

State Estimation of the Autonomic Nervous System from Heart Rate Variability

by

Lindsey Jeanne Marra

B.S. Bioengineering, University of Pittsburgh, 2016

Submitted to the Graduate Faculty of the
Swanson School of Engineering in partial fulfillment
of the requirements for the degree of
Master of Science in Electrical & Computer Engineering

University of Pittsburgh

2021

UNIVERSITY OF PITTSBURGH

SWANSON SCHOOL OF ENGINEERING

This thesis was presented

by

Lindsey Jeanne Marra

It was defended on

November 19, 2020

and approved by

Zhi-Hong Mao, Ph. D., Professor, Department of Electrical and Computer Engineering

Samuel Dickerson Ph. D., Professor, Department of Electrical and Computer Engineering

Thesis Advisor: Ahmed Dallal Ph. D., Professor, Department of Electrical and Computer Engineering

Copyright © by Lindsey Jeanne Marra

2021

State Estimation of the Autonomic Nervous System from Heart Rate Variability Measurements

Lindsey Jeanne Marra, M.S.

University of Pittsburgh, 2021

Heart rate variability (HRV) is an indicator of autonomic nervous system (ANS) activity. HRV is the time series of fluctuations in the intervals between subsequent heartbeats. An opportunity exists to establish real-time tracking of the ANS state based on real time measurements of HRV and predictions from a model of the ANS control of heart rate.

We propose an ANS state estimator. A computational model of the ANS implements a state estimator that is robust to the nonlinear and nonstationary nature of cardiac control. We use a three-state model of the ANS validated in humans, canines, and non-human primates by Champeroux et al. (2018). The state variables are the set of the probabilities that the ANS is in a particular state: $[P(S1), P(S2), P(S3)]'$. S1 is the state of parasympathetic predominance. S2 is the state of parasympathetic and sympathetic coactivation, and S3 is the state of parasympathetic withdrawal and sympathetic activation.

Other state estimation methods were rejected in favor of particle filtering, commonly used in robotics for navigational position estimation. The approach enables visualization of the ANS state based on HRV measurements that may be useful for diagnostic purposes.

Given that the model of ANS regulation of HRV has been validated in pharmacological studies, there is strong qualitative confidence in estimating the ANS state based on HRV measurements. Using this model for long-term state estimation does not directly incorporate the time constants of the PNS and the SNS. Thus, the changes in states may be inaccurate by up to 5

seconds, which is the longest observable delay in ANS control of HRV. Future work to incorporate the dynamics of changes in the ANS state would improve the precision of estimation.

Establishing a state tracking system for the ANS that captures the nature of such a complex physiological system will enable investigation into how the ANS becomes dysregulated in anxiety, depression and PTSD, as well as chronic diseases that, while not mental illnesses, may exacerbate or be exacerbated by ANS dysregulation and mental illness.

Table of Contents

1.0 Introduction..... 1

1.1 Clinical Background..... 3

1.2 Cardiovascular Monitoring 8

1.3 Heart Rate Variability (HRV) 10

1.4 ANS State Estimation with HRV 15

1.5 Particle Filtering..... 18

2.0 Methods..... 22

2.1 ECG Signal Processing..... 22

2.2 Exploratory Data Analysis..... 24

2.3 HRV Control System Modeling 27

2.4 ANS State Estimation with HRV 30

3.0 Results 37

3.1 HRV Analysis Results 37

3.2 ANS State Estimation Results 41

4.0 Discussion..... 47

5.0 Conclusions..... 51

Appendix A Data Summary 53

Appendix B State Estimation Results 55

Appendix C Code Snippets 71

Bibliography 80

List of Tables

Table 1 A selection of models of ANS control of HRV	14
Table 2 Summary of ECG recordings from healthy subjects.....	22
Table 3 Summary of commonly used HRV metrics	25
Table 4 The three states used to represent ANS activity in the model from [44]	29
Appendix Table 1 Summary of ECG data.....	53

List of Figures

Figure 1 Two divisions of the Autonomic Nervous System (ANS)	3
Figure 2 Components of the nervous system in the human stress response.....	6
Figure 3 Raw ECG signal recordings with Physionet annotations	23
Figure 4 The exponential relationship between HRV and HR [63]	27
Figure 5 Autonomic Nervous System State Model	28
Figure 6 Plot HFAM ratio in each animal model [44].....	30
Figure 7 Particle filter in nonlinear system monitoring context [65].....	34
Figure 8 Summary of HRV metrics from 72 healthy-individual recordings	37
Figure 9 Excess kurtosis of successive differences in inter-beat intervals.....	38
Figure 10 Little clinically relevant information in LF and HF band power	39
Figure 11 Variability of HRV itself in a healthy population.....	39
Figure 12 HRV changes over the course of the day	40
Figure 13 Prototype visualization of state estimation of the ANS based on HRV	42
Figure 14 State estimations of the ANS over the course of a day	43
Figure 15 Probability of each of the three possible states dominating for all recordings	44
Figure 16 Example of how the HFAM ratio evolves over the time	45
Appendix Figure 1 ANS state estimation results	70

1.0 Introduction

A state vector can be designed that mirrors the activity of the autonomic nervous system, and specifically the sympathetic response to long term or chronic stress, and acute stress within that context. While the stress system provides adaptive advantages, it's inability to recover completely from overexposure to stimuli can create medical problems that result in poor recovery from physical or emotional trauma, shorter lifespans, and lower quality of life [1]. Continual monitoring of the state of the autonomic nervous system will provide diagnostic information regarding long term regulation. The importance of ANS regulation is reflected in Porges' polyvagal theory that the ANS "sets the limits or boundaries for the range of one's emotional expression, quality of communication, and ability to self-regulate emotions and behaviors [2]."

Human physiology research is undergoing a transformation from a reductive approach to a network approach [3]. While homeostatic control (the regulation of parameters like body temperature and pH to maintain life-sustaining internal conditions) and biomechanical motion control have been the focus of physiological control system studies, a new focus is emerging. Allostatic control mechanisms describe the dynamics of the mediating factors of the human stress response. Allostasis is a concept alternative to homeostasis that recognizes that rather than tracking an ideal set of steady-state conditions for physiological success, regulating to meet changing needs is rather the goal of physiological control mechanisms [4, 5]. These mediators are factors like hormones and cytokines that communicate signals throughout the body in response to changes that necessitate allostatic adaption [6, 7]. The chronic activation of the human stress response leads to dysregulation of the allostatic regulatory system. The clinical implications of overexposure to stress, driven by psychological and adaptive deteriorations, are immense [8, 9]. Adaptations due

to overexposure to stress can even accelerate physiological aging [10]. Monitoring the state of the autonomic nervous system, the ANS, will enable clinical monitoring of the allostatic process, leading to the purpose of this research.

The time-of-day dependent nature of circadian and ultradian fluctuations primes physiological beings for adaptability to the natural, predictable fluctuations of the environment. The possibility of being able to see the fluctuations of the ANS in a visual format could enable not just curious inspection, but also the identification of triggers for each state. In human physiology, glucocorticoids (primarily cortisol) are endocrine mediators of the regulatory mechanisms described by a system called the allostatic control system. In an expansion of the concept of a homeostatic control system which maintains parameters like body temperature and pH at near-constant levels, the allostatic control system in physiology represents an organism's overall capability of the "maintenance of stability through change [11]." The allostatic control system achieves the maintenance of stability through change by promoting adaptability to the predictable and unpredictable changes in the environment. The concept of allostasis is important to bring up here because it takes into account the overall "load" on the stress response of a given individual. It considers the effects of the duration, frequency, and superposition of stressful events as well as the chronic effects of long-term stressors. In fact, allostatic "overload" is the condition which could benefit from further studies. While the stress response encompasses far more than the ANS, ANS dysregulation is an effect of allostatic overload that touches all of the target organs of the system, depicted in Figure 1 [12].

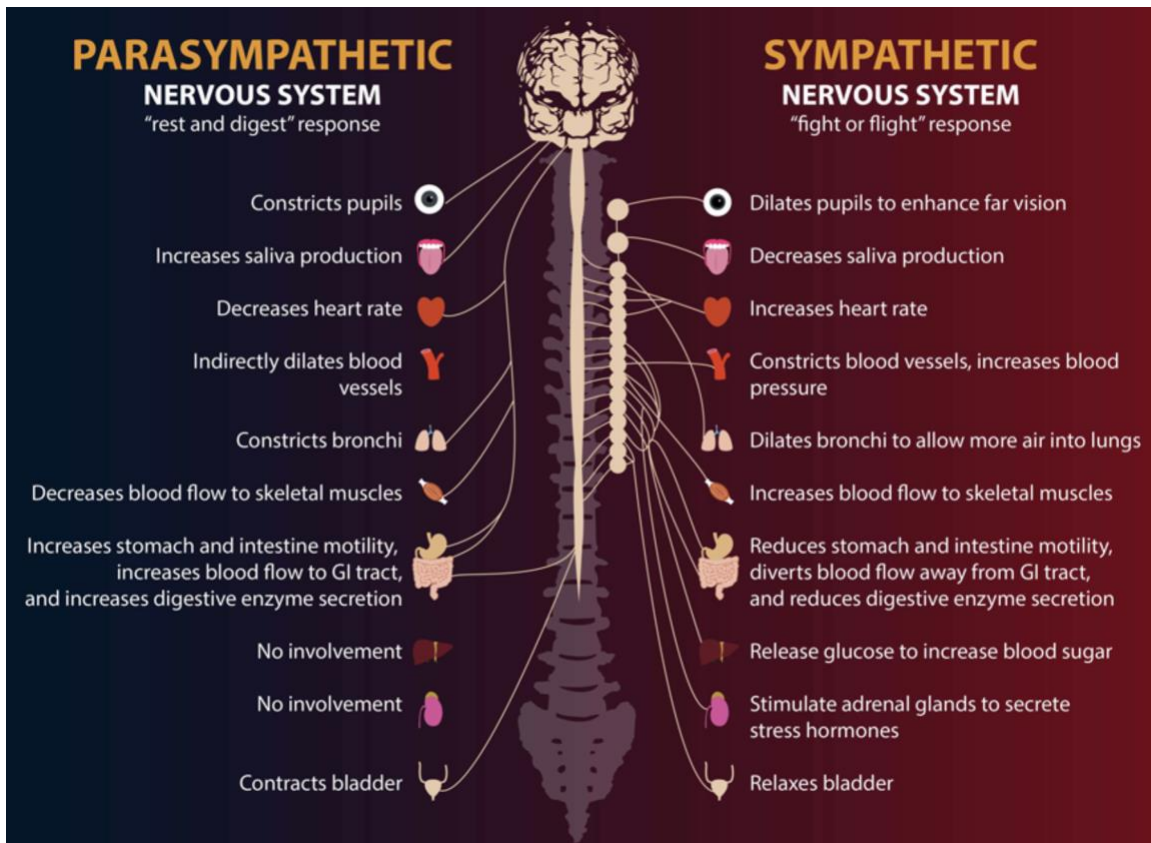


Figure 1 Two divisions of the Autonomic Nervous System (ANS)

The ultimate goal of this work is to provide information and tools for monitoring this system. While the term “allostasis” has gained popularity in stress neurobiology research, this work will use “the stress response” primarily to describe the physiological system of interest.

1.1 Clinical Background

Stress, as an adaptive human response and as an acute or chronic affliction, is complex. The human stress response engages physiological systems across the entire body, and different subsets of these systems are activated to different degrees depending on the timing, magnitude,

repeated or singular nature, and consequences of a stressful stimuli. While anxiety, depression, and post-traumatic stress disorder (PTSD) are the outstanding diseases associated with stress that exceeds levels which provide an adaptive advantage, the consequences of overexposure to stress can have widespread and varied effects. Seemingly separate systems can be affected by overexposure to stress from the immune, digestive, cardiovascular, metabolic and other body systems. The effects to these systems have shown that the lines are blurred between seemingly separate bodily functions. Not only can overexposure to stress cause disease, but it can exacerbate independent disease states and increase recovery times, decrease survival rates, and lower quality of life for individuals and their caretakers.

Stress, as a topic of scientific inquiry, is also consequently complex. Beyond the study of the natural stress response dynamics in acute and chronic conditions, and beyond the study of the afflictions of anxiety, depression, and PTSD themselves... there are lines of scientific inquiry at every scale in space (within and between organelles, cells, organs, organisms, and organizations) and time (across milliseconds, minutes, hours, days, years, and decades) that have been accumulating information about the human experience “stress” for centuries. The diversity of fields beyond physiology and medicine even that require inquiries into the effects of stress can be staggering. The scope of the work enclosed had to be carefully selected and tuned to target stress research as it has been redefined in the last decade while paying tribute to the long-lasting conclusions made in the past century.

Firstly, I will narrow the overall concept of stress to the true topic of interest using the vocabulary offered by reviews of stress literature that aimed to make a more precise definition of the concept for the sake of rigorous inquiry. See Figure 1 for an overview of the autonomic nervous system, the element of the human nervous system that controls the stress response after the

detection of a stressful stimuli and related memories by the central nervous system, which contains the brain and spinal cord.

In response to a physical stressor there is a two-stage response controlled by the central nervous system. First there is an immediate response by the sympathetic-adrenal-medullary (SAM) system, then there is a delayed, slower response by the hypothalamus-pituitary-adrenal (HPA) axis. In a simplification, it can be said that the SAM system activates a response from the ANS. The physical stress response originates in the hypothalamus just above the brainstem. The SAM and HPA axes were illustrated well in [13] shown in Figure 2. The psychological stress response can be said to originate using similar subsystems, but the emotional and memory centers also play a critical role. Both physical and psychological stressors cause a cascade of chemical reactions in the body involving hormones such as the catecholamines like epinephrine and norepinephrine. These hormones increase the activity of the sympathetic division of the autonomic nervous system (sympathetic nervous system: SNS) [6], [8], [11].

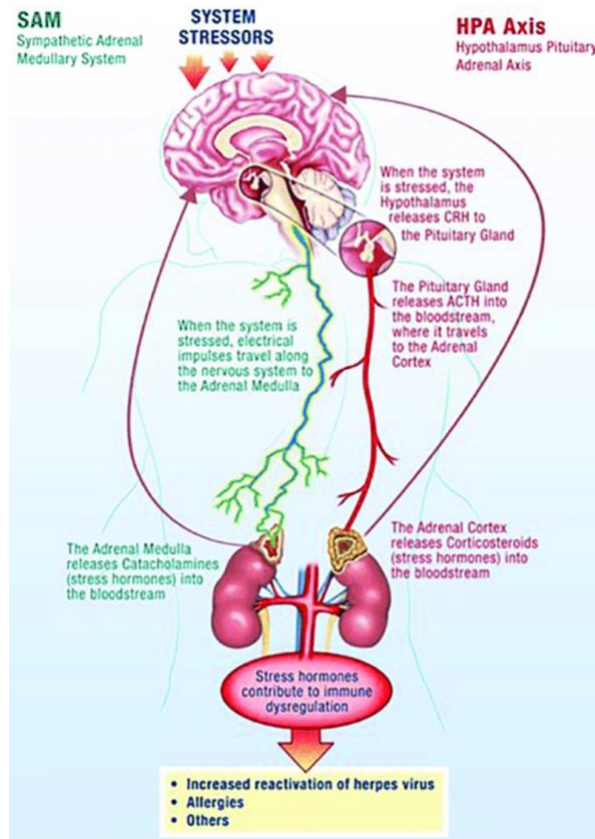


Figure 2 Components of the nervous system in the human stress response

The physiological complement to the SNS is the parasympathetic nervous system (PNS). An accelerator and break control analogy is appropriate as long as one considers that both can be activated at the same time. The PNS is also activated by a signal originating in the hypothalamus. The SNS and the PNS operate independently with the former dominating what is commonly known as the “fight or flight” response, and the latter dominating what is commonly known as the “rest and digest” response. A very important point to note is that not only is the stress response dependent on physical and emotional triggers, but also varies with the cycles of circadian and ultradian (shorter than one day) rhythms. The longer-term effect of the stress response is learning - physiological and behavioral. The dynamics of the stress response are different if one has previously been exposed to a similar stressor. While some of this learning can seem purely

cognitive, memory of stressful events is also stored in tissues as metabolic state changes and even epigenetic changes.

Memory and learning present an interesting challenge in the task of tracking the state of a system based on time-sequential measurements of signals which mirror the state of that system. One example of physiological memory following the overexposure to stress is the reduction of dendritic complexity in the hippocampus and the prefrontal cortex (possibly leading to changes in the cognitive reward system) [14]. Another example is the hypertrophy of the amygdala which is associated with anxiety and learning deficits [15]. Not only is the cause of these effects complex, but so are the downstream impacts of the physiological changes which can even change the stress response itself.

Rotating shift work is an illustrative example of chronic physical stress which can lead to changes in not just cognitive function and physiological structures, but also the stress response itself.

In rotating shift workers, significant measures of circadian rhythm (regulated by the autonomic nervous system) disruption can be seen even during the day shifts given continual HRV monitoring [16]. Changes in HRV outside of the acute time of stress, such as measuring HRV during the daytime despite the acute time of stress being awake during overnight shifts, indicate that monitoring around the clock will be substantially useful in the clinical monitoring of chronic stress states. Health problems are widely recorded in rotating shift workers.

Emotional trauma, even trauma as severe as that which leads to PTSD can have the same long-term effects as physical trauma. PTSD is used as an illustrative example.

Individuals exposed to trauma have shown autonomic dysregulation, and the severity of the symptoms experienced by posttraumatic stress disorder patients correlates with the degree of

parasympathetic impairment experienced during periods of sleep [17]. The study by the U. S. Department of Veterans Affairs even suggests that individuals with more severe PTSD symptoms should be screened early for cardiovascular disease development as indicated by lower adaptability measures (specifically heart rate variability (HRV), explained in following sections) during sleep periods.

1.2 Cardiovascular Monitoring

The amount of physiological data being collected by wearable medical device companies is increasing. First, increases in computer memory capacity allowed more data to be stored locally on a wearable device. Second, increases in the fidelity of wireless communications made routine data uploads possible from the wearable medical device to a company's data servers. Third, the widespread availability of cloud storage and computing increased the limit of data storage and decreased the cost of hardware management to an extent that round the clock monitoring data can simultaneously be collected by medical device companies for (at minimum) tens of thousands of patients at a time. The opportunity to monitor resilience to stressful stimuli in patients at risk of having overtaxed their autonomic nervous system is now within reach [18].

In medical monitoring, physiological signals are a resource that can be tapped into for not only clinical decision making, but also automating the treatment of some acute health conditions such as sudden cardiac arrest. The resource available, electrocardiogram (ECG) data, can be continuously monitored. Arrhythmias can be detected in real time and if they are life threatening, those short clips of data can trigger an automatic defibrillation pulse that prevents sudden cardiac

death. The ZOLL LifeVest has been detecting and treating sudden cardiac arrest using timely clips of ECG recordings since the device approval in 2001 [19].

A patient's heart rate or pulse is measured every time they visit a physician, whether they go to a general practitioner, specialist, or emergency medical facility. The instantaneous heart rate is captured and written on a chart. Is it different than expected by the physician? A patient's heart rate can be continually measured by heart monitors. The ZOLL LifeVest takes periodic measurements of heart rate and if the heart rate is too low it detects a condition called bradycardia. If the electrical firings of the heart increase beyond five "beats" (rather than actual beats detected these are merely peaks in the raw signal due to degradation of ECG morphology in arrhythmia) per second, an arrhythmia is likely occurring, and the patient should be treated with a defibrillation pulse [19].

Now that continuous monitoring of heart rate is possible on a large scale there is an opportunity to monitor the development of chronic conditions. In many of these afflictions, the specific problem of dysregulation of the autonomic nervous system coincides with symptoms like disrupted sleep rhythms, overly active stress responses, and gastrointestinal problems. The parasympathetic (PNS) and sympathetic (SNS) nervous systems primarily control this functionality. Monitoring these systems continuously in real time could lead to insights into the dysregulation of the autonomic nervous system by the conditions listed above.

Sudden death prevention is critical. Thus, physiological data collected by a wearable medical device is used to baseline a normal rhythm and then using sudden changes to detect and treat life threatening situations automatically. Given that such a primary need is taken care of by monitoring technology, we are still left with an endless expanse of data resources and clinical needs. Physiological data is under no threat of exploitation and is only limited in access by

proprietary data ownership. Thus, the opportunity exists to apply the ability to monitor the cardiovascular for less acutely critical afflictions.

1.3 Heart Rate Variability (HRV)

There are many other observable indicators of autonomic activity such as cortisol levels (stress hormone) and cytokine levels (immune protein), breath rate, and blood pressure. One can use any of these parameters to distinguish between PTSD sufferers and healthy controls [20]. Heart rate (HR) and heart rate variability (HRV) are the focus of this work due to their availability in 24-hour recordings, the time scale of interest for this work. There has been a long history of interest in HRV as a sentinel for the autonomic nervous system [15]. The large volume of research based on HRV necessitated a standardization of measuring quantitative biomarkers using the signal [21]. HRV has been studied extensively in the 20 years since the standardization. Researchers from physiology and psychology have since published updated recommendations for others in the field [22], [23].

The HR control system responds to all external and internal regulatory cues to maintain life with respect to stressful stimuli. Thus, the signals it emits are a rich source of information for monitoring purposes. Thus, the focus of this work will be on measuring a patient's HR and how it varies over time brings insights into the stress response. HRV is a widely accepted metric of the autonomic regulation of the heart. Short term HRV measurements (done in a 5-minute time window of HR monitoring) are typically associated with vagal tone which is a term that describes the activity of the vagal nerve, a parasympathetic nervous actuator where the cardiovascular system can be described as the effector that enacts physiological change [24]. Normal values for

HRV in middle-aged individuals have been measured, and there are significant differences with the HRV in individuals who have recently experienced myocardial infarction. Generally, healthy middle-aged individuals have higher HRV than those with recent myocardial infarction or chronic coronary heart disease [25]. The condition of obesity, typically classified as a chronic lifestyle stressor, can have an effect on autonomic dysregulation as early as adolescence as seen in teen circadian rhythm disruption measured by HRV metrics [26]. Current applications of control theory to HRV are encouraging because they have differentiating power between healthy and disease groups [27].

The current state of the research on HRV is evolving quickly. In the 1990's, 2000's, and early 2010's there was a focus on the theoretical application of biophysics concepts like complexity and chaos theory to physiological control and specifically HRV [3], [28] - [33]. In the 2010's researchers established thorough literature reviews of the use of HRV as a clinical indicator, and in 2010 and 2015 Billman et al. established guidelines for its use [22], [34]. These guidelines, along with the preliminary unofficial standard set by [21], were followed in this work.

The first theoretical concept that introduces conceptual complexity and depth into the study of heart rate variability is the concept of memory. A quote from Pittman-Polletta et al (2013) summarizes the concept in the context of cardiac control well:

“... a healthy cardiovascular system seems to remember every adjustment it has made for at least the past 24 h, combining that information with current conditions to make minute, instant-to-instant adjustments in its rate of beating [35].”

Heart rate control is known to have memory on the scale of up to 24-hour periods as is the case in circadian regulation of heart rate variability. Memory exists on much smaller scales as well, down to periods in the range of 10 seconds to 5 minutes. The features of memory and scaling lead to the application of fractal geometry to the problem of analyzing how HRV changes over time. The features demonstrating memory appear to be related to each other in a fractal manner.

A nonlinear landscape topology can be observed in physiological systems and fractional kinetics can describe such systems effectively [28], [31]. Researchers have used fractals to model natural phenomena before [36]. Bruce West in 2010 even surmised specifically that HRV is a fractal random point process [32]. This statement was made in the context of his reiteration that controlling physiological networks to drive their proper operation is one of the goals of medicine, providing validation that this is a worthy approach for future experimentation after the exploratory experimentation presented in this work [29], [30].

In [37], HRV is presented in with a fractional Fokker-Plank equation (equation 14 in that article), for which the approximate asymptotic steady-state solution is the inverse power law (IPL) PDF. From a statistical standpoint, the authors of [38] describe these fractals as being able to “determine the properties of the distribution of intervals in the beating of the mammalian heart”. It should be noted that the concept of fractal geometry encompasses scalability with no limits in the lower or upper scales, and this limitation also applies to cardiac control. Halley et al (2004) used geometric fractals in ecological research despite the limitation of the fractal nature of coast lines for example:

“Why then use fractals at all, if ecological phenomena are not truly fractal? The reason is that fractals may still be as close as simple models can get to the messy multi-scale nature of natural

phenomena. If real distributions are not exactly fractal, they are certainly not Euclidean and so it may be much better to use fractal assumptions than to assume continuous expanses of uniform space. Fractals thus have an important role to play in ecological research, both as a first step towards dealing with scale-dependence and as the null model against which to compare more complex natural patterns [36].”

Given the nonlinear nature explored by theoretical researchers of HRV, there have been practical attempts to apply nonlinear techniques to gain insights into observable HRV behavior and the control of heart rate, but none have been used to track the state of the sympathetic nervous system [39] - [42]. Some of these attempts are summarized in Table 1.

A weakness of these attempts is that the studies do not acknowledge any standard of application of HRV measurement to clinical matters (although there is some standardization in research contexts as described in [21]). Another weakness is that reductive approaches or those employing localized linearization undermine the complex nature of the system in question. One work does check the presence of nonlinear dynamics in experimental models in rats suggests that the extent of nonlinearity present would affect measurements even at very short timescales [43]. Others use frequency analysis of the HRV time series but there is controversy over whether the frequency bands studied are clinically relevant despite being used widely in research [44]. There is evidence that associating LF (between 0.04 and 0.15 Hz) and HF (between 0.15 and 0.4 Hz) components of HRV with autonomic function could lead to misguided medical decisions. Food intake increases parasympathetic activity for digestion, but the heart rate also actually increases to meet the circulatory demand of digestion. Sympathetic regulation can be assessed from HRV with some confidence but claims about parasympathetic activity can be easily misconstrued.

Additionally, the more time spent laying or not doing activity, the more standard HRV measures may predict higher mortality [45]. While this partitioning was assessed in this work (as shown in the data description methods section) it was not used in the end to track the state of the SNS over time, though concepts similar were used.

Table 1 A selection of models of ANS control of HRV

Reference	Year	Description
[41]	2001	Combines the Warner model of norepinephrine and acetylcholine release by SNS and PNS stimulation respectively and the integral pulse frequency modulation to simulate discrete cardiac pulses. Resultant changes in power of frequency bands of interest do not directly reflect the NE/ ACh contributions.
[44]	2018	Canine and non-human primate models of HRV manipulated with drugs that support a three-state system analysis. The drugs used simulated the physiological scenarios caused by beta-blockers, and those that cause sympathetic inhibition and parasympathetic activation.
[43]	2017	Verified the presence of nonlinearities in cardiac control by the ANS in a rat model.
[39]	2013	Simulates LF power decreases during exercise by hypothesizing the presence of a biological dithering effect that “smooths” the presence of nonlinear activity. Focuses on the baroreceptor reflex.

1.4 ANS State Estimation with HRV

The fundamental challenge in the goal of this research is that the state of the ANS cannot be measured directly given readily observable physiological signals. The hidden states can be estimated though, which is the hypothesis of this work. Parasympathetic nervous system cannot be directly monitored using HRV as a signal [45].

Continuous, real time data analysis capabilities have been leveraged in the robotics industry, keeping close to the bleeding edge of possibility in a rapidly moving, fairly unregulated, and highly funded area of research and commerce. The primary monitoring capability in robotics is position monitoring as autonomous robots navigate their task space. This tracking capability estimates the position of the robot in space relative to its previous locations and objects around it using a variety of sensor data from GPS, laser range finding, mono and stereo visual camera streams, and proprioceptive sensors on board the robot. The Kalman filter, extended Kalman filter, unscented Kalman filter, and particle filter methods are all used for state estimation in autonomous robotics in various applications, from flying drones to navigating warehouses.

Continuous monitoring techniques ubiquitous in the autonomous robotics industry are naturally slower to come to prominence in the medical device software industry due to the time spent measuring clinical effectiveness, performing risk analyses to achieve regulatory approval, and time for clinical adoption. The lag between the two industries presents an interesting opportunity to learn more and gain more from the increasing access to physiological data.

The engineering purpose of this work is to solve a nonlinear filtering problem [46]. A Kalman filter approach is inappropriate because the system is neither linear nor Gaussian. If a linear model is not sufficient, may use nonlinear one in the form of an empirical data fit (with artificial neural networks), a high-fidelity dynamic model, either of which may be linearized to

derive a Kalman filter or specify a model for linear model predictive control. As discussed in the next section, it may not be appropriate to make approximations using linearization. Can an extended Kalman filter approach with the Kalman filter applied to a linearized model with Gaussian noise with the same first and second order moments (mean and standard deviation of a stochastic process) be used? The system must be mildly nonlinear where the true posterior PDF is unimodal (one peak) and essentially symmetric. This is not the case in the system of interest [31].

Over the course of decades of HRV research, heart rate control by the autonomic nervous system has been shown to resemble a Levy process [37]. A Levy process can be described as a “continuous-time analog of a random walk.” A random walk is a subcategory of Markov chains, which is a chain of events in which each event depends only on the previous event’s achieved state. The probability density function (PDF) of HRV can be described by a Levy stable PDF that does not vary between healthy and diseased individuals [37]. Since cardiac activity cannot be described as normal or as having a Gaussian distribution, statistically speaking, the non-Gaussian nature of the system must be tolerated by the selected state estimation methodology.

The desire for robotic systems which can adapt to cyclical environmental perturbations prompts the need for a control model for systems that are required to operate in such environments. Environments with both predictable and unpredictable perturbations are often described as complex systems [37]. Complex systems exhibit nonlinear dynamics such as switching between multiple stable states. Bifurcation events such as switching behavior are emergent events from the complex dynamics of the environment [47]. In physiology, organisms mediate the emergent events from the complex dynamics of the environment by generating emergent (bifurcation and switching) behavior themselves [33]. Physiological systems are regulated by a network of molecular clock structures present in the central nervous system and in peripheral regulatory

tissues. An analogous network of clocks may also give rise to regulatory mechanisms in robotics which enable a robot to maintain a level of adaptability to change.

Simultaneous localization and mapping (SLAM) has been used to estimate location in physical space in autonomous robotic agents [48]. The same tool set can be applied to the internal states (states of the analogous allostatic control system) of an autonomous system. This is effectively an internal map. In physiology, the parameter space of analogous interest is the change of dominating frequencies present in heart rate variability calculated from ECG data. The objects in the parameter space in the heart rate variability time series from ECG data are sustained periods with particular frequency range domination and instances of nonlinear events such as bifurcations and bursting patterns. Analogous system level status signals can be used for internal and environmental state estimation in robotics and thus can be applied to state estimation in physiological systems.

In order to select the method for state estimation that applies best to tracking the state of the autonomic nervous system, and specifically the SNS, I first investigated the properties of the control system that regulates HR and HRV, the observable state variables of interest. “Sudden changes in HR (up or down) between one beat and the next are parasympathetically mediated [49].” There is a delay in changes in HR due to sympathetic activity. HRV is also measured by performing a power analysis of the time series of changes in time between heart beats. Low power in the "very low frequency band" (less than 0.04 Hz) has been associated with high inflammation and the presence of PTSD, which can sometimes be an indicator that the SNS is active to an extent that it is causing physiological strain [50] - [53]. Given that power in this frequency band can only be measured from recordings longer than 24 hours, it will not be incorporated in this work but could be useful nonetheless.

Thus, after performing an exploratory analysis of the features available in HRV data and using those features to learn a model for HRV, a particle filter implementation will be tried as a method of state estimation of the stress response, or autonomic nervous system. In ground-roaming robotic position tracking applications the horizontal position (x, y) and the pose are used. Positioning applications and visual tracking drove interest in establishing particle filtering as an accessible state estimation method. In physiological systems, a vector composed of several process variables that convey significant information about autonomic state [53]. An example of defining the state space for a neurophysiological system is that of the brain states in sleep [37].

1.5 Particle Filtering

This section will present the inner mechanics of the particle filter methodology to provide context for how Bayesian inference can be applied to the state estimation of a nonlinear system such as ANS control of HRV. The particle filter is designed for state estimation of a system with both hidden and observable variables. The hidden variables in this case are the ANS state, and we are using the observable variable HRV to estimate them. Because we know how the observable variables of the state are related to the hidden ones, we can estimate the state in the form of the hidden variables in a sequential manner [64].

Particle filtering serves as a numerical approach to state estimation. The particles of the particle filter model an approximate state estimation by forming a statistical distribution of the possible state [46]. The number of particles used to estimate the state determines the resolution with which the state can be estimated. The number of particles used also has a dramatic effect on computational load due to the “curse of dimensionality [63].” There are methods of avoiding this

problem, for example with the feedback particle filter that does not weight the particles according to their measurement likelihoods [78]. In the end, the purpose of using the method is to represent the posterior distribution of the system process of interest given measurements that may not directly define hidden variables:

$$p(x_k | y_0, \dots, y_k) \tag{1-1}$$

First, establish a state (x) vector that describes all relevant information about the system at a given point in time. The dimension of x is the number of state variables (k) that define the state by 1.

$$\bar{x} = [x_1, \dots, x_k]^T \tag{1-2}$$

The posterior distribution can be computed using Bayes' rule for conditional probability where the conditional probability of the measurements occurring given a system state, times the probability of the given system state, divided by the probability of the measurements themselves:

$$p(x_k | y_0, \dots, y_k) = \frac{p(y_0, \dots, y_k | x_0, \dots, x_k) p(x_0, \dots, x_k)}{p(y_0, \dots, y_k)} \tag{1-3}$$

Then, a description of the dynamics of how the state changes over time is typically placed in state space form. The dynamics are represented by function f and different dynamics may describe each state variable in the state vector. For each x_k :

$$x_k = f(x_{k-1}) \quad (1-4)$$

$$y_k = h(x_k) \quad (1-5)$$

The functions f and h are assumed to be known and used to approximate a solution of the state estimation problem to find the posterior probability distribution. In the particle filter methodology, start with the probability distribution of an initial state represented by an initial set of particles:

$$p(x_k | y_0, \dots, y_{k-1}) \quad (1-6)$$

Then, update the values of the initial set of particles using a measurement from the current time step, which in this case is all of the previous measurements and the current one k :

$$p(x_k | y_0, \dots, y_k) = \frac{p(y_k | x_k) p(x_k | y_0, \dots, y_{k-1})}{\int p(x_{k+1} | x_k) p(x_k | y_0, \dots, y_k) dx_k} \quad (1-7)$$

Once the initial posterior distribution has been updated given a measurement from the current time step, we can predict the posterior distribution to be used in the next one:

$$p(x_{k+1} | y_0, \dots, y_k) = \int p(x_{k+1} | x_k) p(x_k | y_0, \dots, y_k) dx_k \quad (1-8)$$

The predicted next step is then used in the next iteration of the computation. In the case of plotting the states over time, a metric summarizing the particles that represent the posterior distribution of a given time step is used to establish an approximate, singular measurement for

each state variable in each time step. This process lends itself well to sequential signal processing where new measurements are incoming with a given sampling frequency. See the Methods section 2.4 (ANS State Estimation with HRV) for a discussion of the state transition matrix that updates the posterior distribution and the measurement likelihood that establishes the weights of the particles in a time step based on the probability that they would properly describe the state of the system.

2.0 Methods

2.1 ECG Signal Processing

Two databases were used from the Physionet [54]. One is called the Normal Sinus Rhythm RR Interval Database v1.0.0 [55]. The other is called the MIT-BIH Normal Sinus Rhythm Database v1.0.0 [56]. A summary of the physiological records available from the two databases is in Table 2 (complete list in Appendix A Table 1).

Table 2 Summary of ECG recordings from healthy subjects

Record	Duration (s)	Skewness	Kurtosis	Mean HR (bpm)	SD HR	Mean HRV (s)	SDNN (s)	LF PWR (ms²)	HF PWR (ms²)	LFHF Ratio
16265	80062	0.404	2.487	75.647	16.188	0.096	0.018	2.55E-05	4.25E-06	5.990
16272	84396	-0.630	2.930	66.226	11.022	0.118	0.017	1.18E-05	1.19E-06	6.185
...
n5r053	81223	0.513	2.412	73.240	14.269	0.106	0.020	1.86E-05	3.56E-06	5.209
n5r054	83754	0.518	2.933	87.333	17.386	0.079	0.011	1.40E-05	1.90E-06	7.367

In total, 72 day-long recordings were available. These 72 recordings were made of 72 healthy adult individuals, typically starting in the morning or afternoon and finishing 24 hours later. The recordings were made in accordance with guidelines made by the Task Force of the European Society of Cardiology and the North American Society of Pacing and Electrophysiology [21]. The Waveform Database (WFDB) Application available on Physionet was used to convert

the available files into two human readable text files for each record available. The first file for each record was the HRV series. The second file for each record was the HR series [57]. Thus, rather than heartbeat event series, time series were acquired through interpolation to synchronize measurements of HR and HRV over time, as well as to perform spectral analyses that were integral to the exploratory phase of this work.



Figure 3 Raw ECG signal recordings with Physionet annotations

ECG was sampled at 128 Hz by the teams who generated and distributed the WFDB recordings. HRV and instantaneous HR annotations were made at the varying heart rate. Figure 3 shows a 10 second snippet of ECG recording along with the annotations made by clinical interpreters. Such annotations (labeled ‘atr’ in Figure 3) were made for all available ECG recordings that were used in this work. Thus, interpolation was necessary to acquire synchronized, evenly spaced HR and HRV time series. The time series were reconstructed at 300 Hz or double

the approximate highest expected HR so as to not lose the frequency information available. After interpolation, both the HR and HRV time series were synchronized along the same time intervals. The HRV toolkit which enabled the extraction of HRV from clinically validated heartbeat annotation files has been benchmarked against other HRV toolboxes made available by researchers in the last 20 years [58], [59]. Detailed steps that went into ECG processing for the available records can be found in [60].

250 Hz ECG sampling is sufficient for time and frequency analysis whereas 100 Hz sampling can be used for just time analysis. Many defibrillator monitors and Holter recorders (heart monitors) are limited to between 100 and 200 Hz [61]. The data used was sampled at 128 Hz. If the overall HRV is very low, such as that measured in heart failure patients, a sampling rate higher than 200 Hz is necessary. Due to the source of the signals analyzed here being healthy individuals, there is no concern in this work about using data captured with a sampling rate of 128 Hz.

2.2 Exploratory Data Analysis

The purpose of the exploratory data analysis is to qualitatively validate the claims made by sources investigated during the literature research phase. Measures of short term HRV and long term HRV were computed following clinical guidelines in [21].

For long term HRV, the full 24-hour length recordings were used to compute metrics for each recording. For short term HRV, the data in each record was trimmed to a length that could be perfectly divided by five-minute intervals. To perform a comparison between five-minute intervals, particularly in the frequency domain, each interval must be the same length [62]. The

remaining datapoints that do not fit into a five-minute interval were trimmed off of the beginning of each record due to the appearance of errant turbulence in the data upon the start of monitoring. Table 3 describes commonly used measures of HRV. The metrics selected for exploratory data analysis are shaded in grey.

Table 3 Summary of commonly used HRV metrics

Metric	Description
SDNN	Standard deviation (square root of variance) of the inter-beat (NN) intervals is a statistical characteristic of HRV. Depends on length of recording, so it has been standardized in this document. HRV must be corrected for HR due to the exponential relationship between the two (shown in Figure 4) to appropriately make conclusions about the change in autonomic regulation over time [63].
RMSSD	Square root of the mean squared differences (RMSSD), another statistical measure of HRV, is the square root of the mean squared differences of successive inter-beat intervals.
NN50	NN50 is the number of interval differences of successive inter-beat intervals greater than 50 ms.
pNN50	pNN50 is the proportion derived by dividing NN50 by the total number of inter-beat intervals in the signal segment of interest.
HRV Triangular Index	The HRV triangular index measurement is the integral of the density distribution (that is, the number of all NN intervals) divided by the maximum of the density distribution. This metric is a geometric characteristic of HRV and

	<p>Table 3 Continued ...</p> <p>is generally useful for long-term changes in HRV, longer than the length of recordings used in this research.</p>
Frequency band power analysis	<p>Frequency analysis of the inter-beat interval differences is clinically relevant in four different frequency bands: ultra-low frequency, very low frequency, low frequency, and high frequency. The low frequency and high frequency bands are relevant to this work as they can be measured in recordings of both 24 hours and 5 minutes. The bounds for these two frequency bands are:</p> <p style="padding-left: 40px;">low LF = 0.04 Hz</p> <p style="padding-left: 40px;">high LF = 0.15 Hz</p> <p style="padding-left: 40px;">low HF = 0.15 Hz</p> <p style="padding-left: 40px;">high HF = 0.4 Hz</p>
Detrended fluctuation analysis	<p>Detrended fluctuation analysis is a spectral approach to computing a scaling exponent that describes the long-term memory present in a given time series.</p>
Heart rate fragmentation	<p>Heart rate fragmentation analysis provides a measure of the presence of seemingly “high” HRV but actually is not the result of the modulation of the parasympathetic nervous system, rather it is the result of aging.</p>

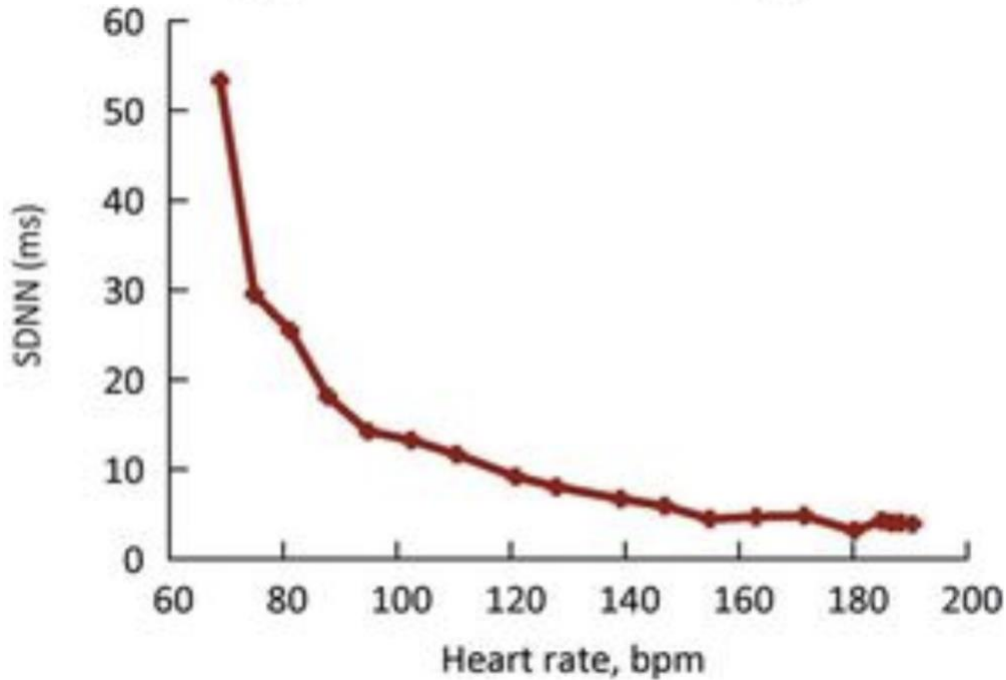


Figure 4 The exponential relationship between HRV and HR [63]

2.3 HRV Control System Modeling

The model of ANS modulation of HR and HRV was based on a new human, canine, and non-human primate model developed and validated pharmacologically by P. Champeroux et al. in 2018 [44]. The group pursued this model due to the weakness of previous models in representing a coactivation state that cannot be assessed directly using classic methods of HRV analysis as described in Table 3. The model breaks HR and HRV oscillations into 10 s intervals for analysis. The group observed changes in HR and HRV due to parasympathetic and sympathetic modulation which can be described with the following algorithm in Figure 5 (after discarding intervals containing arrhythmias), which is used as a state transition model for state estimation. This group

also used standard ECG processing methods, the same used in this thesis document, as outlined in [21].

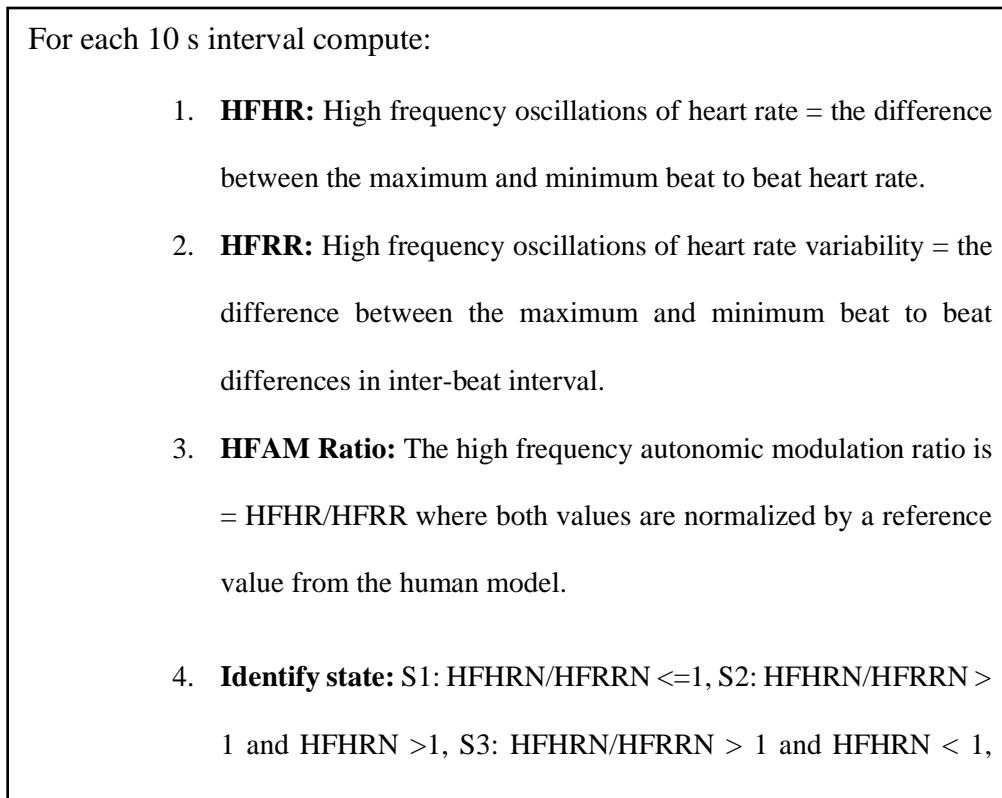


Figure 5 Autonomic Nervous System State Model

Since the two quantities have different units (beats per minute and milliseconds), both HFHR and HFRR are normalized by reference values for healthy humans determined from measurements made in 200 subjects. The reference values used for state estimation in this work were computed for each individual by taking the average HFHR and HFRR for each recording. The group classifies the three different autonomic modulation states as described in Table 4.

Table 4 The three states used to represent ANS activity in the model from [44]

ANS State	Description
S1	This state signifies <i>parasympathetic predominance</i> where normalized HFRR oscillations, a measure of HRV were larger than HFHR oscillations.
S2	This state signifies <i>parasympathetic and sympathetic coactivation</i> where patterns show non-stationary and low amplitude fast oscillations with phases of acceleration or deceleration within the 10 s intervals.
S3	This state signifies the <i>fading of parasympathetic influence and the activation of the sympathetic nervous response</i> . HFRR and HFHR oscillations are stationary and low amplitude compared to S1.

Figure 6 is adopted from [44] and demonstrates the behavior of the model across the circadian rhythm in all three biological models: human, non-human primate, and canine. The figure shows the accordance or agreement between the three different models and will be used as a reference to validate the HFAM patterns computed by the state estimation methodology that follows.

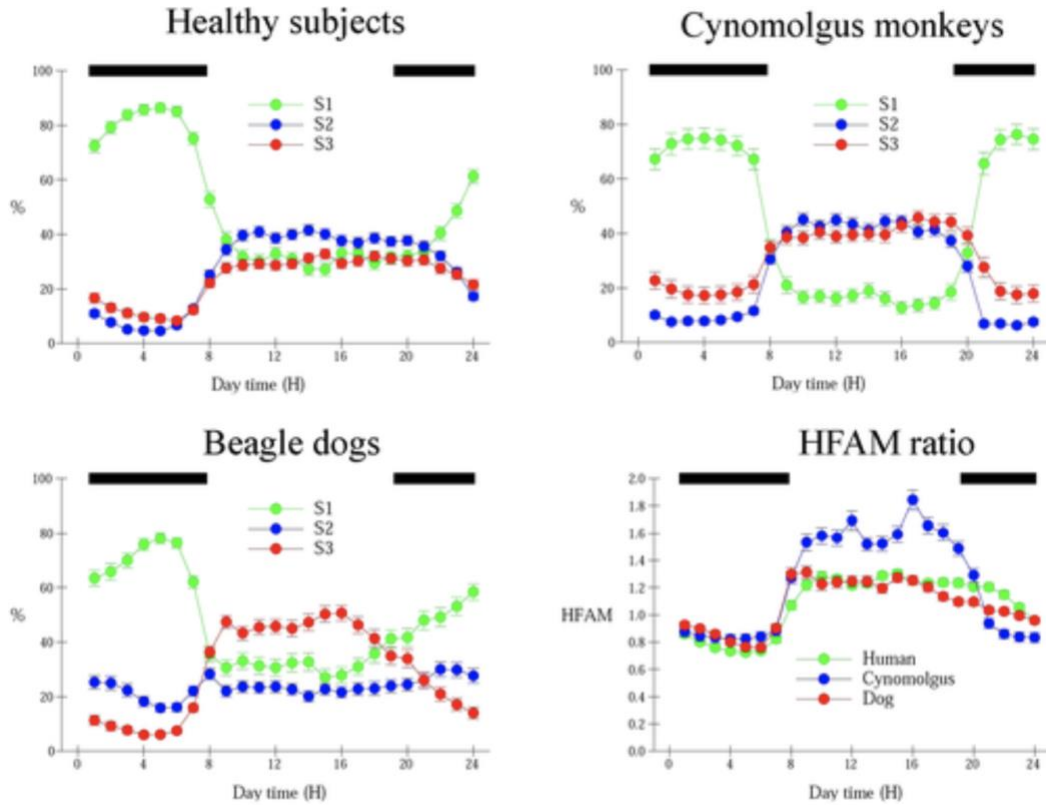


Figure 6 Plot HFAM ratio in each animal model [44]

2.4 ANS State Estimation with HRV

In the end, the goal of this research was to establish methods for the state estimation of the autonomic nervous system. Some requirements for state estimation include the methodology's ability to handle a time series of measurements, input from a model of expected dynamical behavior, measurement noise, and the inevitable likelihood that, rather than there being certainty of one state or another existing, there is a non-zero probability for any of the available states to be active given a measurement and prediction of system state. The results should demonstrate not only a series of state inferences, but also the certainty with which those inferences were made. The

particle filter methodology was chosen due to its ability to handle non-Gaussian systems and to incorporate information from a biological model, and its ability to meet the requirements to achieve state estimation of the autonomic nervous system.

In order to implement state estimation, a particle filter was used to compute the likelihoods of the possible values of a state, changing over time. A set of particles represent the posterior distribution of the process which is the subject of this investigation. The dynamics of the state transitions of the sympathetic nervous system are taken into account in the implementation of the particle filter to make a prediction of what the next possible state could be. The particles are assigned weights that describe the likelihood of each particle being drawn from the probability density function. The probability density function of the system changes as the underlying sympathetic nervous system changes state over time. This is precisely the behavior of interest, and visualizations of the changing state will be the result of this work.

As shown in Table 3, widely used metrics of HRV could be used as measurements for state estimation but have been found to be not suited for the task. For SDNN, significant changes over the course of the day have been shown to be primarily linked to variability in levels of daytime activity level having an effect on the nighttime HRV measurements. Given that daytime activity level will not be controlled for and that the mean squared differences may be warped by the non-Normal distribution of differences, SDNN and RMSSE will not be used in the assessment of the state of the sympathetic nervous system. In the last few decades, the ratio of power in the low frequency (LF) range and the high frequency (HF) range indicated the ratio of activity between the parasympathetic and sympathetic nervous systems. A causal relationship has been discovered between a lower LF/HF ratio in individuals who have spent more time laying down during the daytime which confounds the ultimate effect of a measurable increase in mortality in those with a

lower LF/HF ratio. While there is evidence that some interpretations of HRV metrics that have gained popularity in the last few decades are misleading and oversimplified, HRV analysis beyond the LF and HF measures will still be a useful signal for the extraction of information about cardiac regulation by the central nervous system [45].

In order to incorporate the ANS system model described in the previous section, the new measurements of heart rate variability proposed by [44], HFAM and HFHRN will be computed given instantaneous heart rate measurements and mean inter beat interval difference measurements for each of M ten second segments of data recording. For a given ten second segment m with w measurements per segment the metrics HFHR and HFRR can be computed:

$$y_m = \{y_1, \dots, y_w\} \quad (2-1)$$

Where ‘hr’ is an instantaneous heart rate measurement and ‘rr’ is the change in inter-beat interval since the last beat (interpolated at a resampling frequency for equal length vectors):

$$y_w = [hr_w \ rr_w]^\top \quad (2-2)$$

$$HFHR_m = \max(y_m(1, :)) - \min(y_m(2, :)) \quad (2-3)$$

$$HFRR_m = \max(y_m(2, :)) - \min(y_m(2, :)) \quad (2-4)$$

Now the metric that indicates the values of the hidden state variables, high frequency autonomic modulation (HFAM), can be computed:

$$HFAM_m = \frac{HFHRN_m}{HFRRN_m} \quad (2-5)$$

Where:

$$HFHRN_m = \frac{HFHR_m}{HFHR_{ref}} \quad (2-6)$$

$$HFRRN_m = \frac{HFRR_m}{HFRR_{ref}} \quad (2-7)$$

Where HFHRN and HFRRN are normalized mean “reference” values of expected heart rate measurements and inter-beat interval changes for each individual.

The resultant state calculations will reflect the three possible states described in Table 4. The algorithm validated in [44] provides a definitive answer to the question, “What state is the ANS in right now?” Given the preeminence of the SNS and PNS coactivation state (S2) and the non-binary nature of physiological states due to the heterogeneity of bodily tissues, organs, and time constants of responses, the estimated state will be given as a probability of each of the three states being activated to provide a more wholistic picture of the status of the ANS. Thus, heart rate variability measurements will be used to estimate the following dynamic hidden variables where the probabilities listed are of the likelihood that each of the ANS states listed in Table 4 are activated:

$$\bar{x} = [P(S1) P(S2) P(S3)] \top \quad (2-8)$$

How does the particle filter methodology achieve the intended purpose of this research which is to estimate the state of the autonomic nervous system? A particle filter requires two models in order to have enough information to make inferences about the state of a system [63].

Firstly, it needs a model that describes how the state changes with time. Secondly, it needs a model that relates the noisy measurements to the state [64]. The first model will be called the state transition function and the second model will be called the measurement likelihood in order to mirror the properties needed to implement a particle filter using the MATLAB 2020a System Identification Toolbox. Given a probabilistic model for a state transition function, a particle filter can update its estimation of the state of the system given new information over time. A summary of the goal is to construct a posterior probability density function of the state of the system. Figure 7 shows the context of the particle filter along with the system of interest from the MATLAB 2020b documentation [65]. In this work, x is the state variable of interest, which is calculated using u , which represents the output of the state transition function and m , which is the measurement made that includes measurement noises w .

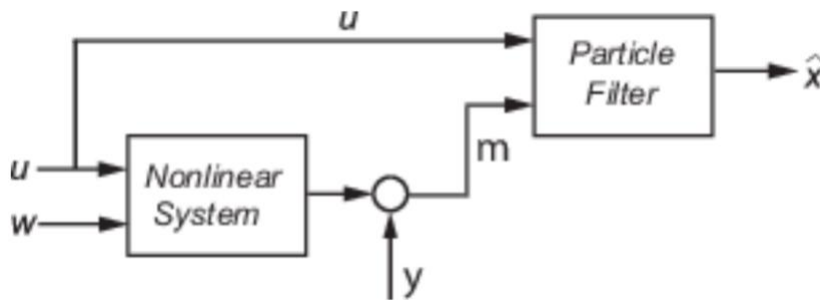


Figure 7 Particle filter in nonlinear system monitoring context [65]

The state transition function, which represents the model of how the system of interest changes through time, more specifically determines how a set of hypotheses of what the state could be, represented by particles, evolves between time steps [66]. The input to the state transition function is the set of particles which represent all of the possible hypotheses of the state of the

system. In this work, the state transition matrix was used to evolve the particle states which applies the algorithm developed by [44] which is described in Figure 5.

This element of the particle filter methodology can be edited in future investigations to incorporate the nonlinear dynamics described in the introduction. The state transition function then outputs all of the particles again but transformed into what the likely hypotheses should be at the subsequent time step. The number of hypotheses provided to the state transition function and thus again returned by it is the number of particles set for use in the particle filter. This contrasts the method of the state transition function in an unscented or extended Kalman filter for example because a state transition function only returns one hypothesis or estimate per time step in those cases. This distinction highlights the usefulness of the particle filter to add another dimension of information in the state estimations if desired. The “state” of the system can be either the most frequently represented hypothesis in the entire set, or the mean of all of the hypotheses in the entire set. Given that the physiological states of interest are not self-exclusionary but rather coexisting to various degrees and feeding back into each other, the entire set of hypotheses provides additional information. Thus, the entire set of hypotheses (all of the “particles” of the particle filter) are used to describe the state of the system, despite the ability to select a single most likely state.

The measurement likelihood function, in turn, takes a measurement and calculates the likelihood of each hypothesized particle being measured given the measurement noise probability model [67]. The sources of noise in the measurement of the two-input metrics, HFAM and HFHRN are ECG measurement noise, inaccuracies in beat annotation, and lost information during the process of interpolation. The overall noise is represented in this work by Gaussian distributed noise with an 0.5 valued covariance matrix. The noise is then combined with the measurement error between the predicted and actual measurement using the probability density function of the

multivariate normal distribution to produce a likelihood for each hypothesis given the measurement. Given more specific noise models, the measurement likelihood could be altered in future investigations. See Appendix C for a summary of the computational tools used to implement ECG signal processing, exploratory data analysis, and particle filtering.

3.0 Results

3.1 HRV Analysis Results

Given the commonly used HRV metrics listed in Table 3, Figure 8 shows a summary of the metrics calculated from the ECG records obtained from PhysioNet. The metrics highlighted in grey in Table 3 were chosen and some other summary statistics were added. The overall duration of each recording in seconds, skewness and kurtosis of the successive differences in inter-beat intervals, and heart rate metrics were added to the analysis.

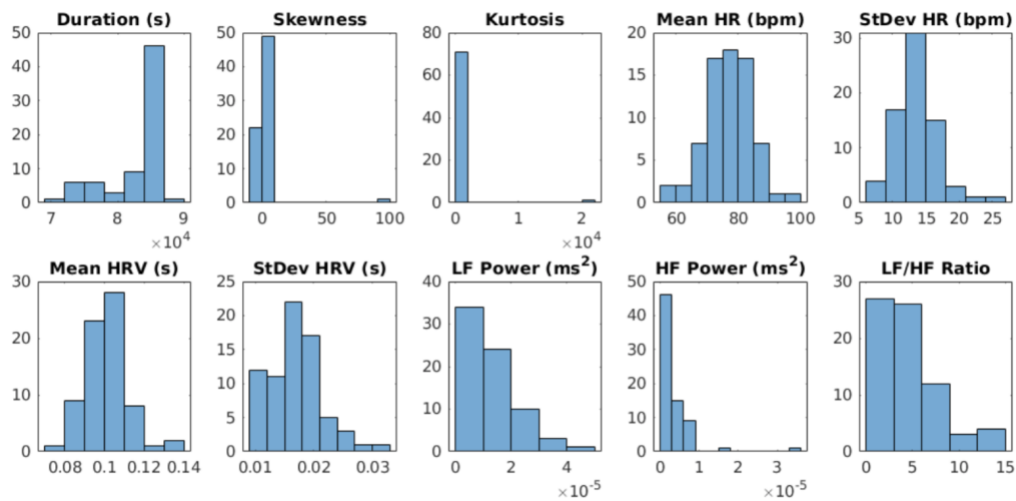


Figure 8 Summary of HRV metrics from 72 healthy-individual recordings

Skewness and kurtosis are measures of how well the distribution of the successive differences in inter-beat intervals for each healthy person from which a recording was taken fits a normal distribution. These were important measurements to add to commonly used HRV analysis methods because the theoretical researchers who have published research about HRV in the last decade have warned about long-tailedness (large outliers) leading to the inappropriate use of a normal distribution to describe the distribution of successive differences in inter-beat intervals.

The kurtosis of the normal distribution is 3, which we can compare to that of the distribution of successive differences in inter-beat intervals. The excess kurtosis (kurtosis - 3) was nearly zero for nearly all of the records, with some slightly negative and some slightly positive as shown in Figure 9. The normal distribution was used for the measurement likelihood function for the particle filter, which we found was in practice acceptable despite deviating from the advice from theoretical biophysicists discussed in the introduction of this thesis.

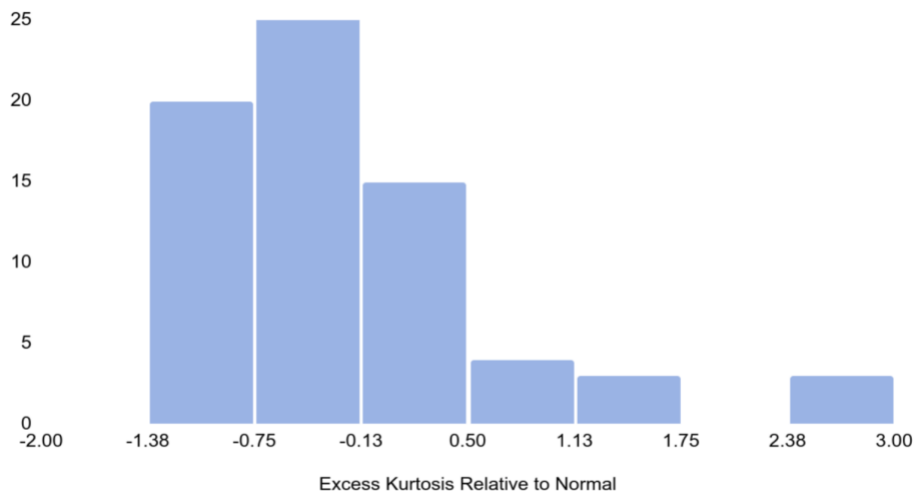


Figure 9 Excess kurtosis of successive differences in inter-beat intervals

Frequency analysis of the low (LF) and high frequency (HF) bands of clinical interest showed the patterns expected in healthy individuals. An example illustration of how the power in the LF and HF bands change over time. As expected, despite the effect being hard to see, HF band power has a smaller amplitude early in the day. Little other information can be gleaned from this plot despite the power in each of the LF and HF bands and the LF/HF ratio being commonly used HRV metrics.

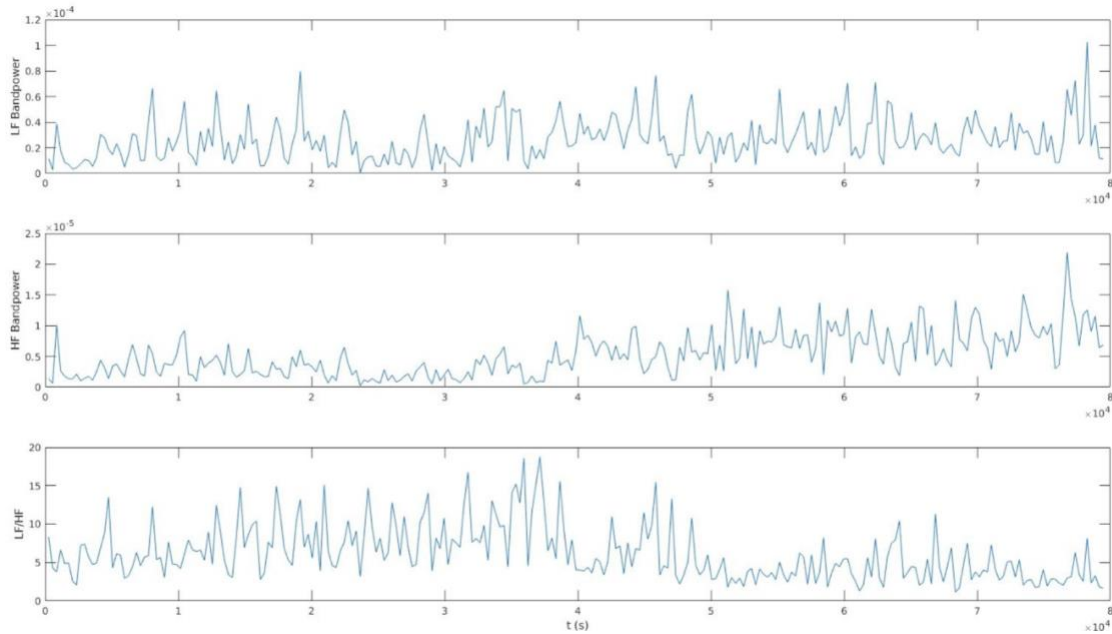


Figure 10 Little clinically relevant information in LF and HF band power

Figure 11 shows how SDNN was distributed across all healthy individuals from which ECG recordings were taken. This figure gives a sense for the variability in heart rate variability itself within a healthy population.

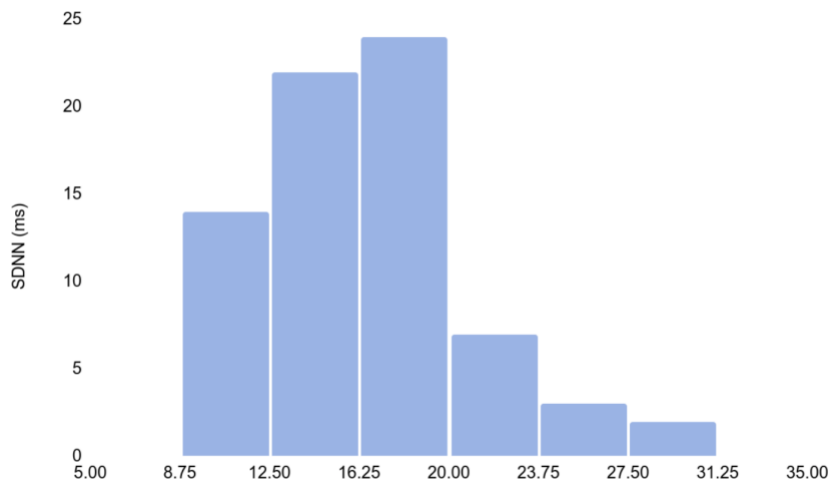


Figure 11 Variability of HRV itself in a healthy population

Heart rate variability, by definition, changes over the course of the day. Figure 12 is illustrative of how the measurements used for state estimation would look to an observer before state estimation filtering took place. This result partially motivated my interest in state estimation because, despite the slightly visible increase in SDNN (a measure of HRV) at nighttime which is expected, there is little else of clinical usefulness to be gathered from the illustration.

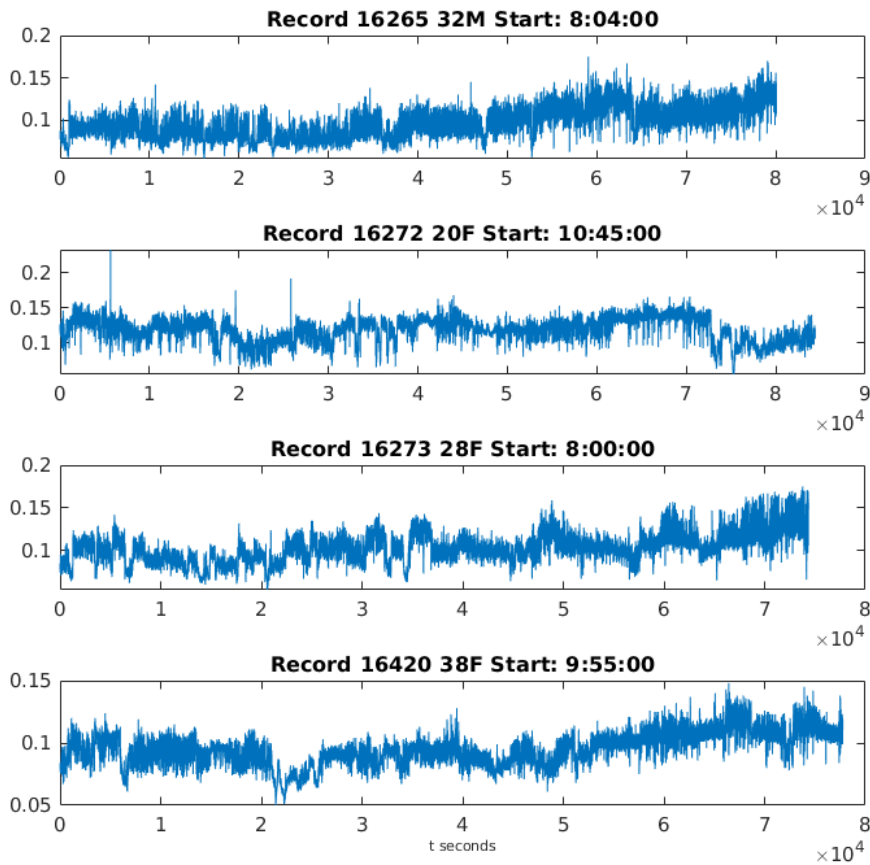


Figure 12 HRV changes over the course of the day

3.2 ANS State Estimation Results

A prototype of state estimation was the first step in implementation. The goal was to show that clinically relevant information could become much more visible given a filtering approach of the time series of HRV metrics. Figure 13 shows the prototype of state estimation that used average metric values over 5-minute increments, the standard width of a short term HRV window used in the literature. The first chart in Figure 13 shows average heart rate over time in beats per minute, over the course of an entire 24-hour (80,000 s) record of a healthy individual's ECG. As expected, heart rate decreases at nighttime. The second chart shows the average change in successive inter-beat interval lengths, showing the predictable pattern of increasingly larger changes in inter-beat intervals in states of rest and digest (PNS activation, or S3 as defined by [44], which can be assumed to be taking place over the nighttime hours. This starts to suggest a clinically relevant pattern from changes in successive inter-beat intervals. The third chart in Figure 13 shows how SDNN, a typically used measure of HRV changes over the course of the day that mirrors the patterns in Figure 12. As was also shown in Figure 12, clinically relevant information is difficult to extract visually from SDNN despite its popularity as an instantaneous HRV metric. This result leads to the particle filter methodology which was performed in order to extract clinically relevant information from HRV data that has previously not been used yet to demonstrate the changing ANS state over time, over the course of at least 24 hours.

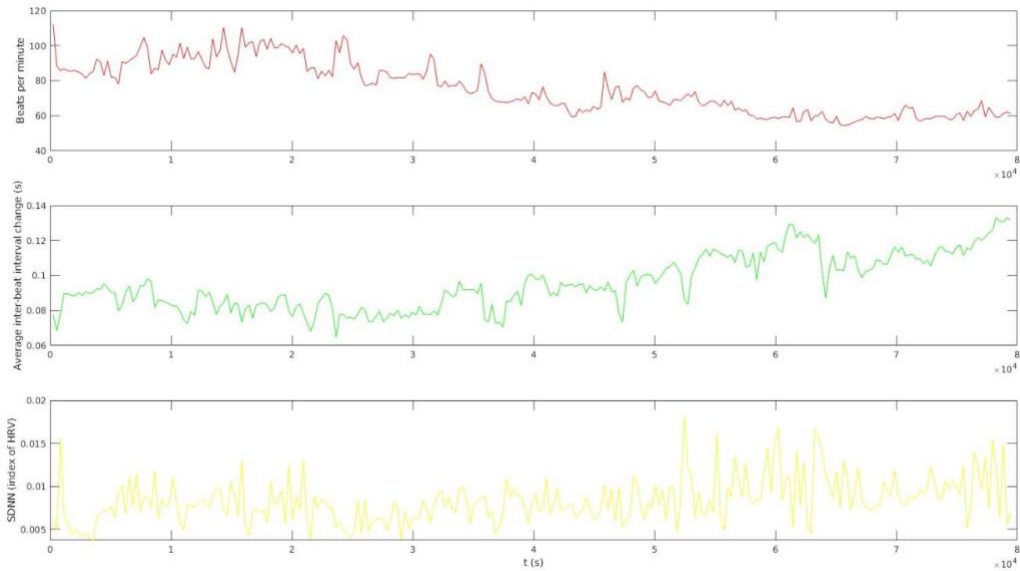


Figure 13 Prototype visualization of state estimation of the ANS based on HRV

State estimation was performed, as described in the Methods section, with the particle filter methodology using a state transition matrix that models the three states of the ANS as described in Table 4 and represents a pharmacologically validated model of ANS control of HRV by [44].

Figure 14 shows the day-long output of the particle filter-based estimations of the state of the ANS for four of the healthy individuals (nsr050, nsr051, nsr052, nsr053) from which ECG recordings were taken. Appendix B contains the output of the particle filter methodology from all of the individual day-long recordings summarized in Table 2 and Appendix A.

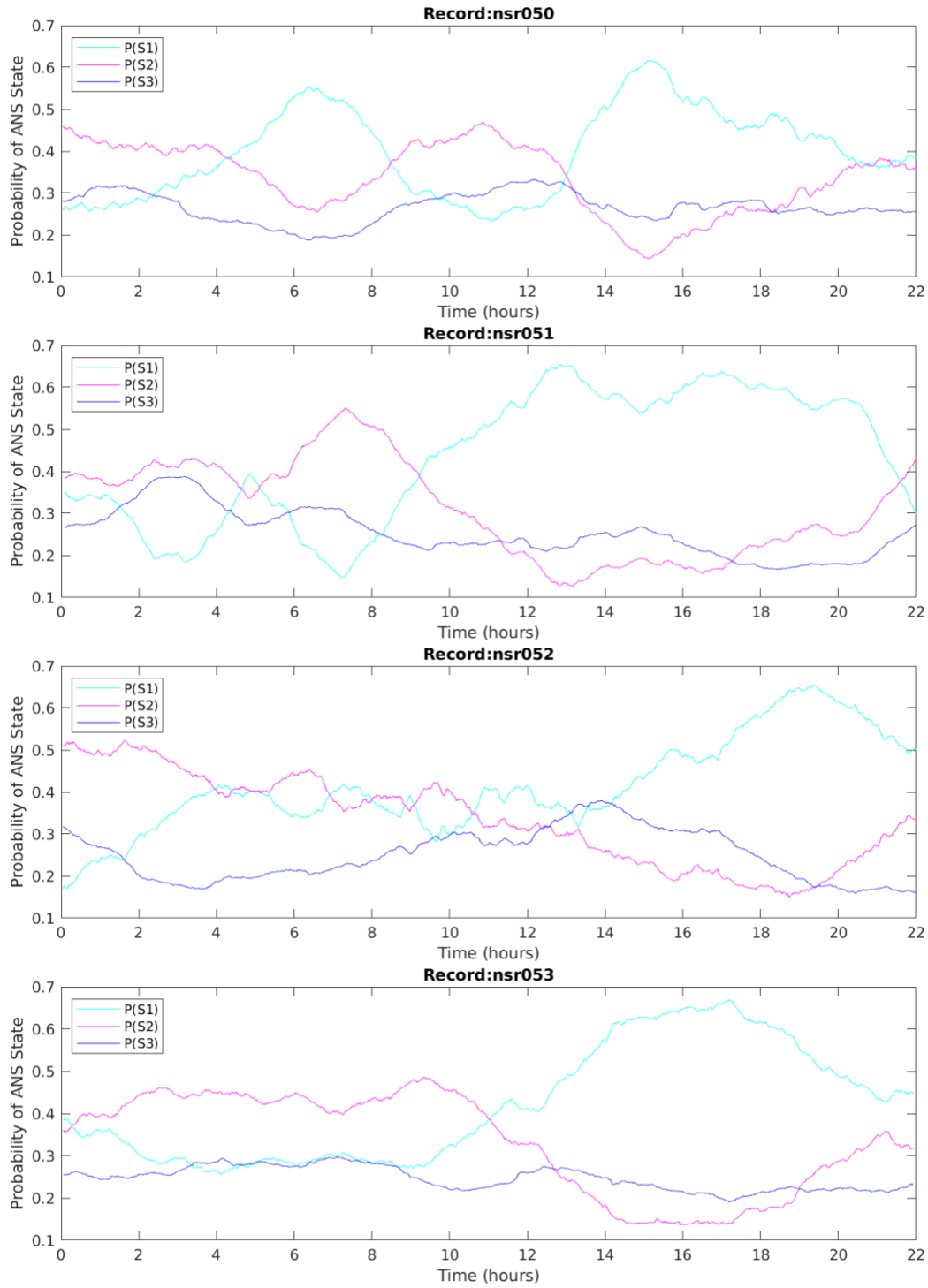


Figure 14 State estimations of the ANS over the course of a day

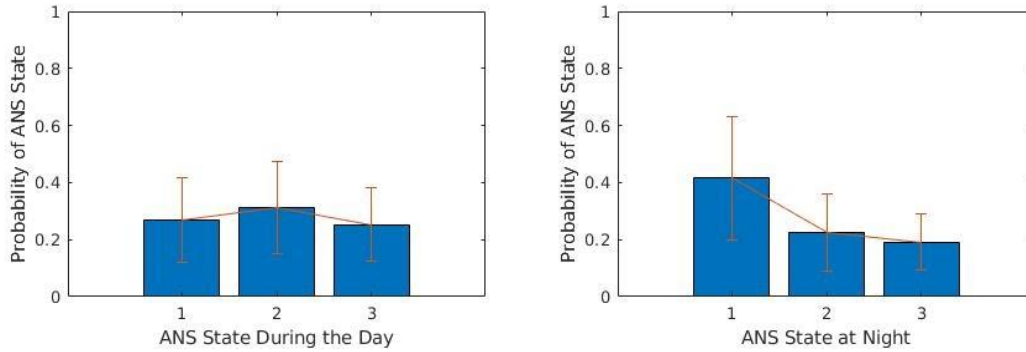


Figure 15 Probability of each of the three possible states dominating for all recordings

Table 4 (Reproduced from Section 2.3)

ANS State	Description
S1	This state signifies <i>parasympathetic predominance</i> where normalized HFRR oscillations, a measure of HRV were larger than HFHR oscillations.
S2	This state signifies <i>parasympathetic and sympathetic coactivation</i> where patterns show non-stationary and low amplitude fast oscillations with phases of acceleration or deceleration within the 10 s intervals.
S3	This state signifies the <i>fading of parasympathetic influence and the activation of the sympathetic nervous response</i> . HFRR and HFHR oscillations are stationary and low amplitude compared to S1.

The HFAM ratio of the values of HFHR and HFRR, normalized by reference values, can show us how well the measurements of HRV fit the model generated by [44]. From Figure 6 we have:

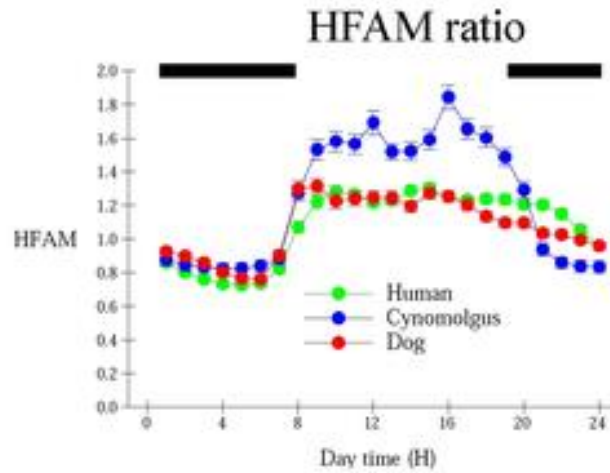


Figure 6 (Reproduced from Section 2.3)

We can extract the HFAM ratio measurements from the state estimation program and plot them over the course of a full day to see how well the measurements accord with the model used for ANS control of HRV. These measurements are shown in Figure 16.

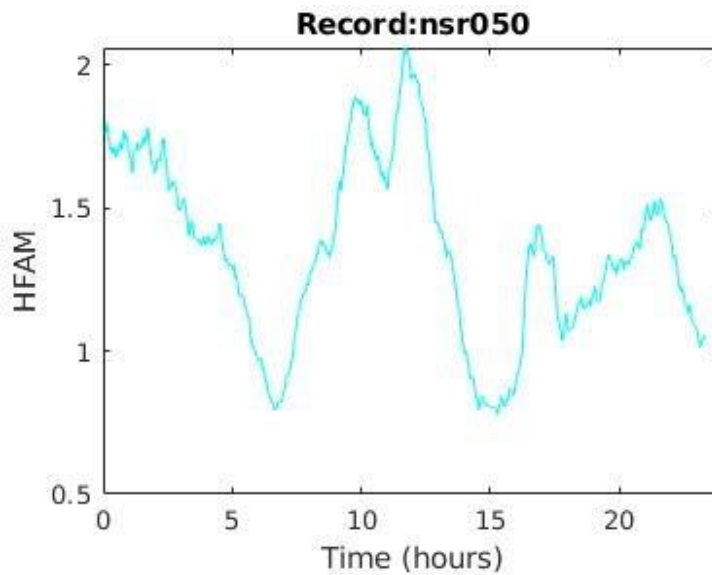


Figure 16 Example of how the HFAM ratio evolves over the time

The qualitative accordance with the model provides confidence that the measurements themselves are valid and typical, and well suited for use in state estimation in this context where a model is used to update the posterior distribution of a state at a given time step.

4.0 Discussion

Some of the same challenges must be faced in any work attempting to use heart rate variability as a single measurement source.

The presence of ectopic heart beats, heart beats that arise from cardiac fibers outside of the sinoatrial node, can cause misleading inter-beat interval measurements. The datasets used for exploratory analysis, [55], [56], were reviewed carefully by clinicians and ectopic beats were manually eliminated from analysis. There are other methods of estimating heart rate given the presence of ectopic beats if careful, manual clinical review is not possible [71]. Another source of variability introduced by signal processing methodologies is the designated choice in peak detection to label heart beats. For example, a first derivative method was used in [16].

Abnormally raised HRV occurs in the elderly and is associated with higher mortality rates. Thus, a method for the state estimation of the autonomic nervous system, and specifically the sympathetic nervous system, may be misled in these situations as discussed in [69]. This risk can be continually monitored though, ancillary to or incorporated into the method of state estimation by repeatedly measuring heart rate fragmentation. [72] The following is a quote from [72] explaining the basis of the methodology:

“These considerations led to the development of a novel approach to the analysis of short-term heart rate variability, termed heart rate fragmentation, accompanied by a set of simple-to-implement statistical metrics. A framework for the proposed approach is the concept that adaptive control of the heartbeat, particularly on short time scales, requires a hierarchy of interacting networks comprising neuroautonomic (especially the parasympathetic) and electrophysiologic

components (sinus node pacemaker cells and their connections to the atrial syncytium). The integrity of these networks allows for their correlated function, evinced in part by the smoothness (fluency) of the output. At the same time, their functionality provides for sufficiently rapid (short-term or high frequency) responsiveness to physiologic stresses, while protecting against excessive volatility on a beat-to-beat basis.”

Frequency analysis of the low frequency and high frequency bands of interest was useful during the exploratory analysis phase but has limitations in its use for clinical decision making. One study noted that the power in each frequency band of interest does not in fact vary between healthy individuals and sick individuals. This phenomenon was specifically observed in patients with chronic or subacute coronary heart disease [25].

While it is assumed in this work that the probability density function of subsequent changes in inter-beat intervals is stationary, in progressive disease states increased non-Gaussianity of HRV can predict mortality [73]. Nonstationarity would need to be considered specifically in conditions studied outside of this work.

Normal HRV is coupled to respiratory rate (the control of heart rate and respiratory rate are two coupled simultaneous stochastic processes), which wasn't taken into account in this attempt at state estimation of the autonomic nervous system [74]. Inaccuracies may arise if, at some time during the measurement interval, the individual being monitored were to consciously control their breath rate in a manner that ignored their current respiratory needs.

The heart rate control system responds to all external and internal regulatory cues to maintain life with respect to stressful stimuli (allostasis). Thus, the signals it emits are a rich source of information for monitoring purposes, especially given the widespread use of heart rate

monitoring equipment in 2020. What can be learned from normal monitoring? Specifically, this work is useful for normal monitoring in situations with a high risk of traumatic stress infliction.

The ANS controls heart rate and heart rate variability. Thus, changes in heart rate indicate a change in the activity of the autonomic nervous system. There is evidence already that the autonomic nervous system becomes dysregulated in PTSD sufferers. The dysregulation causes a lot of problems such as: overreaction long after trauma, irregular sleep patterns, and extreme difficulty with focus during the day. The changes in heart rate at various times of the day look significantly different in PTSD sufferers compared to those without it.

Given the tool provided by this research, clinicians will be able to characterize the extent of the damage to the autonomic nervous system in PTSD sufferers compared to those without PTSD. This clinical usefulness extends to disorders including anxiety, depression, and chronic illnesses like diabetes and lupus. In the long term, characterizing a problem is the start to solving a problem. The ability to estimate the state of the autonomic nervous system over time enables the characterization of the problem in individuals in a way that has not been done previously. The ultimate goal would be to "fix" the problems PTSD sufferers and others experience due to autonomic nervous system dysregulation.

Psychiatric medicine encounters physiological problems faced by patients with mental health diagnoses. Beyond the presenting diagnostic symptoms, individuals experience sleep disruption, among other autonomic driven problems. The symptoms that arise unrelated to the primary diagnostic symptoms interfere with the individual's daily activities to the extent that it actually worsens the presenting psychiatric problem.

The current state of the art in diagnostics experienced by the majority of patients today is to address the mental health problem and target each of the physiological symptoms which may

present themselves due to the dysregulation of the autonomic nervous. Each physiological problem is targeted on a symptom-by-symptom basis with no use of feedback on how well the underlying problem is being addressed when the driver of the source of the symptoms is autonomic nervous system. The call to action which motivated this research was the call to enable the study the dysregulation of the autonomic nervous system that could provide feedback mechanisms during treatment.

A reminder must be added. The human stress response is an adaptive rather than maladaptive system if a person is not saturated by inflammatory signals for prolonged periods of time. The human stress response enables an individual to be adaptive to changes in the environment, cyclical and spontaneous as well as normal and anomalous. Individuals are particularly good at anticipating cyclical changes in both the internal and the external environments yet are also good at being ready for non-cyclical changes in the environment, where the stress response activates systems for alertness and energy usage when a stressor is detected. The benefit of having a working stress response is the maximization of alertness for normal active times and to activate restorative processes in inactive times.

5.0 Conclusions

The particle filter methodology is effective in the task of estimating the state of the autonomic nervous system using heart rate variability. The preliminary report exploration of the methodology showed that the particle filter could estimate the state of the ANS with [insert certainty]. This result was achieved with a state transition transformation of particles based on a pharmacological model of ANS control of HRV and a measurement likelihood based on the multivariate normal distribution with a noise amplitude set to consider all possible sources of noise rather than directly developing a sensor model. Improvements to the certainty with which the state of the ANS can be estimated can be made with a more finely tuned measurement likelihood function.

The most interesting result was the demonstration that, during the daytime, healthy controls are quite often in the S2 state when the parasympathetic and the sympathetic nervous systems are coactivated. The result leads to curiosity about whether the coactivation state can be further subdivided into physiologically relevant states. Exploration of this concept will certainly require experimentation with a multi fractal model of heart rate variability control in order to capture the effects of multi scale, coupled physiological control mechanisms.

Further validation of clinical usefulness is required from a human factors engineering standpoint. The research question that still needs to be asked and answered relative to the work done in this thesis is, “How can the continually changing state of the ANS be displayed to give clinicians the most helpful information?”

In future work, we want to modify the state transition function and the measurement likelihood function to gain the resolution of more hidden states. Given a more complex, higher

dimension of states, more work must be done in the knowledge representation domain. The question is raised, “How can we encode multidimensional experiential knowledge in a Bayesian graphical form?”

Functionally, the work of establishing a state estimation methodology provides information about the frequency and duration of stress response activations as well as insight into the amount of time spent in a rest and digest state recovering. Given that the two states are often coactivated during the day, further resolution into that physiological state is the next goal based on this work.

Appendix A Data Summary

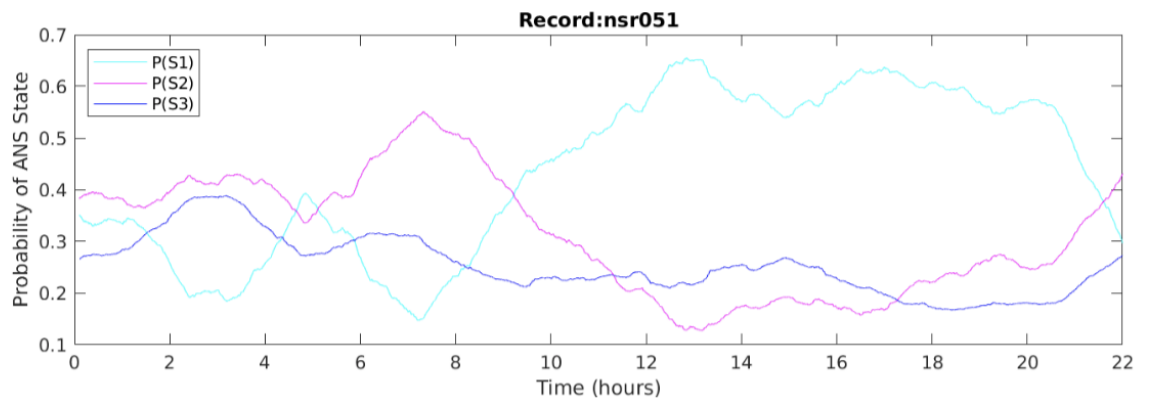
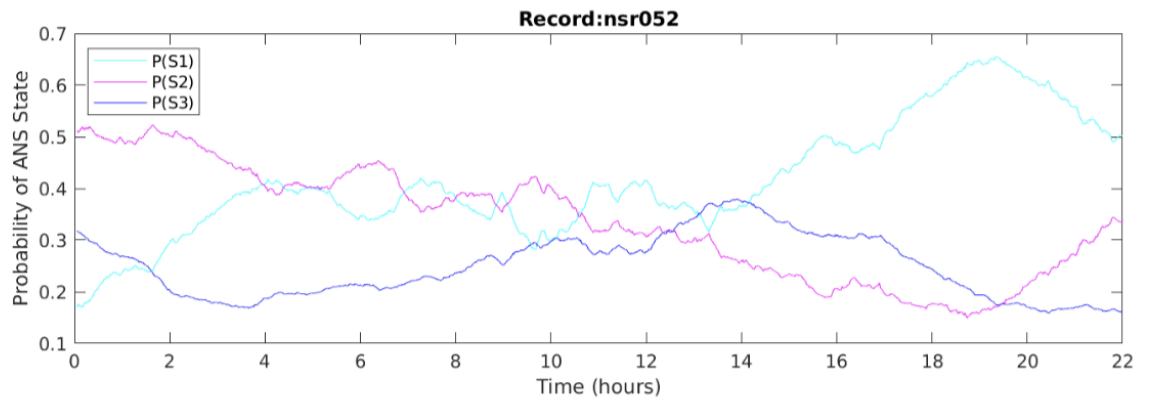
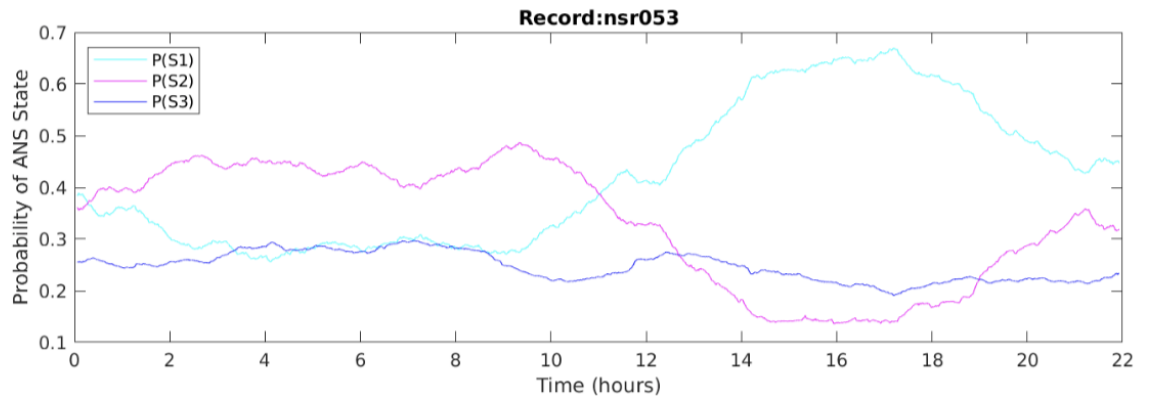
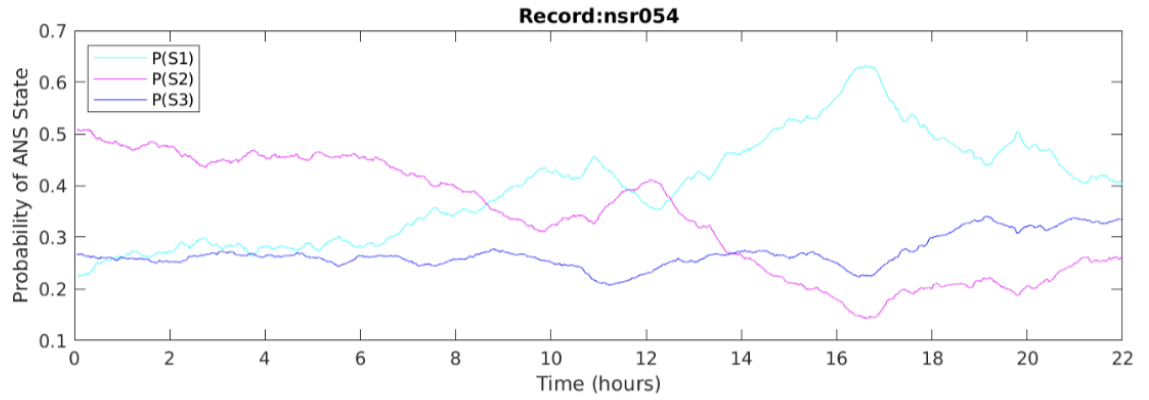
Appendix Table 1 Summary of ECG data

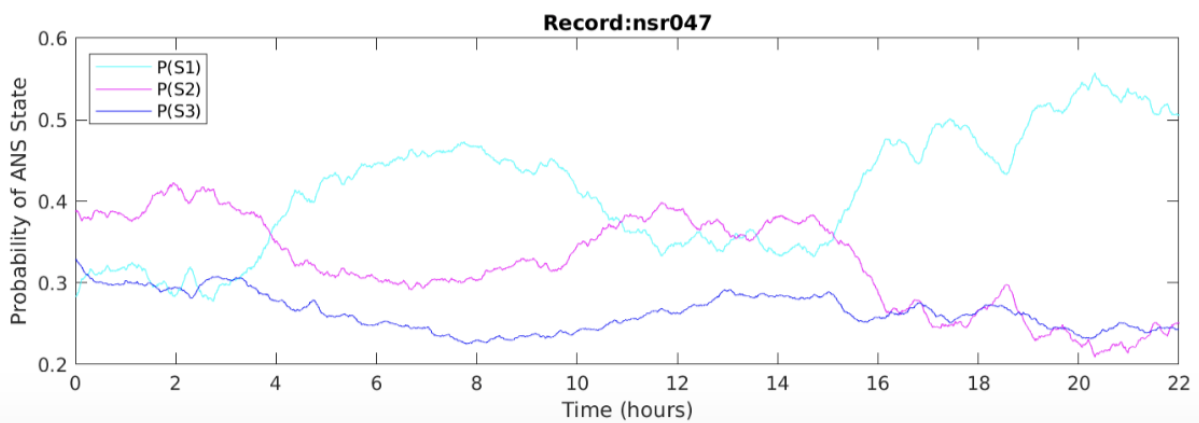
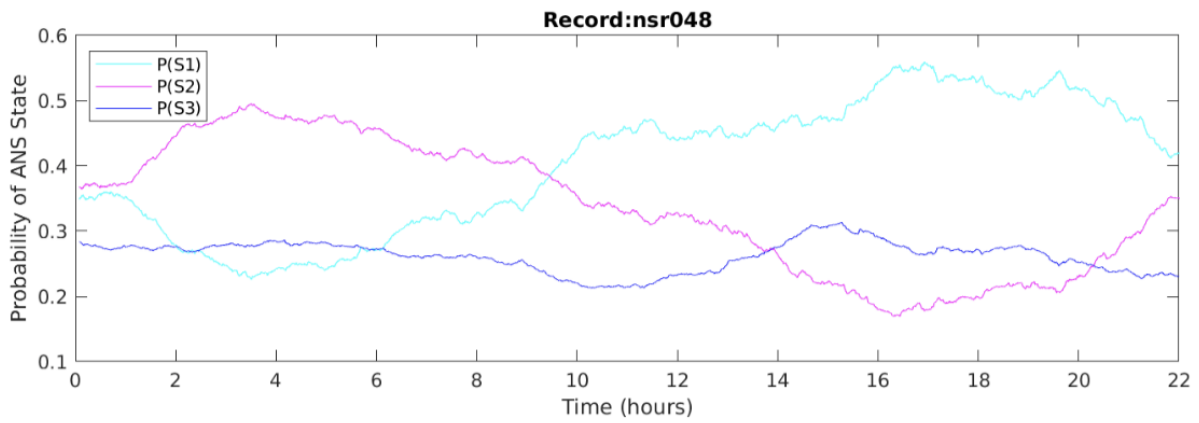
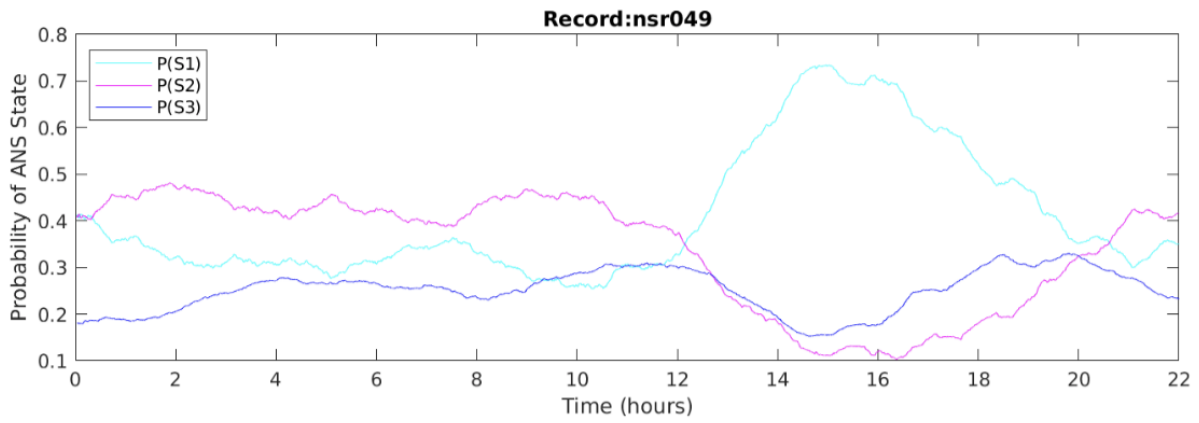
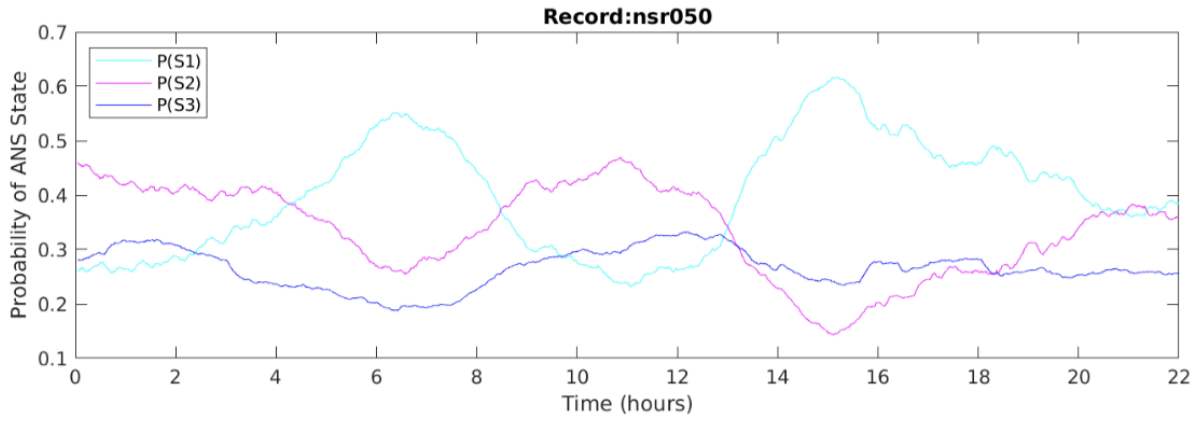
Record	Duration (s)	Skewness	Kurtosis	Mean HR (bpm)	SDHR	Mean HRV	SDNN	LF PWR	HF PWR	LFHF Ratio
16265	80062	0.404	2.497	76	16.2	0.095	0.0179	2.55E-05	4.25E-06	5.99
16272	84396	-0.630	2.930	66	11.0	0.118	0.0172	1.18E-05	1.90E-06	6.19
16273	74348	0.097	3.220	73	12.4	0.102	0.0157	1.02E-05	4.07E-06	2.50
16420	77759	-0.052	2.962	79	10.8	0.095	0.0130	6.13E-06	1.83E-06	3.35
16483	76099	0.328	2.644	82	10.1	0.089	0.0098	7.16E-06	5.94E-07	12.04
16539	84668	0.791	4.571	78	12.8	0.096	0.0162	3.60E-05	1.73E-05	2.09
16773	78141	0.718	5.939	63	15.5	0.108	0.0155	3.19E-05	8.82E-06	3.62
16786	84052	-0.039	2.137	73	10.2	0.106	0.0148	1.30E-05	3.89E-06	3.35
16795	74734	0.818	2.940	70	16.8	0.106	0.0253	1.99E-05	7.33E-06	2.72
17052	76400	0.265	2.722	69	12.3	0.115	0.0196	1.52E-05	7.99E-06	1.90
17453	74482	0.742	3.789	81	10.7	0.090	0.0105	1.16E-05	2.44E-06	4.77
18177	80903	0.787	3.861	87	13.9	0.082	0.0094	7.71E-06	1.48E-06	5.21
18184	75230	0.775	5.495	82	10.7	0.091	0.0117	1.60E-05	5.13E-06	3.12
19088	72613	0.448	2.878	82	13.6	0.089	0.0123	1.09E-05	3.26E-06	3.34
19090	69234	-0.078	2.241	71	8.5	0.109	0.0133	1.22E-05	2.73E-06	4.46
19093	72236	-0.088	2.815	63	8.7	0.122	0.0158	4.22E-05	7.22E-06	5.85
19140	72038	0.527	3.593	81	10.7	0.092	0.0115	1.34E-05	4.26E-06	3.15
19830	75964	0.488	3.319	87	16.5	0.080	0.0112	3.29E-06	5.32E-07	6.18
nsr001	81191	0.624	2.374	79	16.9	0.096	0.0195	6.20E-06	1.52E-06	4.06
nsr002	84471	0.502	2.113	80	13.5	0.096	0.0179	4.03E-06	3.11E-07	12.97
nsr003	85220	-0.711	2.927	69	8.5	0.113	0.0117	3.07E-06	3.58E-06	0.86
nsr004	83461	0.037	1.914	71	14.8	0.109	0.0233	1.02E-05	5.30E-06	1.92
nsr005	86232	0.248	2.179	82	24.3	0.101	0.0288	2.08E-05	2.51E-06	8.28
nsr006	83711	-0.605	2.651	75	16.9	0.108	0.0190	6.36E-06	1.15E-06	5.52
nsr007	85343	-0.321	2.473	76	9.9	0.101	0.0134	1.80E-06	6.26E-07	2.88
nsr008	86231	0.302	2.036	75	13.5	0.104	0.0190	1.71E-05	3.71E-06	4.61
nsr009	86232	0.561	3.302	72	14.2	0.102	0.0180	1.30E-05	2.36E-06	5.52
nsr010	82857	-0.186	2.258	70	16.5	0.110	0.0248	3.37E-05	2.73E-06	12.32
nsr011	86231	0.395	1.983	81	12.7	0.095	0.0157	2.03E-06	9.41E-07	2.16
nsr012	86457	-0.179	2.472	69	14.2	0.114	0.0211	1.21E-05	1.73E-06	6.99

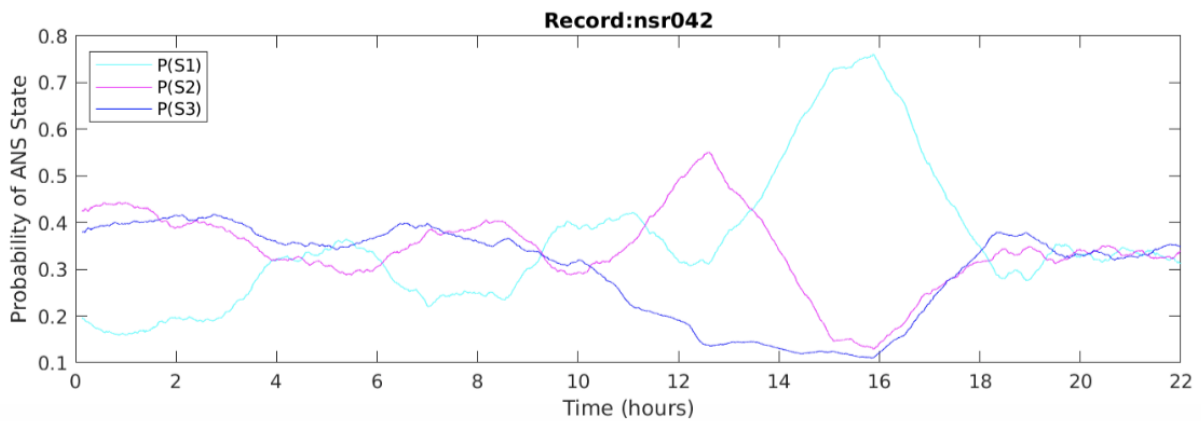
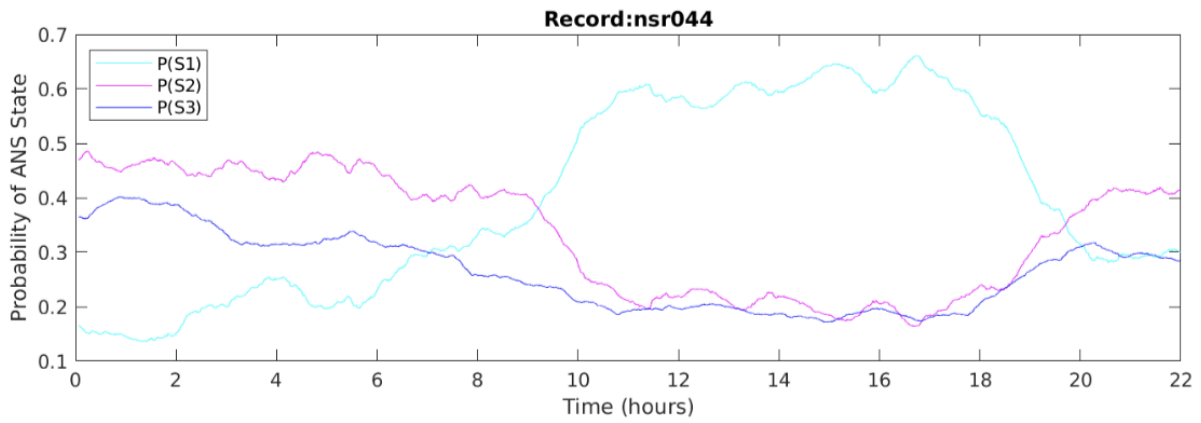
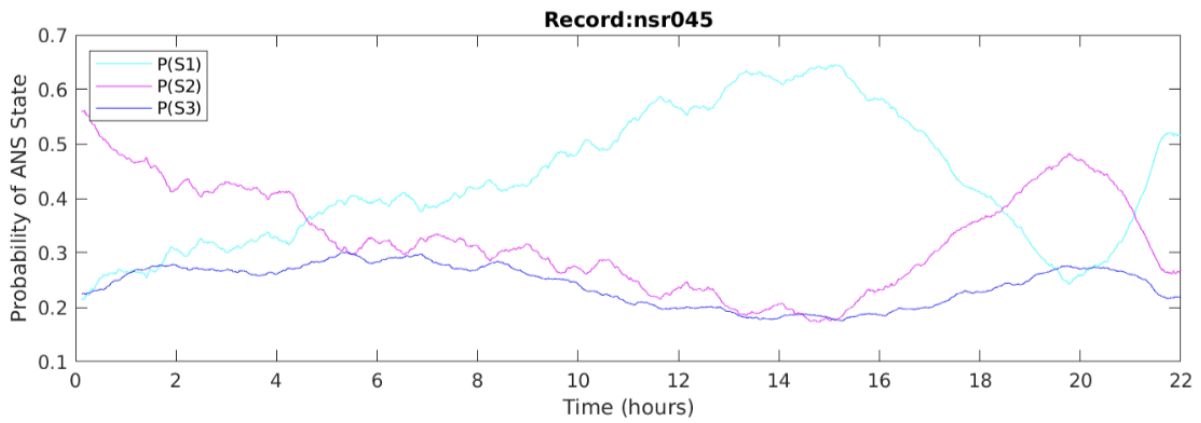
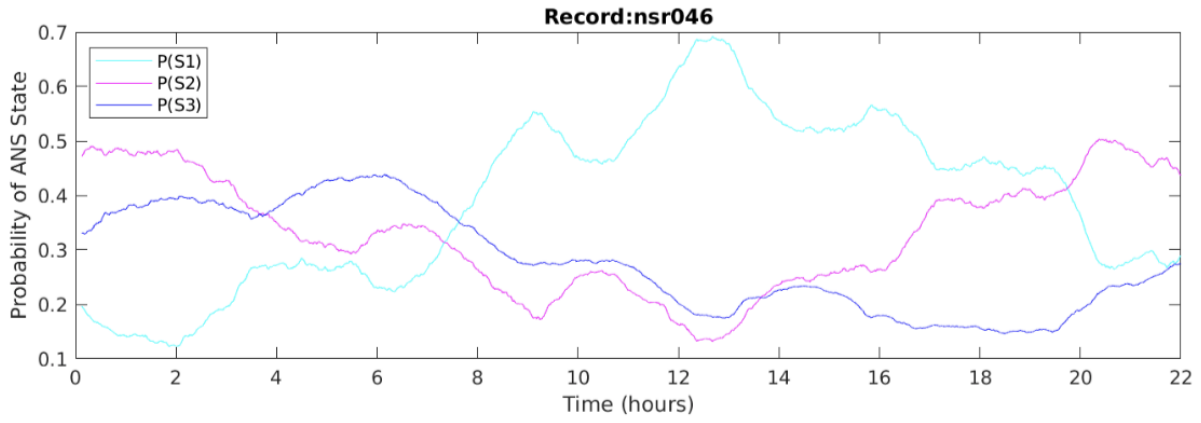
nsr013	84865	-0.028	1.887	82	18.3	0.093	0.0220	6.19E-06	8.69E-07	7.12
nsr014	86457	0.555	2.960	79	13.9	0.100	0.0201	2.87E-05	3.44E-05	0.83
nsr015	86230	-0.101	2.045	77	10.4	0.102	0.0134	4.07E-06	7.26E-07	5.61
nsr016	86457	-0.019	2.074	79	11.6	0.101	0.0143	2.56E-06	1.06E-06	2.42
nsr017	86231	0.275	2.628	71	12.5	0.111	0.0192	2.44E-05	8.97E-06	2.72
nsr018	86147	0.753	3.447	78	12.5	0.102	0.0172	1.93E-05	3.67E-06	5.26
nsr019	86231	-0.210	1.890	86	14.4	0.093	0.0159	1.94E-06	8.44E-07	2.30
nsr020	84206	0.913	3.512	98	15.1	0.082	0.0147	6.80E-06	8.14E-07	8.35
nsr021	86232	0.630	2.460	72	11.5	0.107	0.0185	6.43E-06	2.50E-06	2.57
nsr022	85496	0.045	2.877	58	6.9	0.133	0.0153	2.11E-05	7.27E-06	2.90
nsr023	86457	0.028	1.962	78	11.6	0.100	0.0150	3.95E-06	1.79E-06	2.21
nsr024	86231	1.056	2.999	70	19.6	0.106	0.0309	2.02E-05	8.77E-06	2.30
nsr025	86329	1.185	5.518	92	12.2	0.087	0.0123	2.64E-05	7.44E-06	3.55
nsr026	86457	0.862	2.749	81	15.4	0.093	0.0183	7.58E-07	2.89E-07	2.62
nsr027	86032	-0.283	1.728	82	17.8	0.099	0.0198	4.19E-06	2.44E-06	1.71
nsr028	86081	0.170	2.302	77	13.4	0.104	0.0152	1.09E-05	1.67E-06	6.50
nsr029	86457	0.586	2.428	89	21.1	0.092	0.0223	1.83E-05	3.19E-06	5.72
nsr030	86226	-0.135	1.986	75	13.9	0.105	0.0188	1.95E-06	1.02E-06	1.92
nsr031	86457	0.401	2.407	83	13.1	0.096	0.0157	1.53E-05	2.13E-06	7.20
nsr032	86457	-0.081	2.203	75	12.0	0.106	0.0159	2.18E-06	1.28E-06	1.70
nsr033	82631	0.086	2.485	59	9.4	0.132	0.0195	2.12E-05	2.70E-06	7.83
nsr034	85481	-1.086	4.289	71	14.9	0.110	0.0197	8.94E-06	1.03E-06	8.69
nsr035	86231	1.003	4.234	84	11.5	0.094	0.0145	7.80E-06	2.61E-06	2.99
nsr036	84888	-0.189	2.355	83	11.7	0.092	0.0115	3.64E-06	3.57E-06	1.02
nsr037	82631	0.368	2.322	69	12.0	0.116	0.0174	4.01E-06	8.58E-07	4.67
nsr038	76940	0.081	2.230	82	15.7	0.097	0.0192	1.08E-05	2.58E-06	4.17
nsr040	85001	0.094	2.026	83	14.1	0.093	0.0170	2.07E-06	1.24E-06	1.67
nsr041	84662	0.032	2.554	80	9.2	0.099	0.0102	2.59E-06	1.37E-06	1.89
nsr042	86457	0.070	2.410	76	12.7	0.101	0.0167	2.14E-05	5.39E-06	3.97
nsr043	84739	0.193	2.412	79	14.7	0.102	0.0147	3.18E-06	6.43E-07	4.94
nsr044	86231	0.459	2.487	82	13.9	0.096	0.0173	5.64E-06	2.80E-06	2.01
nsr045	86259	0.180	2.174	74	12.1	0.107	0.0164	7.73E-06	5.31E-06	1.46
nsr046	82857	-0.156	2.230	70	14.8	0.111	0.0219	8.00E-06	1.96E-06	4.07
nsr047	86575	-0.132	2.823	79	13.2	0.092	0.0110	1.45E-05	2.06E-06	7.02
nsr048	87194	0.821	3.265	84	15.7	0.089	0.0153	1.92E-05	1.34E-06	14.33
nsr049	86456	0.176	2.175	74	12.5	0.106	0.0181	1.95E-05	1.96E-06	9.91
nsr050	86457	-0.059	2.861	89	15.6	0.082	0.0106	6.44E-06	6.75E-07	9.54
nsr051	86457	0.241	2.295	75	17.3	0.106	0.0245	2.58E-05	7.82E-06	3.30
nsr052	86457	0.530	2.926	88	18.9	0.083	0.0157	4.22E-06	4.28E-07	9.86
nsr053	81223	0.513	2.412	73	14.3	0.106	0.0198	1.86E-05	3.56E-06	5.21
nsr054	83754	0.518	2.933	87	17.4	0.079	0.0105	1.40E-05	1.90E-06	7.37

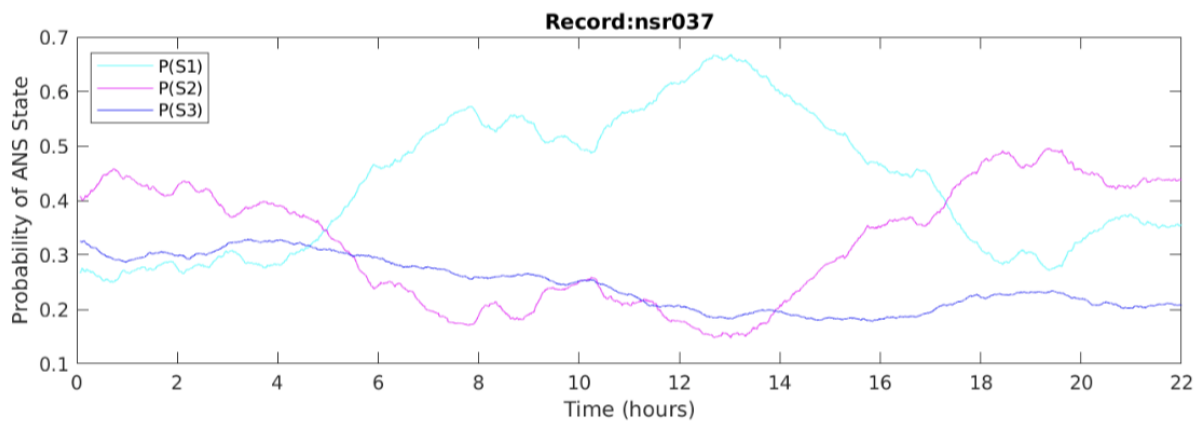
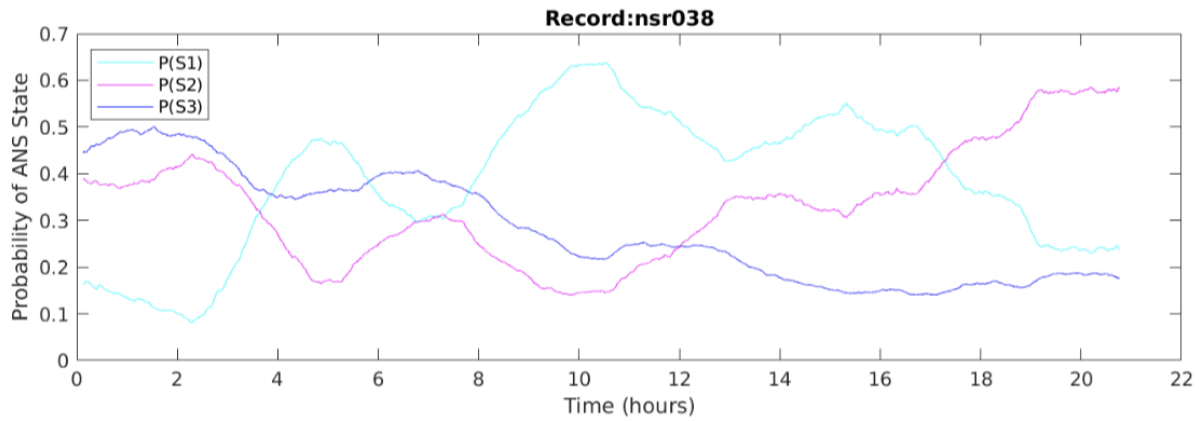
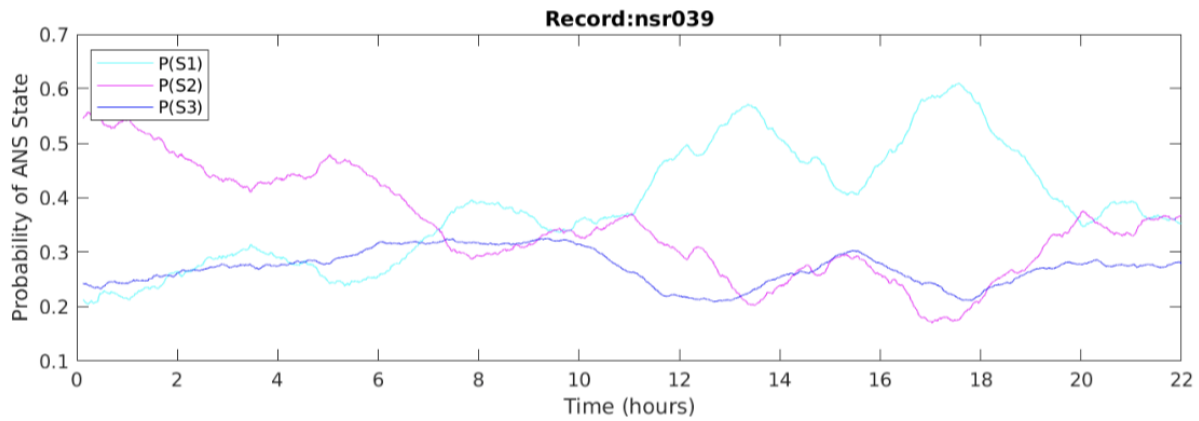
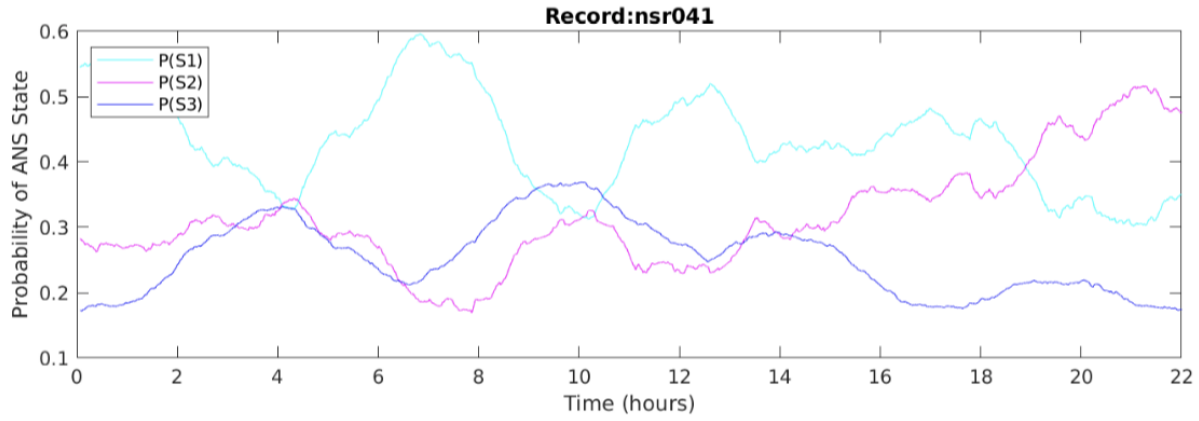
Appendix B State Estimation Results

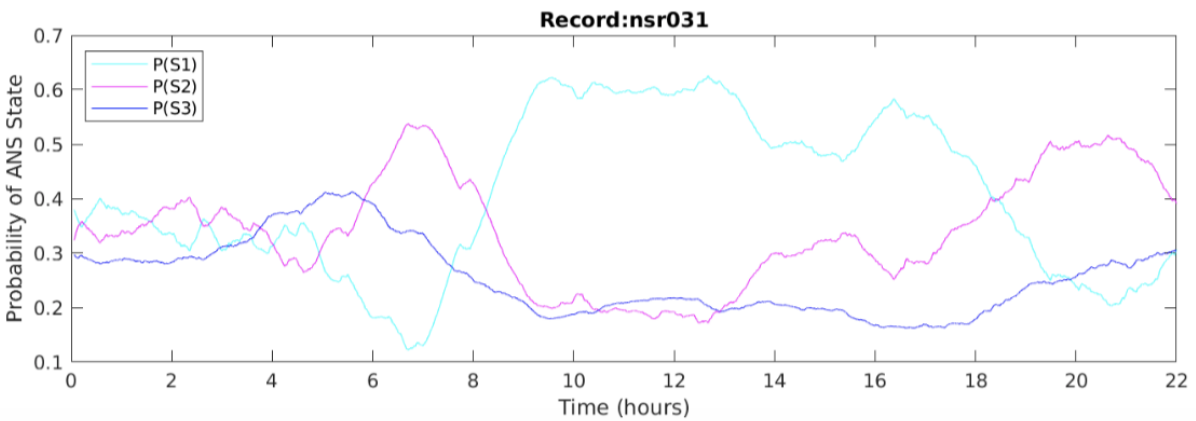
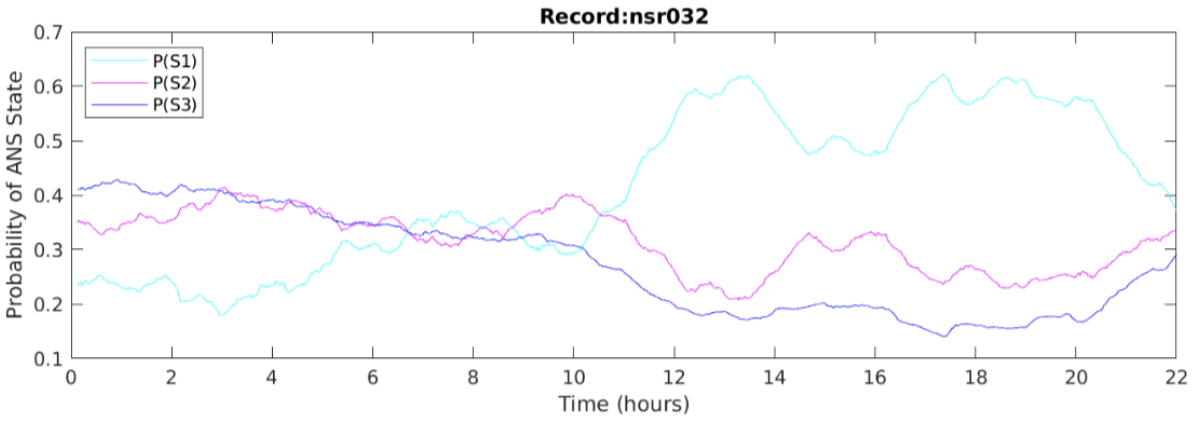
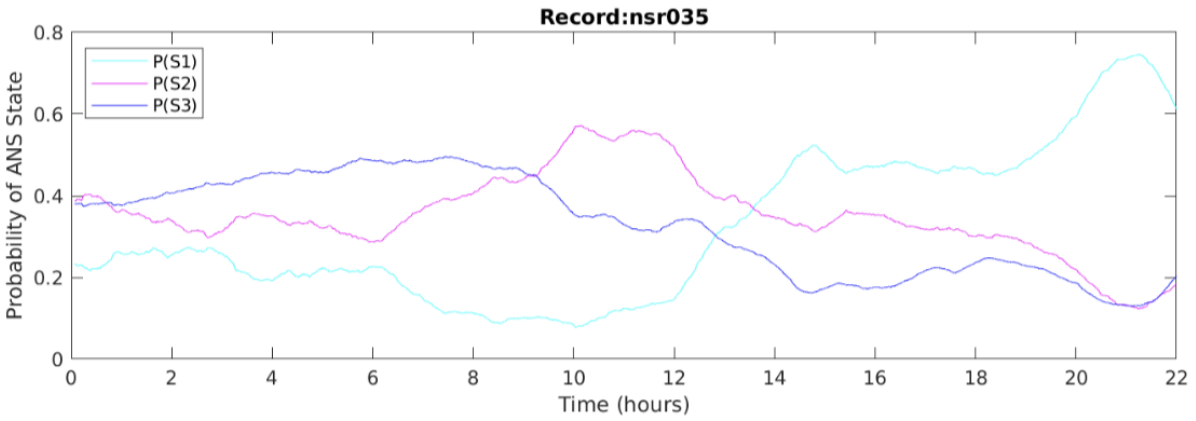
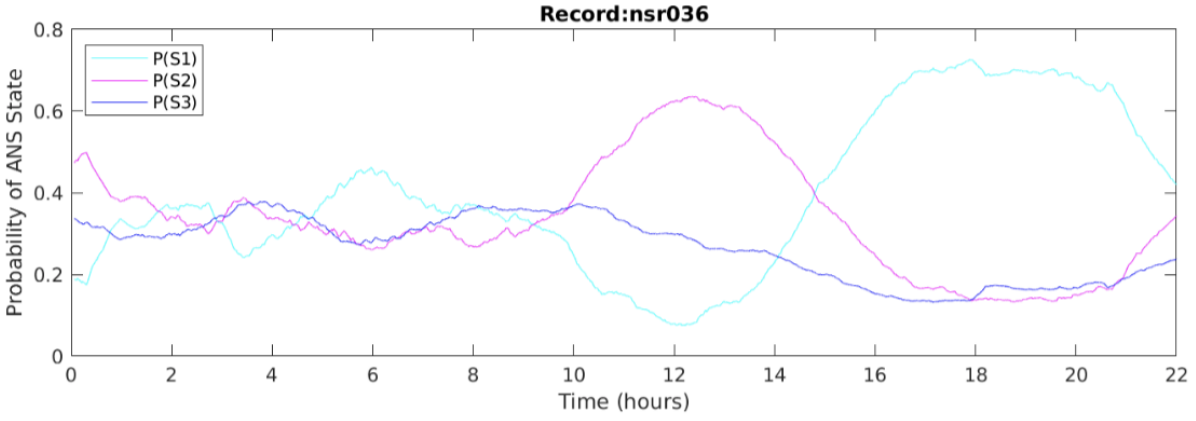
(See next page.)

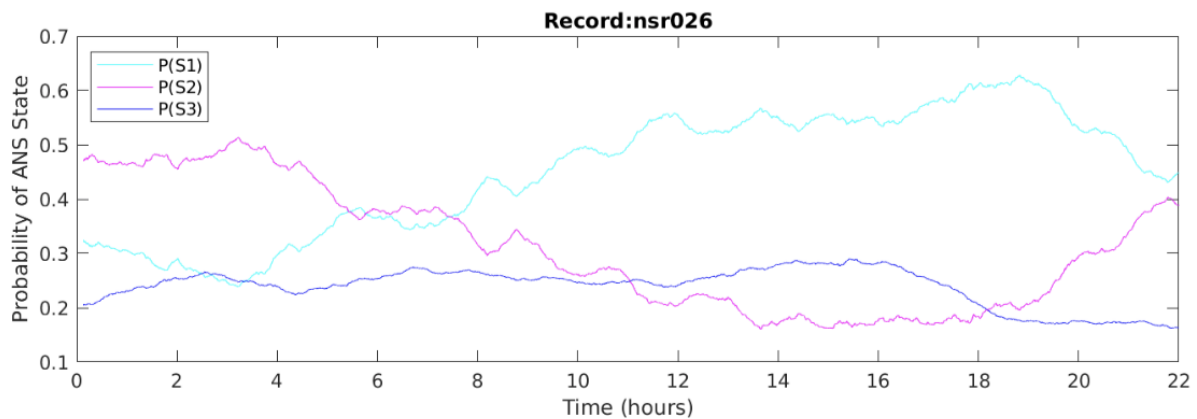
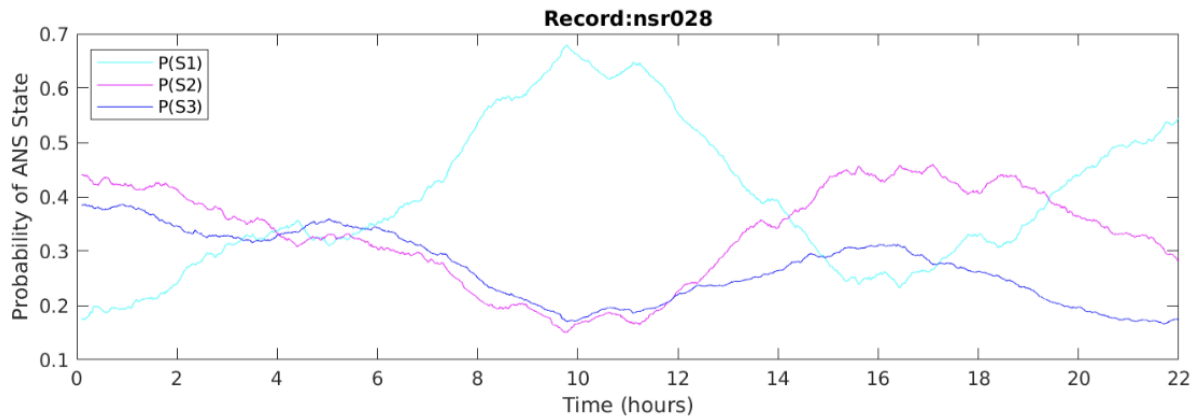
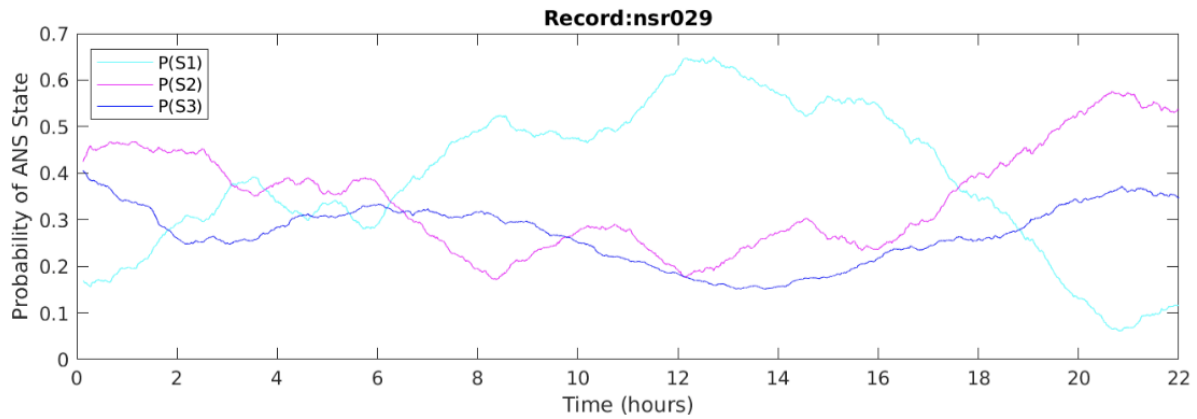
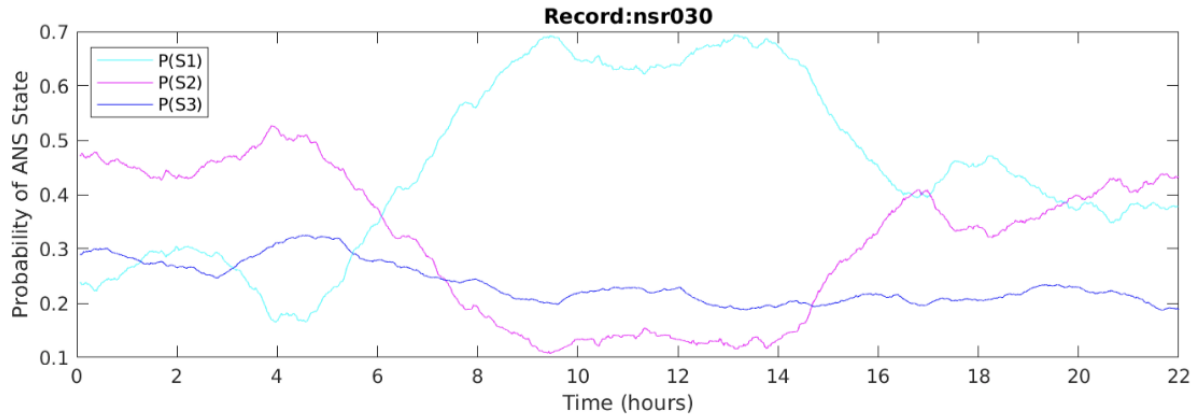


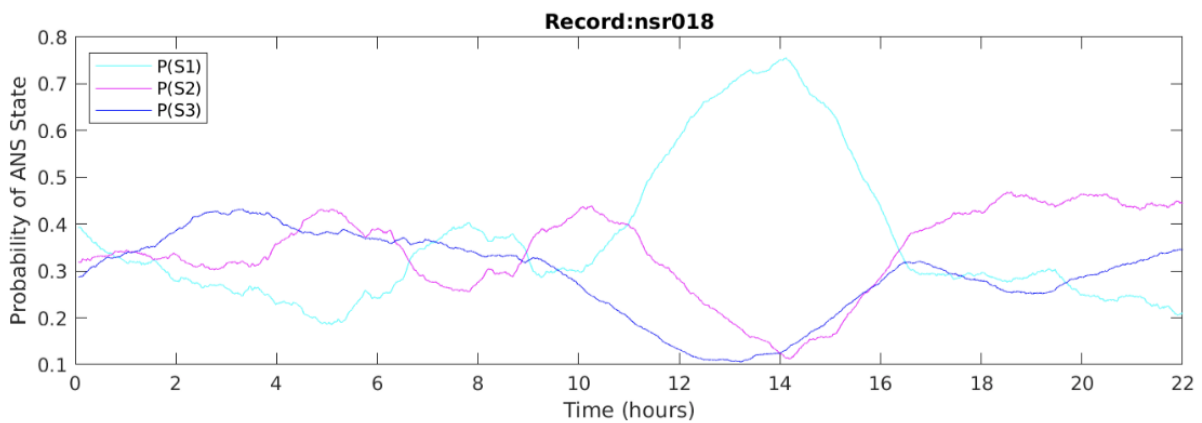
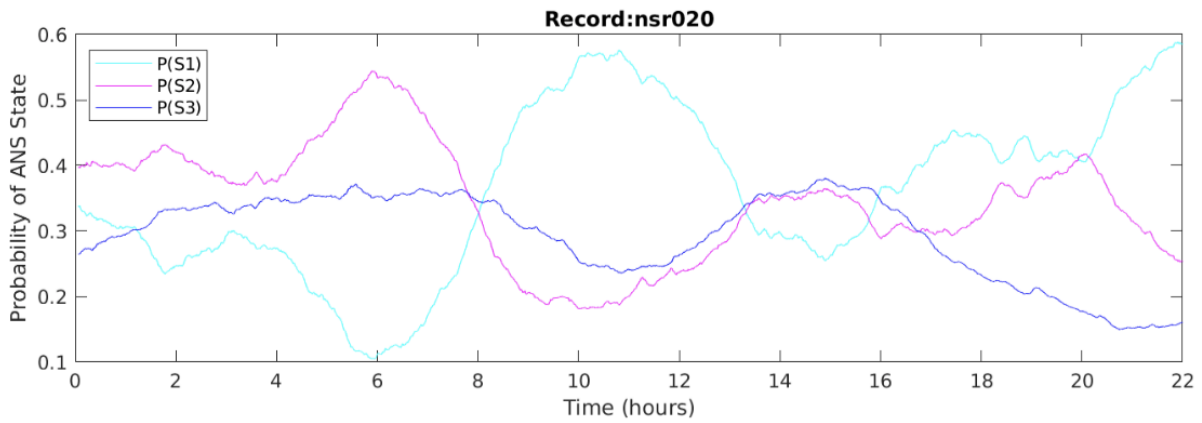
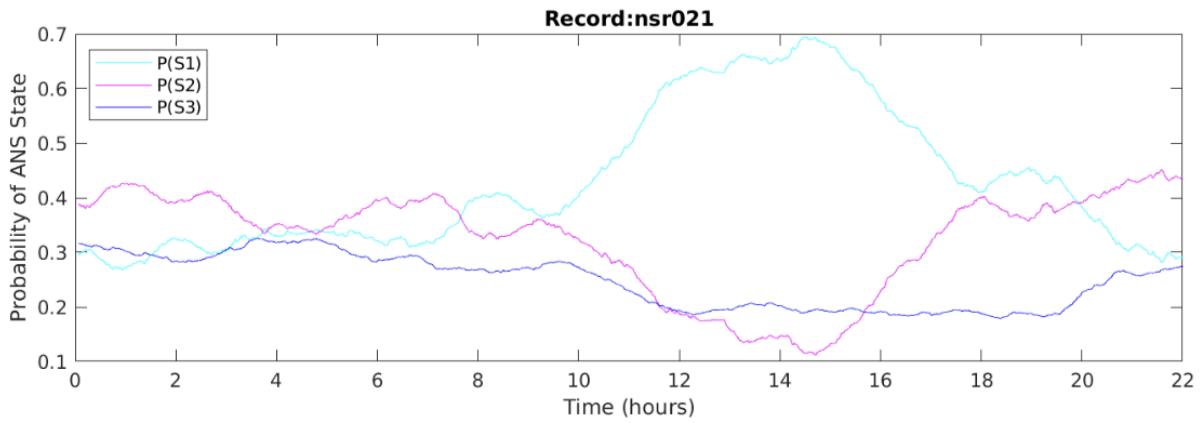
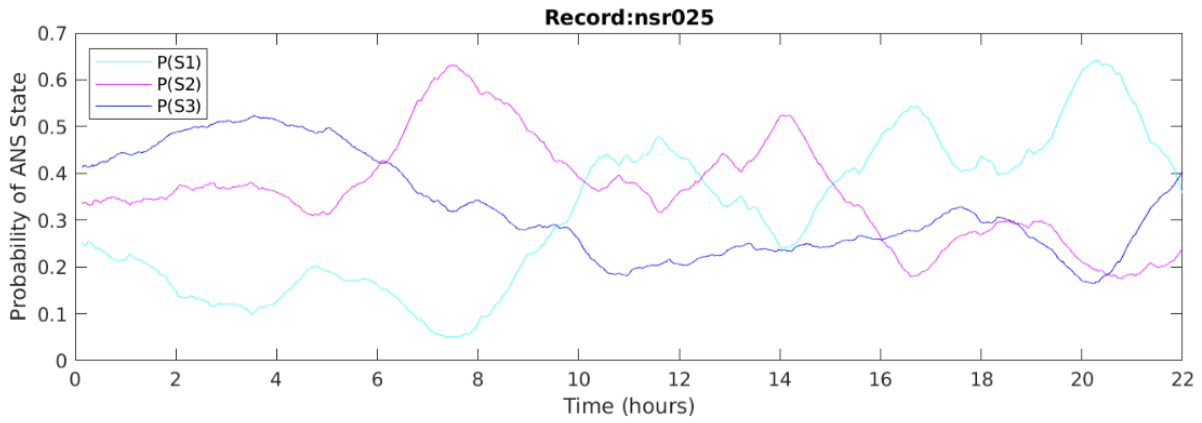


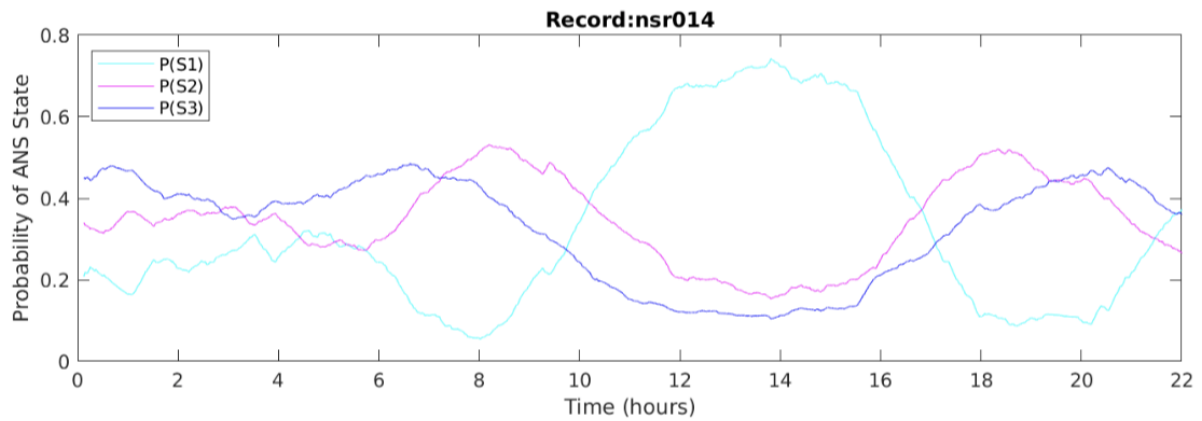
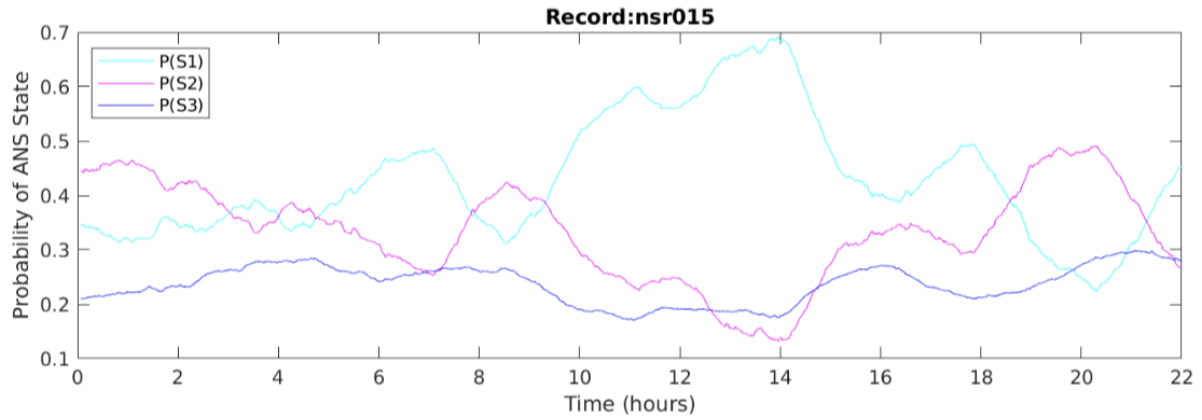
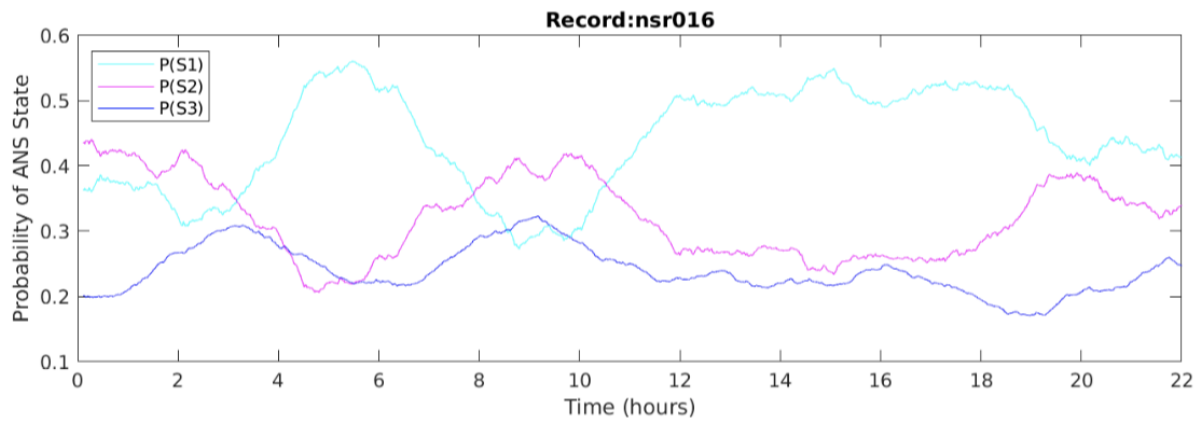
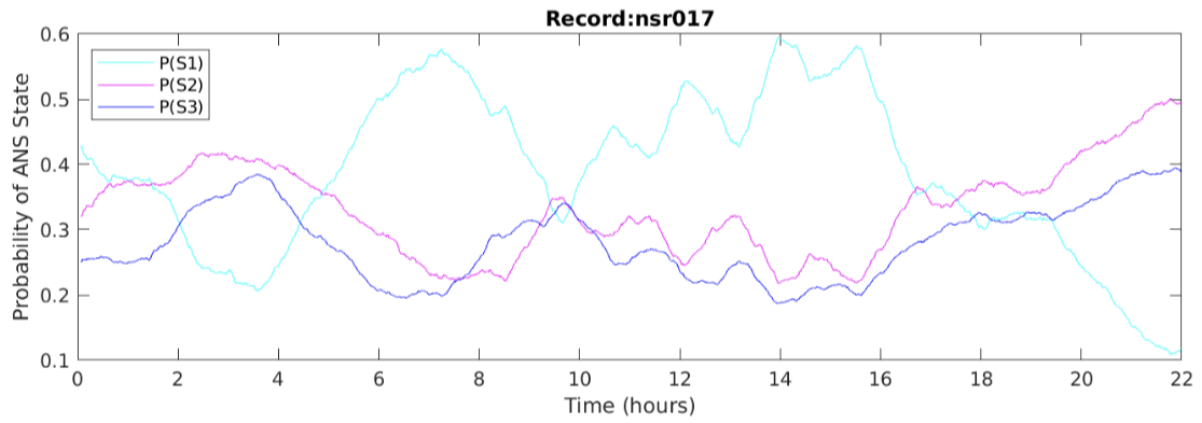


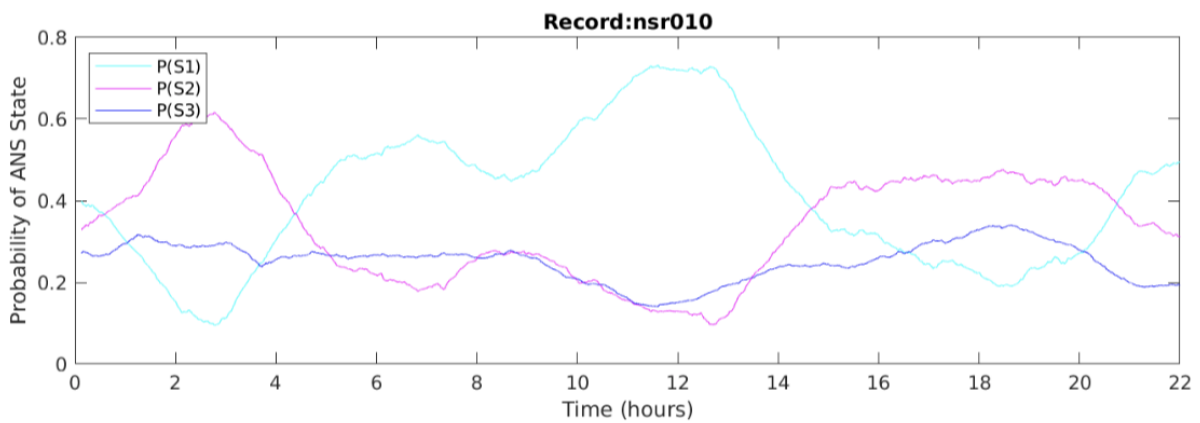
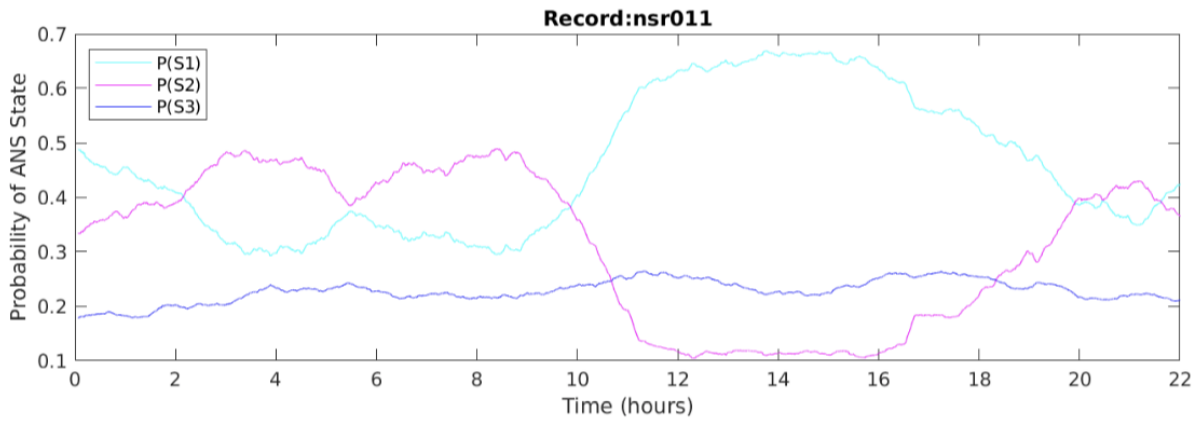
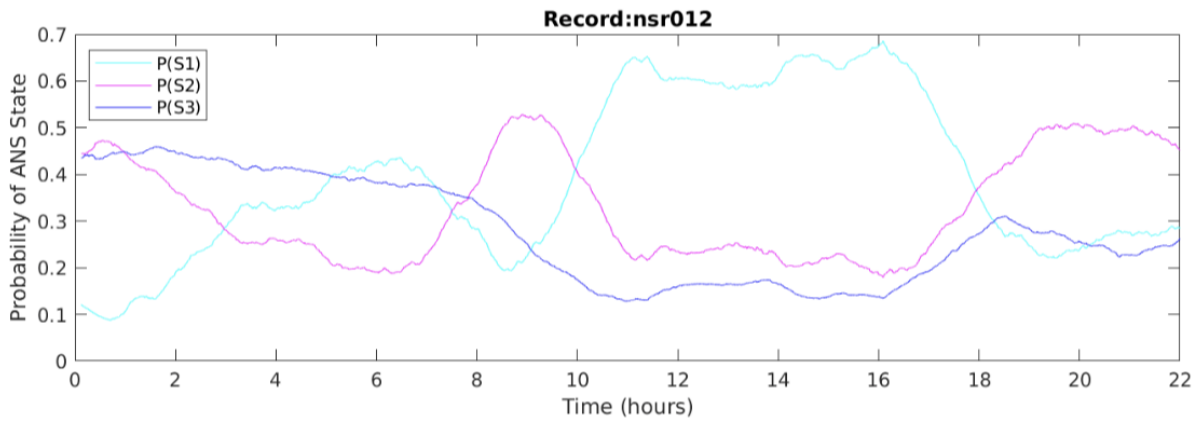
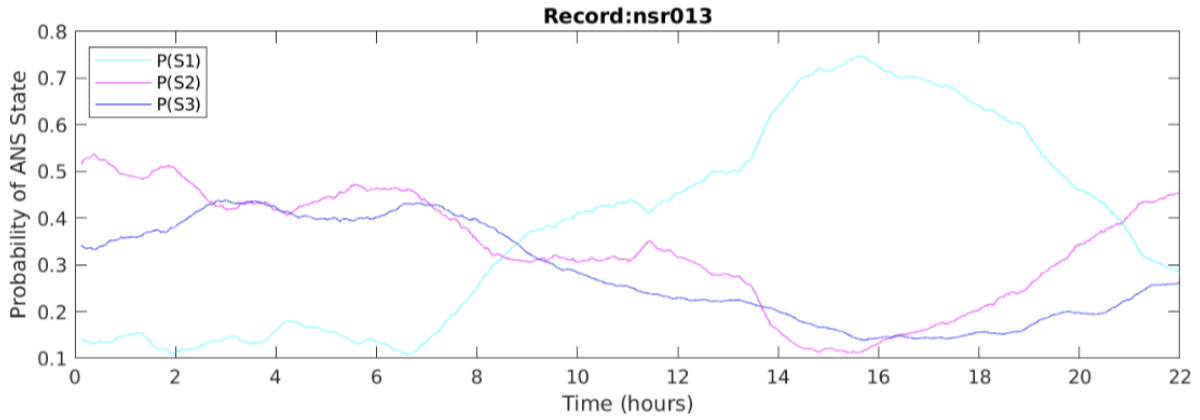


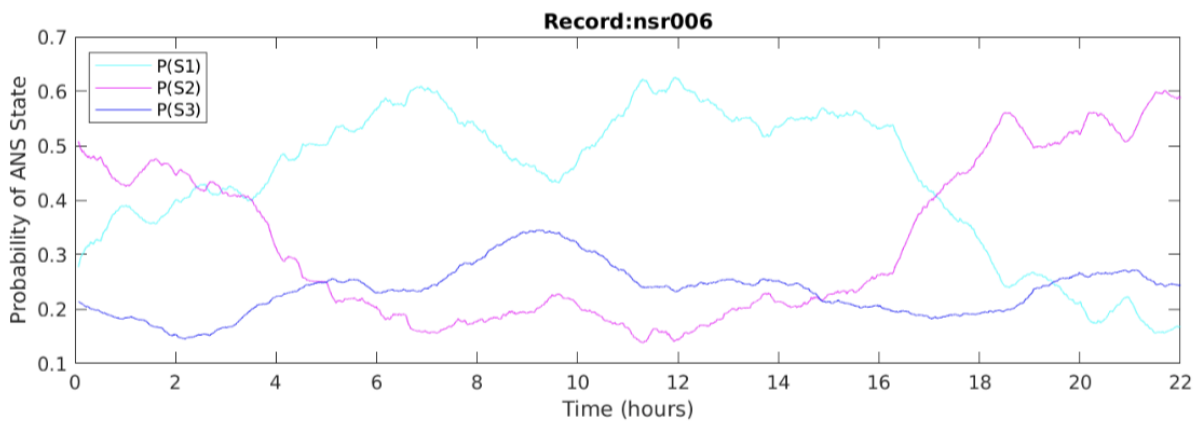
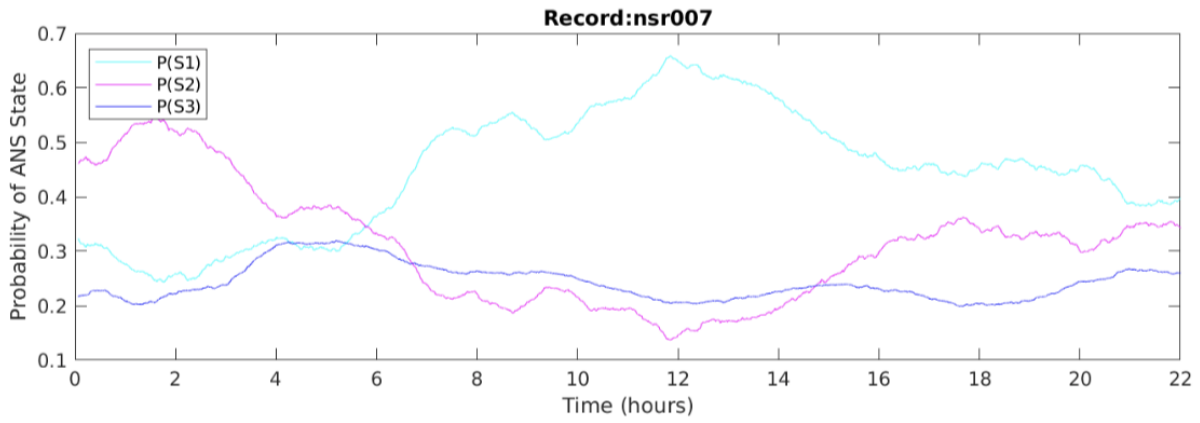
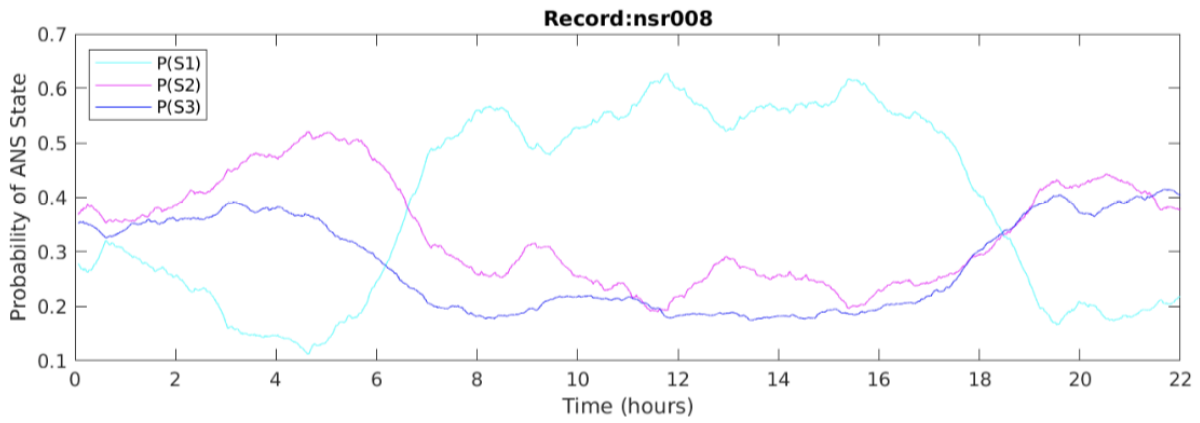
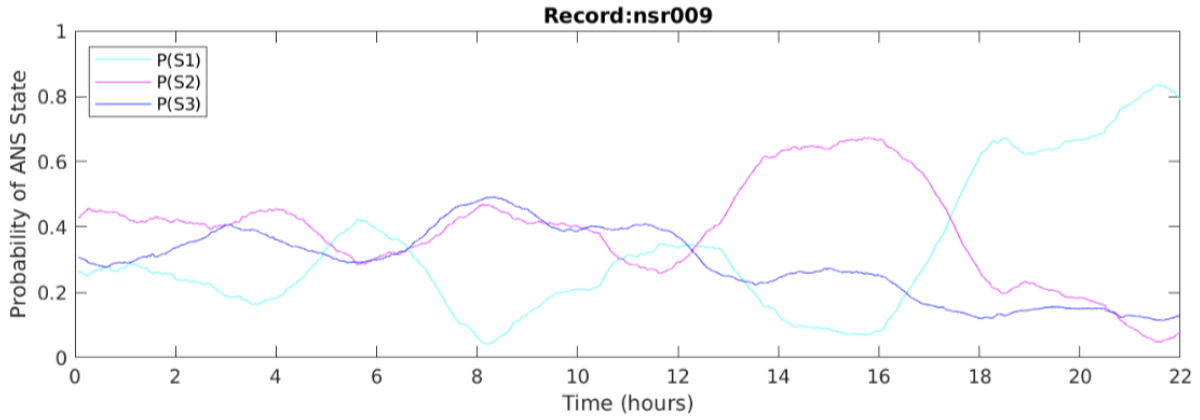


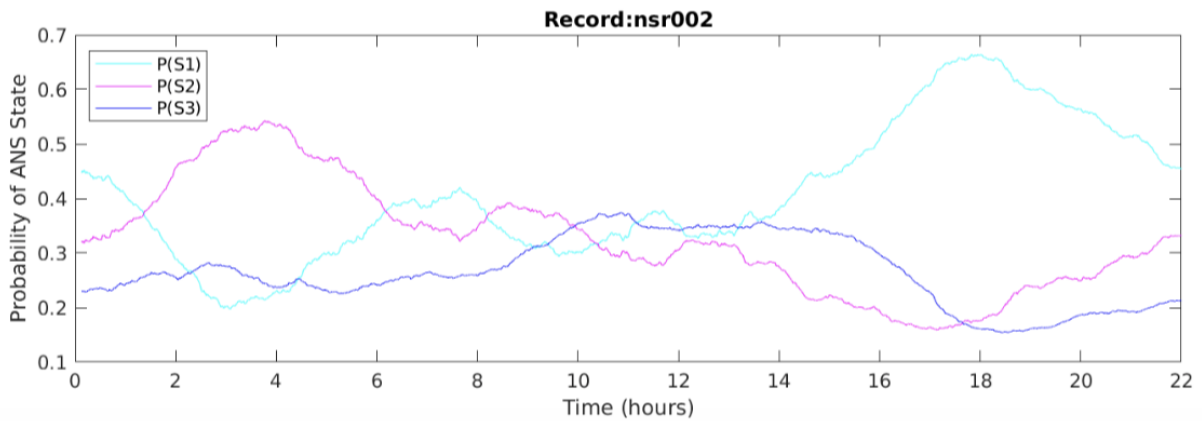
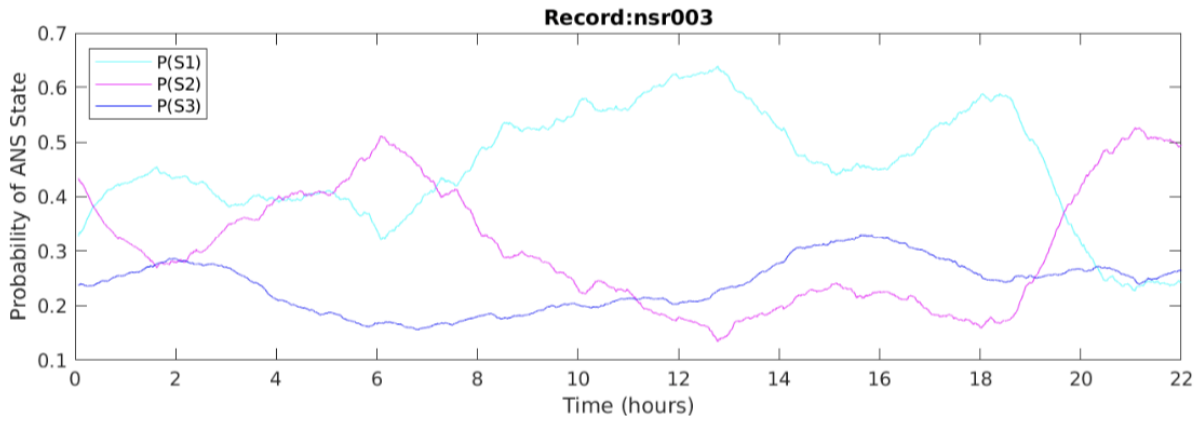
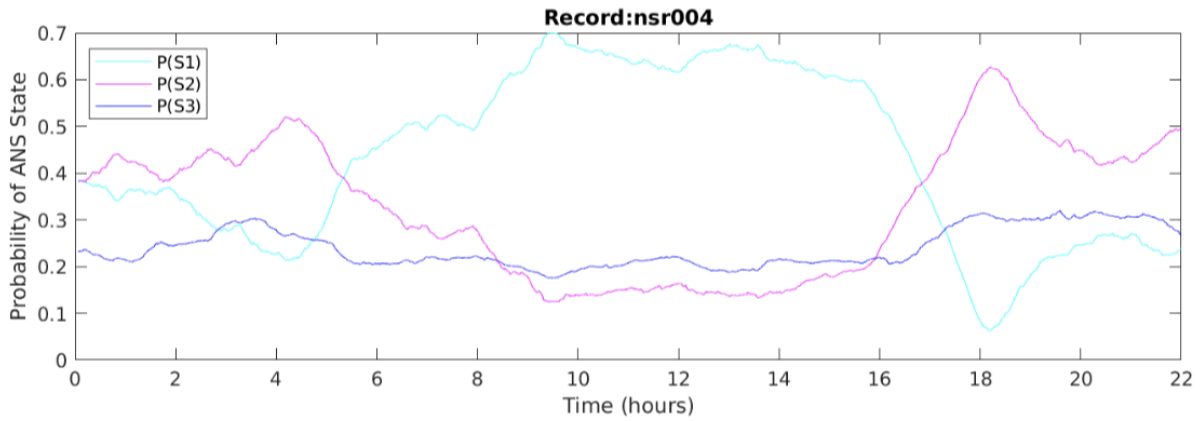
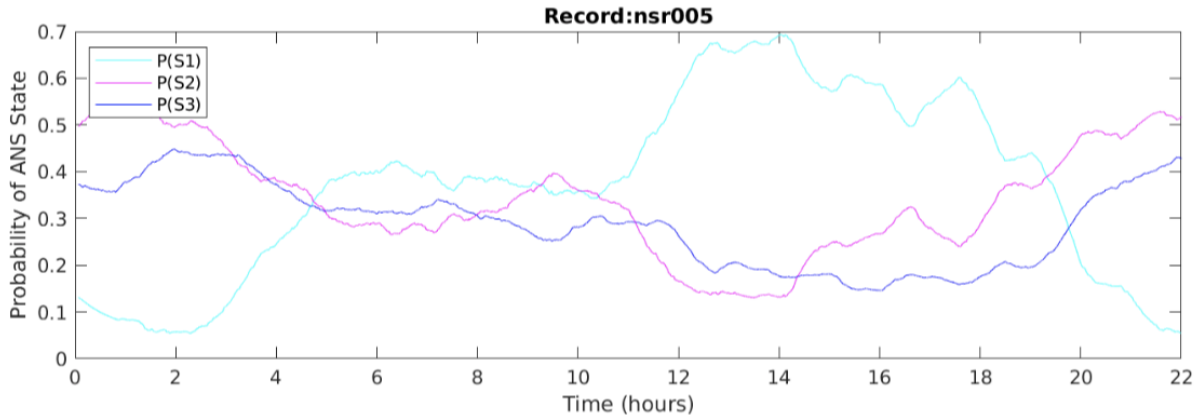


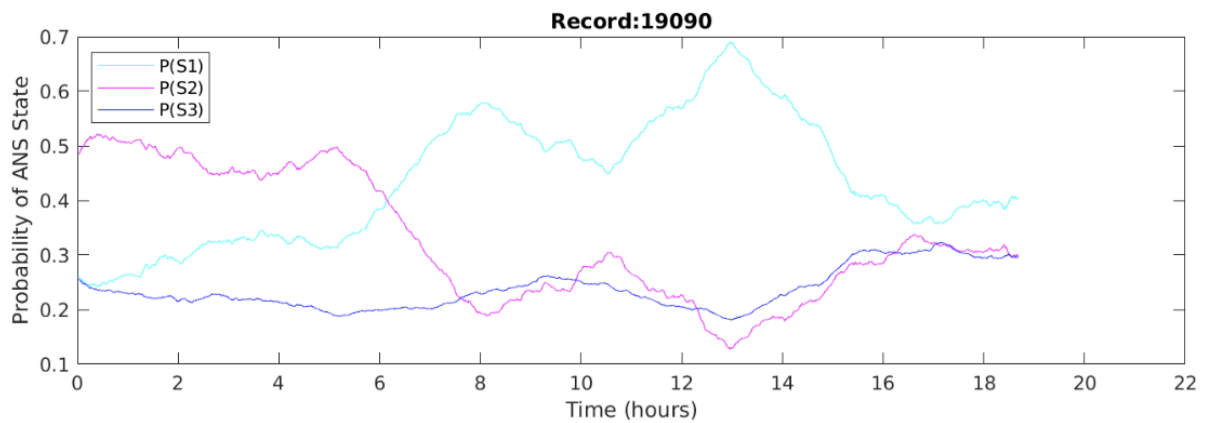
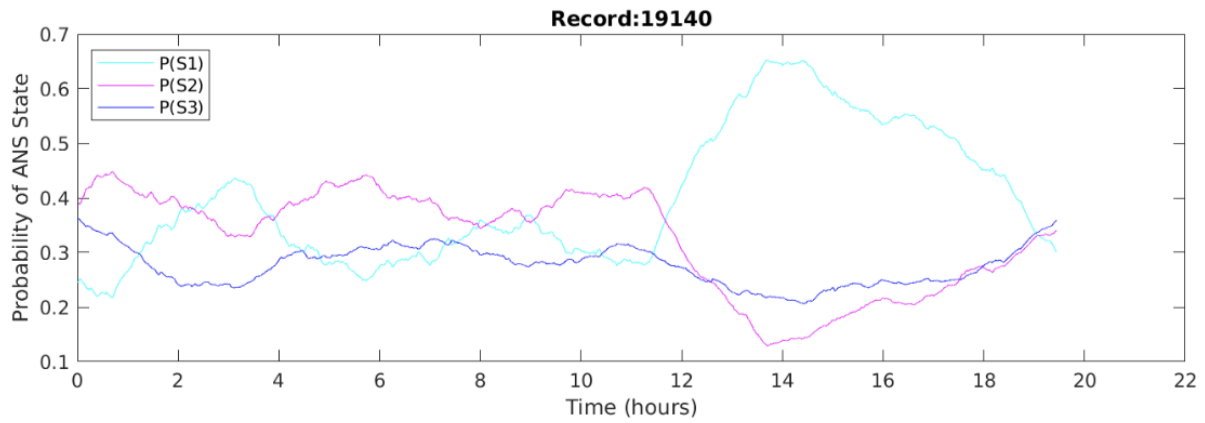
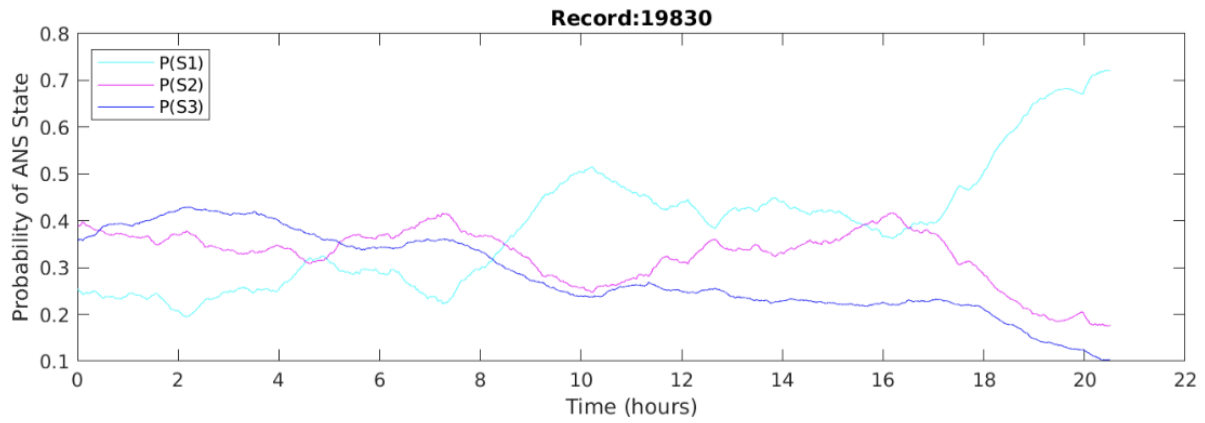
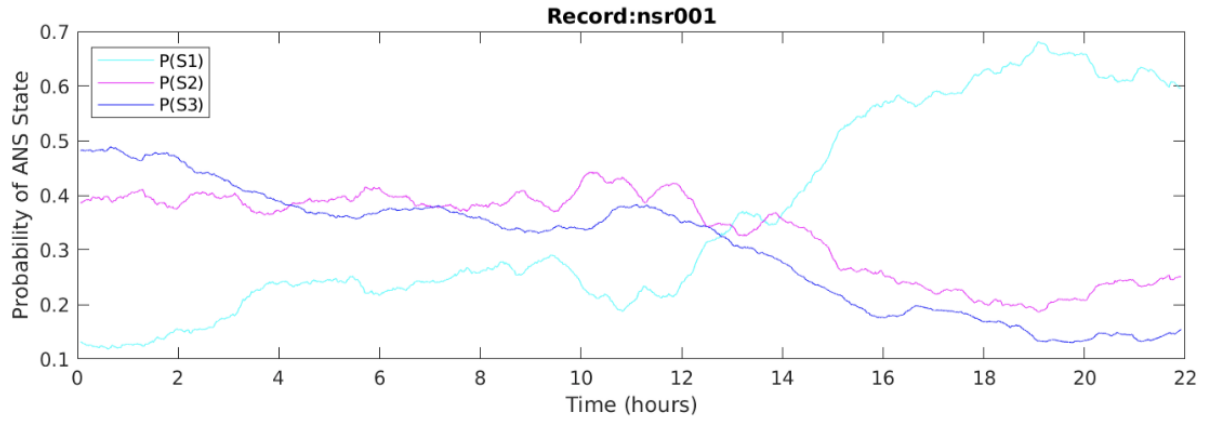


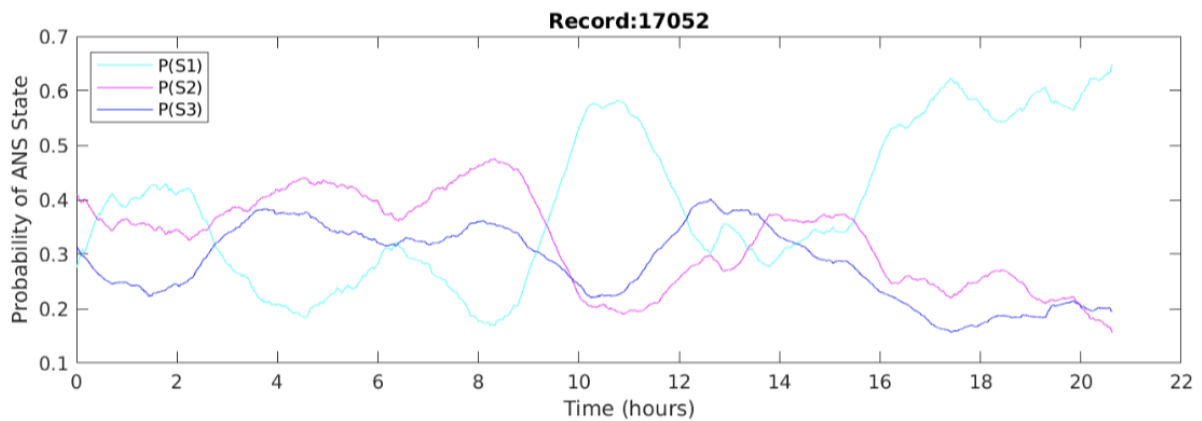
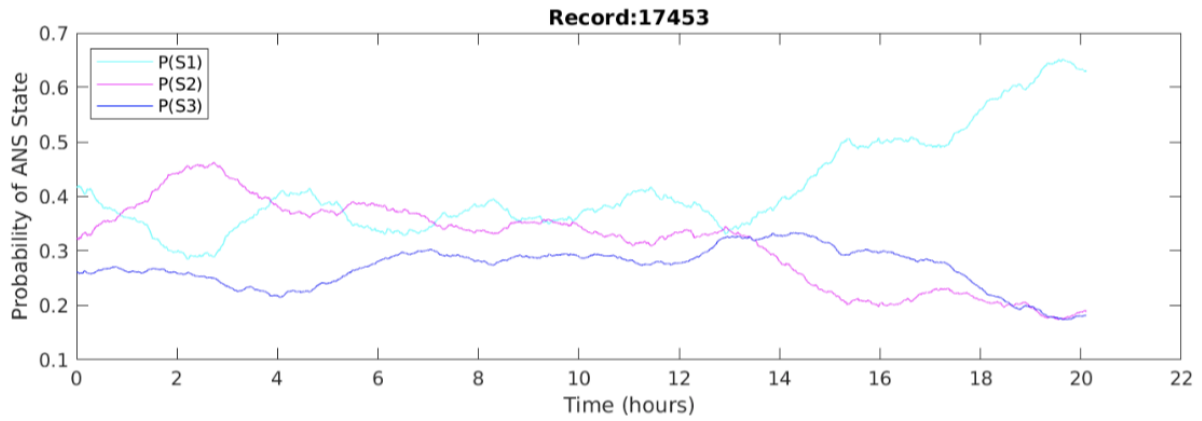
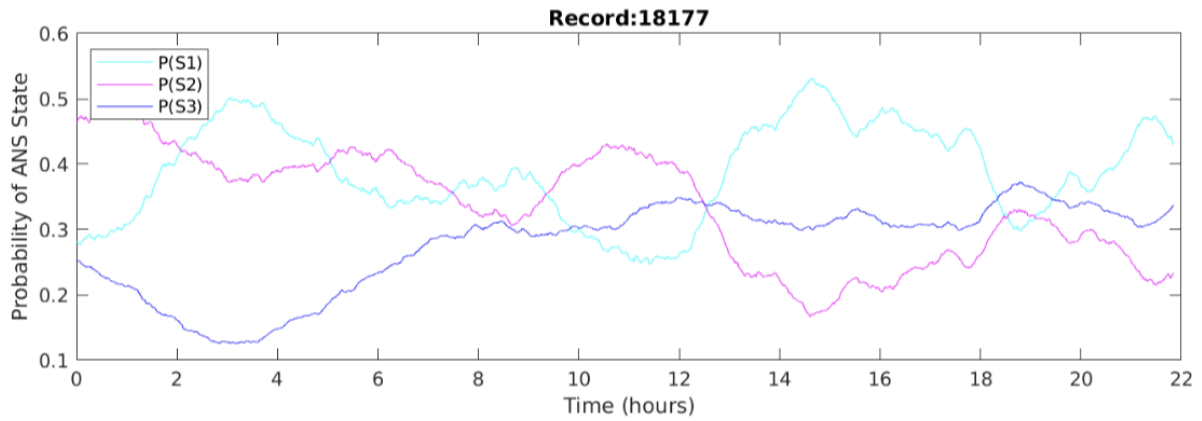
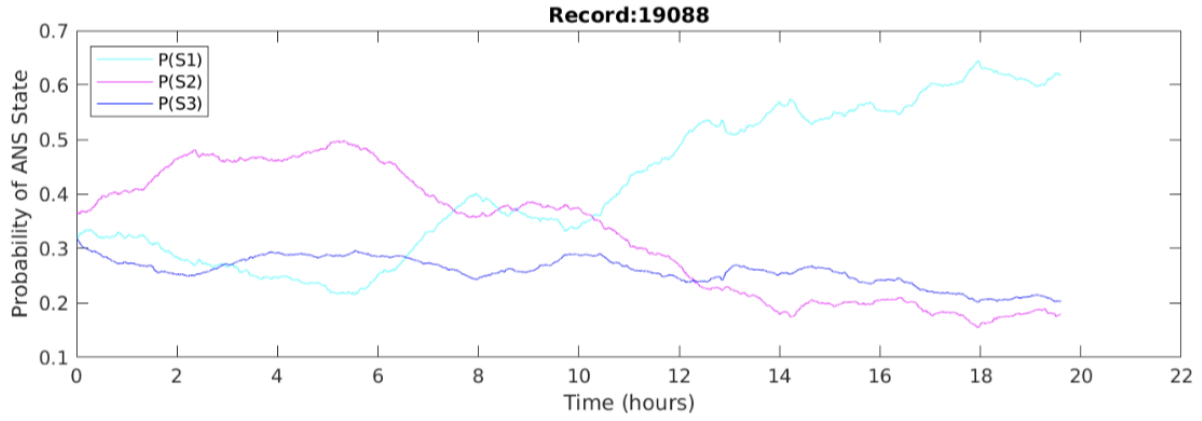


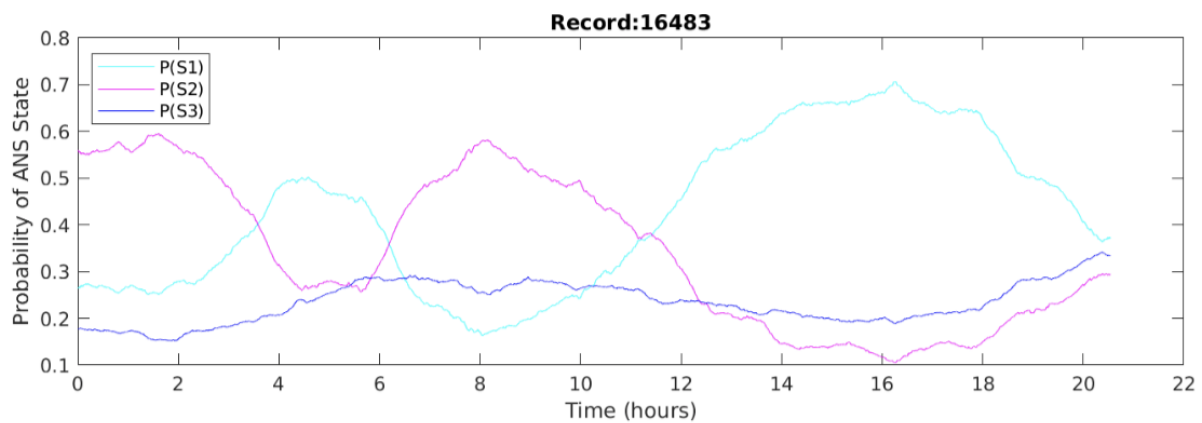
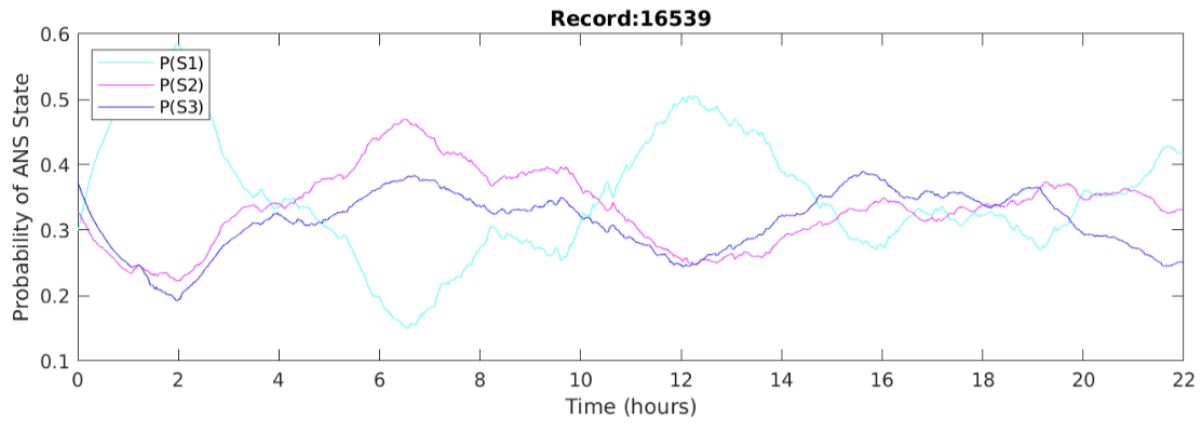
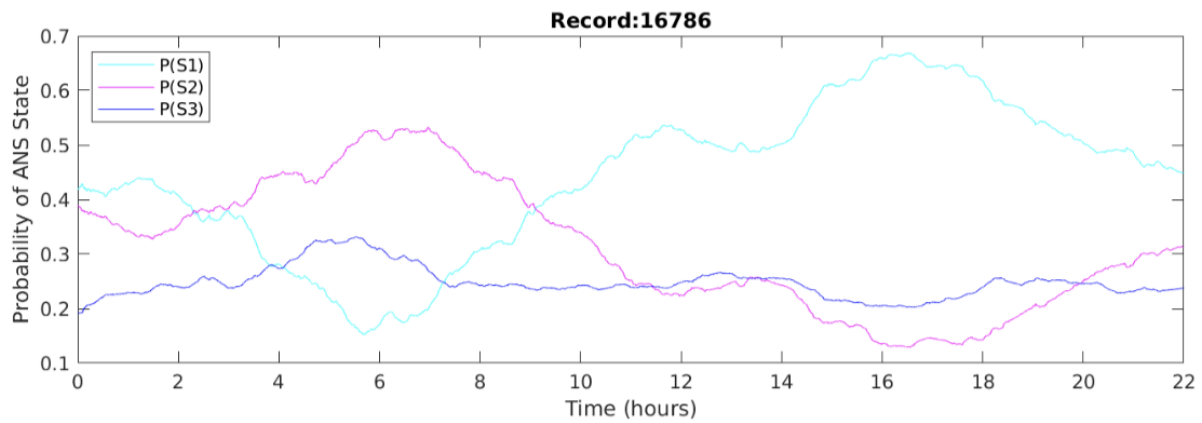
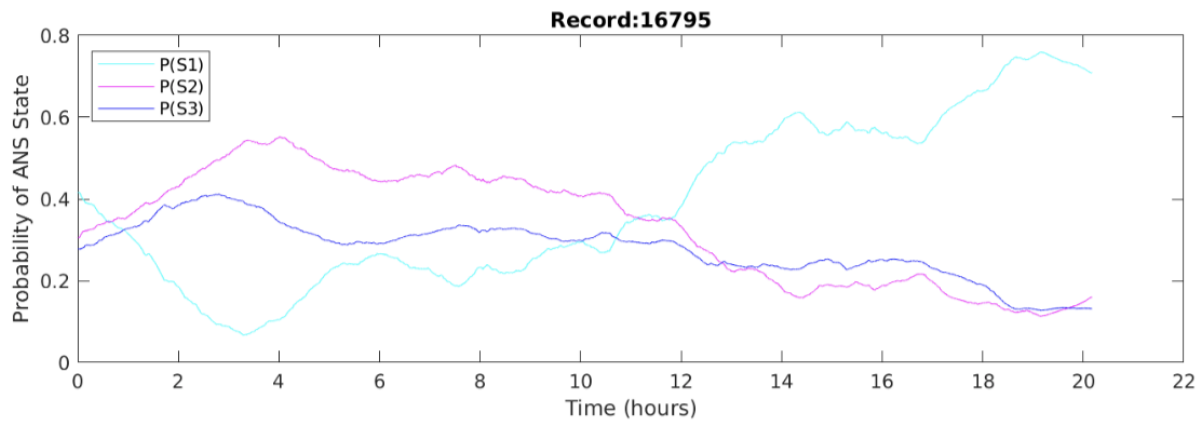


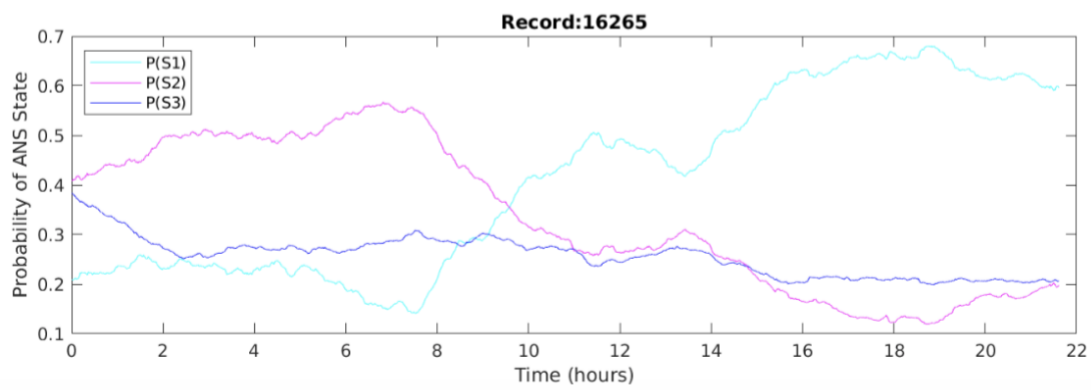
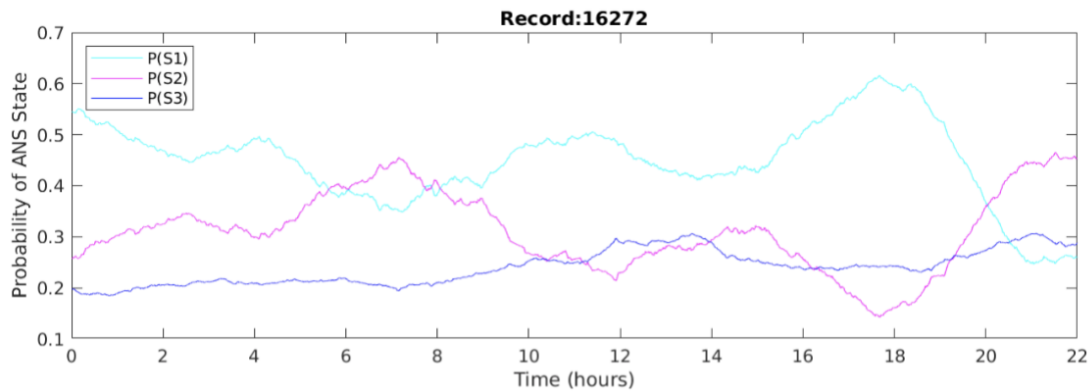
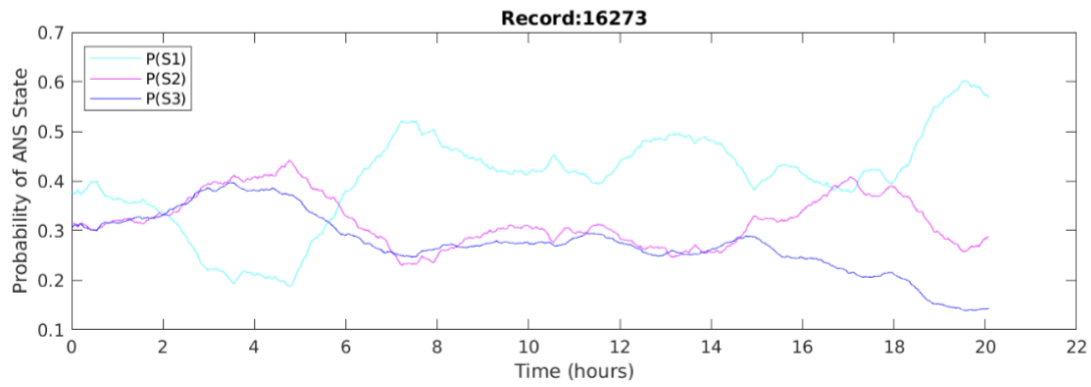
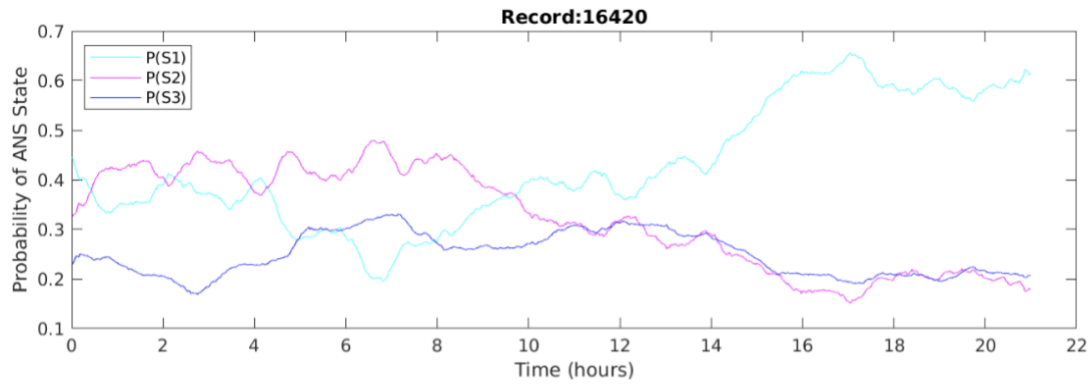












Appendix Figure 1 ANS state estimation results

Appendix C Code Snippets

ECG Processing

MIT-BIH RR interval and instantaneous HR (Python3)

```
import os
import subprocess
def main():

# read in RECORDS list
with open('/path/RECORDS') as f:
    for line in f:
        line = line.strip()
        file_rr = '/path/' + line + '.rr.txt'
        file_hr = '/path/' + line + '.hr.txt'
        # iterate through RECORDS list, running ann2rr on each
        FNULL = open(os.devnull, 'w')
        args = 'ann2rr -r ' + line + ' -a atr -c -P N -p N > ' + file_rr
        subprocess.run(args, stdout=FNULL, stderr=FNULL, shell=True)

        args2 = 'ihr -r ' + line + ' -a atr > ' + file_hr
        subprocess.run(args2, stdout=FNULL, stderr=FNULL, shell=True)
        # print output of ann2rr for each record to a rr.txt file
        # print output of ihr for each record to a hr.txt file

if __name__ == '__main__':
    main()
```

NSR RR interval and instantaneous HR (Python3)

```
import os
import subprocess

def main():
# read in RECORDS list
with open('RECORDS') as f:
    for line in f:
        line = line.strip()
        # iterate through RECORDS list, running ann2rr on each
        FNULL = open(os.devnull, 'w')
        args = 'ann2rr -r ' + line + ' -a ecg -c -P N -p N > ' + line + '.rr.txt'
        subprocess.run(args, stdout=FNULL, stderr=FNULL, shell=True)
        args2 = 'ihr -r ' + line + ' -a ecg > ' + line + '.hr.txt'
```

```

        subprocess.run(args2, stdout=FNNULL, stderr=FNNULL, shell=True)
    # print output of ann2rr for each record to a rr.txt file
    # print output of ihr for each record to a hr.txt file

```

```

if __name__ == '__main__':
    main()

```

Export to MAT (Python3)

```

import matplotlib.pyplot as plt
import numpy as np
import math
import scipy.io as io
import pdb
# the purpose of this script is to zip the rr
# and hr time series together with a time
# index and save to a file to give to matlab
# for each record.

def main():

# read in RECORDS list
with open('RECORDS', 'r') as f:
    for line in f:
        line = line.strip()
        file_rr = line + '.rr.txt'
        file_hr = line + '.hr.txt'
        file_mat = line + '.mat'
        rr_hr_ibis = []
        with open(file_rr, 'r') as fr:
            for delta_ibi in fr:
                delta_ibi = float(delta_ibi)
                rr_hr_ibis.append(delta_ibi)
            rr_hr_ibis = np.array(rr_hr_ibis)
            l_fr = len(rr_hr_ibis)
            print('done reading rrs')
            with open(file_hr, 'r') as fh:
                all_t = []
                all_hr = []
                i = -1
                for sample in fh:
                    sample = sample.split('\t')
                    all_t.append(float(sample[0]))
                    all_hr.append(float(sample[1]))
            #plt.plot(range(l_fr), rr_hr_ibis)
        #plt.show()

```

```

print('done reading hrs')
all_t = np.array(all_t)
all_hr = np.array(all_hr)
breakpoint()
sampling_frequency = 300 # about twice the highest expected heart rate
time_start = math.ceil(all_t[0])
time_end = math.ceil(all_t[-1])
time_increment = float(1/sampling_frequency)
interpolated_t = np.arange(time_start, time_end, time_increment)
interpolated_hr = np.interp(interpolated_t, all_t, all_hr)
print('interpolated hr')
interpolated_hrv = np.interp(interpolated_t, range(0, len(rr_hr_ibis)), rr_hr_ibis)
print('interpolated hrv')
mat_data = {}
mat_data['t'] = interpolated_t
mat_data['hrv'] = interpolated_hrv
mat_data['hr'] = interpolated_hr
io.savemat(file_mat, mat_data)
save_msg = 'saved ' + file_mat
print(save_msg)
if __name__ == '__main__':
main()

```

Exploratory Analysis

Exploratory analysis and long term HRV (MATLAB 2020a)

```

ms_to_s = 1/1000; % s/ms
sampl_rate = 300; % /s

files = dir('*.*mat');
records = zeros(length(files),1);
duration = zeros(length(files),1);
skewnessr = zeros(length(files),1);
kurtosisr = zeros(length(files),1);
mean_hr = zeros(length(files),1);
std_hr = zeros(length(files),1);
mean_hrv = zeros(length(files),1);
sdnn = zeros(length(files),1);
lfpwr = zeros(length(files),1);
hfpwr = zeros(length(files),1);
lfhfr = zeros(length(files),1);
% HRV metrics for each file
i = 1;
for file = files'
records(i) = convertCharsToStrings(file.name);
rdata = load(file.name);

```

```

t = rdata.t;
duration(i) = t(length(t));
hr = rdata.hr;
hrv = (rdata.hrv)*ms_to_s;
skewnessr(i) = skewness(hrv);
kurtosisr(i) = kurtosis(hrv);
mean_hr(i) = mean(hr);
std_hr(i) = std(hr);
mean_hrv(i) = mean(hrv);
sdnn(i) = std(hrv);
lfpwr(i) = bandpower(hrv,sampl_rate, [0.04, 0.15]); % signal processing toolbox
hfpwr(i) = bandpower(hrv,sampl_rate, [0.15, 0.4]); % signal processing toolbox
lfhfr(i) = lfpwr(i)/hfpwr(i);
i = i + 1;
end
ex_analysis = [duration, skewnessr, kurtosisr, mean_hr, std_hr, mean_hrv, sdnn, lfpwr, hfpwr,
lfhfr];
Short term HRV (MATLAB 2020a)
i = 1;
record = [];
for file = files'
record(i) = convertCharsToStrings(file.name);
rdata = load(file.name);
t = rdata.t;
hr = rdata.hr;
hrv = (rdata.hrv)*ms_to_s;

% trim data to get multiple of 5 minutes
orig_length = length(t);
trim = rem(orig_length, block_length) + 1;
num_blocks = fix((orig_length - trim)/block_length);
t = t(trim:orig_length);
hr = hr(trim:orig_length);
hrv = hrv(trim:orig_length);
% subdivide data into cells, each containing a 5 minute interval of t, hr,
% and hrv data
hr_blocks = reshape(hr, block_length, []);
hrv_blocks = reshape(hrv, block_length, []);
time_blocks = reshape(t, block_length, []);
block_start = zeros(num_blocks,1);
mean_hrv = zeros(num_blocks,1);
std_hrv = zeros(num_blocks,1);
mean_hr = zeros(num_blocks,1);
lf_bandpower = zeros(num_blocks,1);
hf_bandpower = zeros(num_blocks,1);
lf_hf = zeros(num_blocks,1);

```

```

for i = 1:num_blocks
    block_start(i) = time_blocks(1,i);
    mean_hrv(i) = mean(hrv_blocks(:,i));
    std_hrv(i) = std(hrv_blocks(:,i));
    mean_hr(i) = mean(hr_blocks(:,i));
    lf_bandpower(i) = bandpower(hrv_blocks(:,i),sampl_rate, [0.04, 0.15]);
    hf_bandpower(i) = bandpower(hrv_blocks(:,i),sampl_rate, [0.15, 0.4]);
    lf_hf(i) = lf_bandpower(i)/hf_bandpower(i);
end
end

```

State Transition Design (MATLAB 2020a)

```

sampl_rate = 300; % interpolation sample rate of hr and hrv time series
block_length = 10*sampl_rate; % samples per 10 second block

```

```

files = dir('*.*mat');
length(files)
rec_name_m = [];
st_m = [];
shrv_m = [];
sdnn_m = [];
shr_m = [];
lfp_m = [];
hfp_m = [];
lfhf_m = [];
hfhr_m = [];
hfrr_m = [];
hfam_m = [];
c = cell(1, length(files));
c_i = 1;
for file = files'
    c_i
    record = convertCharsToStrings(file.name)
    rdata = load(file.name);
    t = rdata.t; % s
    hr = rdata.hr; % bpm
    hrv = rdata.hrv; % ms

    % trim data to get multiple of 10 s
    orig_length = length(t);
    trim = rem(orig_length, block_length) + 1;
    num_blocks = fix((orig_length - trim)/block_length);
    t = t(trim:orig_length);
    hr = hr(trim:orig_length);
    hrv = hrv(trim:orig_length);

```

```

% subdivide data into cells, each containing a 10s interval of t, hr,
% and hrv data
hr_blocks = reshape(hr, block_length, []);
hrv_blocks = reshape(hrv, block_length, []);
time_blocks = reshape(t, block_length, []);
rec_name = zeros(num_blocks,1);
st = zeros(num_blocks,1);
shrv = zeros(num_blocks,1);
sdnn = zeros(num_blocks,1);
shr = zeros(num_blocks,1);
lfp = zeros(num_blocks,1);
hfp = zeros(num_blocks,1);
lfhf = zeros(num_blocks,1);
hfhr = zeros(num_blocks,1);
hfrr = zeros(num_blocks,1);

for i = 1:num_blocks
    rec_name(i) = record;
    st(i) = time_blocks(1,i);
    shrv(i) = mean(hrv_blocks(:,i));
    sdnn(i) = std(hrv_blocks(:,i));
    shr(i) = mean(hr_blocks(:,i));
    lfp(i) = bandpower(hrv_blocks(:,i),sampl_rate, [0.04, 0.15]);
    hfp(i) = bandpower(hrv_blocks(:,i),sampl_rate, [0.15, 0.4]);
    lfhf(i) = lfp(i)/hfp(i);
    hfhr(i) = max(hr_blocks(:,i)) - min(hr_blocks(:,i)); % in bpm
    hfrr(i) = max(hrv_blocks(:,i)) - min(hrv_blocks(:,i)); % in ms
end
baseline_hfhr = mean(hfhr);
baseline_hfrr = mean(hfrr);
hfhrn = hfhr./baseline_hfhr;
hfrrn = hfrr./baseline_hfrr;
hfam = hfhrn./hfrrn;% hf autonomic modulation ratio
raw_state = zeros(length(st),1);
for k = 1:length(st)
    if hfam(k) <=1
        raw_state(k) = 1;
    else
        if hfhrn(k) >1
            raw_state(k) = 2;
        else
            raw_state(k) = 3;
        end
    end
end
end
end

```

```
c{c_i} = table(st, shrv, sdn, shr, hfp, raw_state);
c_i = c_i + 1;
```

```
end
```

Particle Filtering (MATLAB 2020a)

```
load('/home/lindsey/sthrv_env/stHRV/stHRV/all_data_thesis/16265.mat')
```

```
% create time series of information
```

```
ms_to_s = 1/1000; % s/ms
```

```
sampl_rate = 300; % /s
```

```
d_sampl_rate = 0.01; % new block rate
```

```
% hrv = hrv.*ms_to_s; % convert ms to s
```

```
block_length = 10*sampl_rate; % samples per 10 s block
```

```
% trim data to get multiple of 10 s
```

```
orig_length = length(t);
```

```
trim = rem(orig_length, block_length) + 1;
```

```
num_blocks = fix((orig_length - trim)/block_length);
```

```
t = t(trim:orig_length);
```

```
hr = hr(trim:orig_length);
```

```
hrv = hrv(trim:orig_length);
```

```
% subdivide data into cells, each containing a 10s interval of t, hr,
```

```
% and hrv data
```

```
hr_blocks = reshape(hr, block_length, []);
```

```
hrv_blocks = reshape(hrv, block_length, []);
```

```
time_blocks = reshape(t, block_length, []);
```

```
st = zeros(num_blocks,1);
```

```
shrv = zeros(num_blocks,1);
```

```
sdnn = zeros(num_blocks,1);
```

```
shr = zeros(num_blocks,1);
```

```
lfp = zeros(num_blocks,1);
```

```
hfp = zeros(num_blocks,1);
```

```
lfhf = zeros(num_blocks,1);
```

```
hfhr = zeros(num_blocks,1);
```

```
hfrr = zeros(num_blocks,1);
```

```
for i = 1:num_blocks
```

```
st(i) = time_blocks(1,i);
```

```
shrv(i) = mean(hrv_blocks(:,i));
```

```
sdnn(i) = std(hrv_blocks(:,i));
```

```
shr(i) = mean(hr_blocks(:,i));
```

```
lfp(i) = bandpower(hrv_blocks(:,i),sampl_rate, [0.04, 0.15]);
```

```
hfp(i) = bandpower(hrv_blocks(:,i),sampl_rate, [0.15, 0.4]);
```

```
lfhf(i) = lfp(i)/hfp(i);
```

```

hfhr(i) = max(hr_blocks(:,i)) - min(hr_blocks(:,i)); % in bpm
hfrr(i) = max(hrv_blocks(:,i)) - min(hrv_blocks(:,i)); % in ms
end
baseline_hfhr = mean(hfhr);
baseline_hfrr = mean(hfrr);
hfhrn = hfhr./baseline_hfhr;
hfrrn = hfrr./baseline_hfrr;
hfam = hfhrn./hfrrn;% hf autonomic modulation ratio
raw_state = zeros(length(st),1);
for l = 1:length(st)
if hfam(l) <= 1
    raw_state(l) = 1;
else
    if hfhrn(l) > 1
% =====
predict ==
duration = length(y.st); % ceil(length(y.st)/100);
num_particles = 200;
pf = stateEstimatorPF;
pf.StateTransitionFcn = @nav.algs.gaussianMotion;
pf.MeasurementLikelihoodFcn = @nav.algs.fullStateMeasurement;
pf.StateEstimationMethod = 'maxweight';
pf.ResamplingMethod = 'systematic';
mhfhrrn = mean(y.hfhrn);
mhfhrrn = mean(y.hfhrn);
%
%
initialize(pf, num_particles, [mhfhrrn, mhfhrrn], eye(2));
hStatePredicted = [];
hStateCorrected = [];
my_state = zeros(duration, 3); % array of probabilities for each state

for i = 1:duration
hStatePredicted(i,:) = predict(pf);
hStateCorrected(i,:) = correct(pf, [y.hfam(i), y.hfhrn(i)]);
my_particles_hfam = pf.Particles(:, 1);
my_particles_hfhrn = pf.Particles(:, 2);
pf.Particles(1,:)
raw_state = zeros(num_particles,1);
for m = 1:num_particles
    if my_particles_hfam(m) <= 1
        raw_state(m,1) = 1;
    else
        if my_particles_hfhrn(m) > 1
            raw_state(m,1) = 2;
        else

```

```
        raw_state(m,1) = 3;
    end
end
end
p1 = sum(raw_state == 1)/num_particles;
p2 = sum(raw_state == 2)/num_particles;
p3 = sum(raw_state == 3)/num_particles;
my_state(i,:) = [p1, p2, p3];
status = 100*i/duration
%break
end
```

Bibliography

- [1] Ginsberg J. P. (2016). Editorial: Dysregulation of Autonomic Cardiac Control by Traumatic Stress and Anxiety. *Front. Psychol.* 21. 10.3389/fpsyg.2016.00945
- [2] Porges, S. W. (2011). *The Polyvagal Theory: Neurophysiological Foundations of Emotions, Attachment, Communication, and Self-regulation* (Norton Series on Interpersonal Neurobiology). New York, NY: W. W. Norton & Company.
- [3] Ivanov P. C., Liu K. K. L., Bartsch R. P. (2016). Focus on the emerging new fields of network physiology and network medicine. *New Journal of Physics.* 10.1088/1367-2630/18/10/100201
- [4] Goldstein D. S., McEwen B. (2002). Allostasis, homeostasis, and the nature of stress. *Stress.* 10.1080/102538902900012345.
- [5] Shaffer F., McCraty R., Zerr C. L. (2014). A healthy heart is not a metronome: an integrative review of the heart's anatomy and heart rate variability. *Front. Psychol.* 30. 10.3389/fpsyg.2014.01040
- [6] Day T. A. (2005). Defining stress as a prelude to mapping its neurocircuitry: no help from allostasis. *Prog Neuropsychopharmacol Biol Psychiatry.* 10.1016/j.pnpbp.2005.08.005
- [7] Rao R., Androulakis I. P. (2019). The physiological significance of the circadian dynamics of the HPA axis: Interplay between circadian rhythms, allostasis and stress resilience. *Horm. Behav.* 10.1016/j.yhbeh.2019.02.018
- [8] Godoy L. D., et al. (2018). A Comprehensive Overview on Stress Neurobiology: Basic Concepts and Clinical Implications. *Front Behav Neurosci.* 10.3389/fnbeh.2018.00127
- [9] Ginsberg J. P., Pietrabissa G., Manzoni G. M., Castelnuovo G. (2015). Treating the mind to improve the heart: the summon to cardiac psychology. *Front. Psychol.* 10.3389/fpsyg.2015.01101
- [10] Williamson J. B., Porges E. C., Lamb D. G, Porges S. W. (2015). Maladaptive autonomic regulation in PTSD accelerates physiological aging. *Front Psychol.* 21. 10.3389/fpsyg.2014.01571
- [11] McEwen B. S., Wingfield J. C. (2003). The concept of allostasis in biology and biomedicine. *Horm. Behav.* 10.1016/s0018-506x(02)00024-7
- [12] <https://brain-bodyhealth.com/rheumatoid-arthritis-autonomic-nervous-system-imbalance/>

- [13] Rooney B., Crucian B. E., Pierson D. L., Laudenslager M. L. (2019). Herpes Virus Reactivation in Astronauts During Spaceflight and Its Application on Earth. *Frontiers in Microbiology*. 10.3389/fmicb.2019.00016
- [14] Holmes, A., and Wellman, C. L. (2009). Stress-induced prefrontal reorganization and executive dysfunction in rodents. *Neurosci. Biobehav.* 10.1016/j.neubiorev.2008.11.005
- [15] Mitra, R., and Sapolsky, R. M. (2008). Acute corticosterone treatment is sufficient to induce anxiety and amygdaloid dendritic hypertrophy. *Proc. Natl. Acad. Sci.* 10.1073/pnas.0705615105
- [16] Yoshizaki T., Kawano Y., Tada Y. (2013). Diurnal 24-Hour Rhythm in Ambulatory Heart Rate Variability during the Day Shift in Rotating Shift Workers. *Journal of Biological Rhythms*. 10.1177/0748730413489957
- [17] Calhoun P., Watkins L. L., Dennis P. A., Rissling M. (2016). Circadian Contrasts in Heart Rate Variability Associated with Posttraumatic Stress Disorder Symptoms in a Young Adult Cohort: Heart Rate Variability, Sleep, and PTSD Symptoms. *Journal of Traumatic Stress*. 10.1002/jts.22125
- [18] Drury R. L. (2014). Wearable biosensor systems and resilience: a perfect storm in health care? *Front. Psychol.* 6. 10.3389/fpsyg.2014.00853
- [19] <https://lifestest.zoll.com/medical-professionals/frequently-asked-questions>, accessed July 2020.
- [20] Cohen H., Kotler M., Matar M. A., Loewenthal U., Miodownik H., Cassuto Y. (1998) Analysis of heart rate variability in posttraumatic stress disorder patients in response to a trauma-related reminder. *Biological Psychiatry*. 44. 10.1016/S0006-3223(97)00475-7
- [21] HRV Task Force. (1996). Heart rate variability: standards of measurement, physiological interpretation and clinical use. Task Force of the European Society of Cardiology and the North American Society of Pacing and Electrophysiology. *Circulation* 93, 1043–1065. doi: 10.1161/01.CIR.93.5.1043
- [22] Billman G. E., Huikuri H. V., Sacha J., Trimmel K. (2015). An introduction to heart rate variability: methodological considerations and clinical applications. *Front. Physiol.* 6. 10.3389/fphys.2015.00055
- [23] Laborde S., Mosley E., Thayer J. F. (2017) Heart Rate Variability and Cardiac Vagal Tone in Psychophysiological Research - Recommendations for Experiment Planning, Data Analysis, and Data Reporting. *Front Psychol.* 8. 10.3389/fpsyg.2017.00213
- [24] Breit S., Kupferberg A., Rogler G., Hasler G. (2018). Vagus Nerve as Modulator of the Brain-Gut Axis in Psychiatric and Inflammatory Disorders. *Front. Psychiatry*. 13. 10.3389/fpsyg.2018.00044

- [25] Bigger J. T., Fleiss J. L., Steinman R. C., Rolnitzky L. M., Schneider W. J., Stein P. K. (1995). RR Variability in Healthy, Middle-Aged Persons Compared with Patients with Chronic Coronary Heart Disease or Recent Acute Myocardial Infarction. *Circulation*. 10.1161/01.CIR.91.7.1936
- [26] Rodriguez-Colon S. et al. (2015). The Circadian Pattern of Cardiac Autonomic Modulation and Obesity in Adolescents. *Clin Auton Res*. 10.1007/s10286-014-0257-7
- [27] Rodriguez J., Correa C., Paez J., Cortes J., Prieto S., Castro M., Montenegro C. (2019). Application of the theory of probability and dynamic systems in the evaluation of cardiac dynamics: Study of diagnostic agreement. *J. Phys.: Conf. Ser.* 1160. 10.1088/1742-6596/1160/1/012019
- [28] Zaslavsky G. M. (2002). Chaos, fractional kinetics, and anomalous transport. *Physics Reports*. 10.1016/S0370-1573(02)00331-9
- [29] Goldberger, A., Rigney, D., and West, B. (1990). Chaos and fractals in human physiology. *Sci. Am.* 262, 42–49. doi: 10.1038/scientificamerican0290-42
- [30] Goldberger, A., and West, B. (1987). Fractals: a contemporary mathematical concept with applications to physiology and medicine. *Yale J. Biol. Med.* 60, 104–119.
- [31] West B. J. (2010). Fractal Physiology and the fractional calculus: a perspective. *Front. Physiol.* 10.3389/fphys.2010.00012
- [32] Valverde S., Ohse S., Turalska M., West B. J., Garcia-Ojalvo J. (2015). Structural determinants of criticality in biological networks. *Front. Physiol.* 10.3389/fphys.2015.00127
- [33] Goldberger A. L., Amaral L. A. N., Hausdorff J. M., Ivanov P. C., Peng C.-K., Stanley H. E. (2002). Fractal dynamics in physiology: Alterations with disease and aging. *PNAS*. 10.1073/pnas.012579499
- [34] Billman G. E. (2011). Heart rate variability - a historical perspective. *Front. Physiol.* 29. 10.3389/fphys.2011.00086
- [35] Pittman-Polletta B., Scheer F. A. J. L., Butler M. P., Shea S. A. (2013). The role of the circadian system in fractal neurophysiological control: The circadian system and fractal neurophysiology. *Biological Reviews*. 10.1111/brv.12032
- [36] Halley J. M., Hartly S., Kallimanis A. S., Kunin W. E., Lennon J. J., Sgardelis S. P. (2004). Uses and abuses of fractal methodology in ecology. *Ecology Letters*. 7. 10.1111/j.1461-0248.2004.00568.x
- [37] West B. J., Turalska M. (2019). Hypothetical Control of Heart Rate Variability. *Front. Physiol.* 10.3389/fphys.2019.01078

- [38] Peng C. K., Mietus J., Hausdorff J. M., Havlin S., Stanley H. E., Goldberger A. L. (1993). Long-range anticorrelations and non-Gaussian behavior of the heartbeat. *Phys Rev Lett.* 70:1343–1346.
- [39] Dvir H., Bobrovsky B. Z., Gabbay U. (2012). A novel heart rate control model provides insights linking LF-HRV behavior to open-loop gain. *Int. J. Cardiology.* 168. 10.1016/j.ijcard.2012.09.073
- [40] Canuto D., Chong K., Bowles C., Dutson E. P., Eldredge J. D., Beenharash P. (2018). A regulated multiscale closed-loop cardiovascular model, with applications to hemorrhage and hypertension. *International Journal for Numerical Methods in Biomedical Engineering.* 34. 10.1002/cnm.2975
- [41] Chiu H. W., Kao T. (2001). A Mathematical Model for Autonomic Control of Heart Rate Variation. *IEEE Engineering in Medicine and Biology.* 10.1109/51.917726
- [42] Su S. W. et al. (2007). Nonparametric Hammerstein Model Based Model Predictive Control for Heart Rate Regulation. 2007 Annual International Conference of the IEEE Engineering in Medicine and Biology Society. 10.1109/IEMBS.2007.4352956
- [43] Silva L. E. V. (2017). Nonlinearities of heart rate variability in animal models of impaired cardiac control: contribution of different time scales. *Journal of Applied Physiology.* 123. 10.1152/jappphysiol.00059.2017
- [44] Champeroux P., Fesler P., Jude S., Richard S., Guennec J. Y., Thoreau J. (2018). High-frequency autonomic modulation: a new model for analysis of autonomic cardiac control. *British Journal of Pharmacology.* 175. 10.1111/bph.14354
- [45] Hayano J., Yuda E. (2019). Pitfalls of assessment of autonomic function by heart rate variability. *J Physiol Anthropol.* 38. 10.1186/s40101-019-0193-2
- [46] Gustafsson F. (2010). Particle Filter Theory and Practice with Positioning Applications. *IEEE A&E Systems Magazine.* 25. 10.1109/MAES.2010.5546308
- [47] Spasic S. Z., Kesic S. (2019). Editorial: Nonlinearity in Living Systems: Theoretical and Practical Perspectives on Metrics of Physiological Signal Complexity. *Front. Physiol.* 10.3389/fphys.2019.00298
- [48] Durrant-Whyte H., Bailey T. (2006). Simultaneous localization and mapping: part I. *IEEE Robotics & Automation Magazine.* 10.1109/MRA.2006.1638022
- [49] Hainsworth, R. (1995). The control and physiological importance of heart rate. In Malik, M., Camm, J. (Eds.). *Heart rate variability*, 3-19. New York: Futura publishing company Inc.
- [50] Shah, A. J., Lampert, R., Goldberg, J., Veledar, E., Bremner, J. D., and Vaccarino, V. (2013). Posttraumatic stress disorder and impaired autonomic modulation in male twins. *Biol. Psychiatry* 73, 1103–1110. doi: 10.1016/j.biopsych.2013.01.019

- [51] Carney, R. M., Freedland, K. E., Stein, P. K., Miller, G. E., Steinmeyer, B., Rich, M. W., et al. (2007). Heart rate variability and markers of inflammation and coagulation in depressed patients with coronary heart disease. *J. Psychosom. Res.* 10.1016/j.jpsychores.2006.12.004
- [52] Lampert, R., Bremner, J. D., Su, S., Miller, A., Lee, F., Cheema, F., et al. (2008). Decreased heart rate variability is associated with higher levels of inflammation in middle-aged men. *Am. Heart J.* 10.1016/j.ahj.2008.07.009
- [53] Konstantinov K. B. (1996). Monitoring and control of the physiological state of cell cultures. *Biotechnol Bioeng.* 52. 10.1002/bit.260520203.
- [54] Goldberger, A. L., Amaral, L. A. N., Glass, L., Hausdorff, J. M., Ivanov, P. C., Mark, R. G., et al. (2000). PhysioBank, PhysioToolkit, and PhysioNet: components of a new research resource for complex physiologic signals. *Circulation* 101, e215–e220. doi: 10.1161/01.CIR.101.23.e215
- [55] Normal Sinus Rhythm RR Interval Database v1.0.0.
<https://physionet.org/content/nsr2db/1.0.0/>, accessed May 2020.
- [56] MIT-BIH Normal Sinus Rhythm Database <https://physionet.org/content/nsrdb/1.0.0/>, accessed May 2020.
- [57] Heart rate variability tutorial <https://archive.physionet.org/tutorials/hrv/>, accessed May 2020.
- [58] Heart rate variability toolkit <https://archive.physionet.org/tutorials/hrv-toolkit/>, accessed May 2020.
- [59] Vest A. N., Li Q., Liu C., Nemati S., Shah A., Clifford G. D. (2018). Benchmarking Heart Rate Variability Toolboxes. *J. Electrocardiol.* 10.1016/j.jelectrocard.2017.08.006
- [60] Jarrin D. C., McGrath J. J., Lambert M. (2012). Measurement fidelity of heart rate variability signal processing: The devil is in the details. *Int. J. Psychophysiol.* 86. 10.1016/j.ijpsycho.2012.07.004
- [61] Kwon O., Jeong J., Choi Y., et al. (2018). Electrocardiogram Sampling Frequency Range Acceptable for Heart Rate Variability Analysis. *Healthc Inform Res.* 24. 10.4258/hir.2018.24.3.198
- [62] Li K., Rudiger H., Ziemssen T. (2019). Spectral Analysis of Heart Rate Variability: Time Window Matters. *Front. Neurol.* 10.3389/fneur.2019.00545
- [63] Monfredi O. et al. (2014). Biophysical Characterization of the Underappreciated and Important Relationship Between Heart Rate Variability and Heart Rate. *Hypertension.* 10.1161/HYPERTENSIONAHA.114.03782
- [63] Kutschireiter A., Surace S. C., Pfister J. P. (2019). The Hitchhiker’s guide to nonlinear filtering. *Journal of Mathematical Psychology.* 10.1016/j.jmp.2019.102307

- [64] Arulampalam M. S., Maskell S., Gordon N., Clapp T. (2002). A Tutorial on Particle Filters for Online Nonlinear/Non-Gaussian Bayesian Tracking. *IEEE Transactions on Signal Processing*. 11053-587X(02)00569-X
- [65] <https://www.mathworks.com/help/ident/ref/particlefilter.html>, accessed November 2020.
- [66] Speekenbrink M. (2016). A tutorial on particle filters. *Journal of Mathematical Psychology*. 73. 10.1016/j.jmp.2016.05.006.
- [67] Doucet A., Johansen A. M. (2008). A Tutorial on Particle Filtering and Smoothing: Fifteen years later. <https://www.stats.ox.ac.uk/~doucet/>.
- [68] Feng M., Cai S. M., Tang M., Lai Y. C. (2019). Equivalence and its invalidation between non-Markovian and Markovian spreading dynamics on complex networks. *Nature Communications*. 10. 10.1038/s41467-019-11763-z
- [69] Stein P. K., Domitrovich P. P., Hui N., Rautaharju P., Gottdiener J. (2005). Sometimes Higher Heart Rate Variability Is Not Better Heart Rate Variability: Results of Graphical and Nonlinear Analyses. *J. Cardio. Electrophysiology*. 16. 10.1111/j.1540-8167.2005.40788.x
- [70] Bryce R. M., Sprague K. B. (2012). Revisiting detrended fluctuation analysis. *Scientific Reports*. 2. 0.1038/srep00315
- [71] Albrecht P., Cohen R. J. (1998). Estimation of heart rate power spectrum bands from real-world data: dealing with ectopic beats and noisy data. *IEEE*. 10.1109/CIC.1988.72624
- [72] Costa M. D., Davis R. D., Goldberger A. L. (2017). Heart Rate Fragmentation: A New Approach to the Analysis of Cardiac Interbeat Interval Dynamics. *Front. Physiol*. 10.3389/fphys.2017.00255
- [73] Hayano, J., Kiyono, K., Struzik, Z., Yamamoto, Y., Watanabe, E., Stein, P., et al. (2011). Increased non-Gaussianity of heart rate variability predicts cardiac mortality after an acute myocardial infraction. *Front. Physiol*. 2:65. doi: 10.3389/fphys.2011.00065
- [74] Buchner T., Petelczyc M., Zebrowski J., et al. (2009). On the nature of heart rate variability in a breathing normal subject: A stochastic process analysis. *Chaos*. 19. 10.1063/1.3152008
- [75] Kamath M. V., Watanbe M., Upton A. (2012). Heart Rate Variability (HRV) Signal Analysis: Clinical Applications. Taylor & Francis Group. Ch 2. p 11.
- [76] <https://www.whoop.com/>, accessed September 2020.
- [77] <https://apolloneuro.com/>, accessed September 2020.
- [78] Blom Y. T., H. A. P., Mehta P. G. (2014). The continuous-discrete time feedback particle filter. *Proceedings of the American Control Conference*. 10.1109/ACC.2014.6859259